PhD Program in Neuroscience

Natural and pathological aging distinctively impacts the vomeronasal system and social behavior

Doctoral Thesis presented by

Adrián Portalés Montes

Thesis Director:

Dra. Sandra Jurado Sánchez

Instituto de Neurociencias

Universidad Miguel Hernández de Elche

- 2024 -

UNIVERSITAS Miguel Hernández

CSIC UNIVERSITAS Miguel Hernández

INSTITUTO DE NEUROCIENCIAS

EXCELENCIA SEVERO OCHOA 2014 - 2027

La presente Tesis Doctoral titulada "**Natural and pathological aging distinctively impacts the vomeronasal system and social behavior**" ha sido desarrollada por mí mismo, Adrián Portalés Montes. Esta tesis se presenta bajo la modalidad de tesis por compendio de publicaciones y presenta como índice de calidad un artículo de investigación del que soy primer autor:

- Portalés A, Chamero P, Jurado S. Natural and Pathological Aging Distinctively Impacts the Pheromone Detection System and Social Behavior. Mol Neurobiol. 2023 Aug;60(8):4641-4658. doi: 10.1007/s12035-023-03362-3. Epub 2023 May 2. PMID: 37129797; PMCID: PMC10293359.

Dra. Dª Sandra Jurado Sánchez, diretora de la Tesis Doctoral titulada “Natural and pathological aging distinctively impact the vomeronasal system and social behavior“

AUTORIZO

La presentación de la Tesis Doctoral “Natural and pathological aging distinctively impact the vomeronasal system and social behavior“ realizada por D. Adrián Portalés Montes, bajo mi inmediata dirección y supervisión como directora de su Tesis Doctoral en el Instituto de Neurociencias (CSIC-UMH) y que se presenta para la obtención del grado de Doctor en Neurociencias por la Universidad Miguel Hernández.

Y para que conste, a los efectos oportunos, firmo el presente certificado.

Dra. Sandra Jurado Sánchez

Sant Joan d'Alacant, 25 de 03 2024

Dña. Cruz Morenilla Palao, Coordinadora del programa de Doctorado en Neurociencias del Instituto de Neurociencias de Alicante, centro mixto de la Universidad Miguel Hernández (UMH) y de la Agencia Estatal Consejo Superior de Investigaciones Científicas (CSIC),

INFORMA:

Que D./Dña. Adrián Portalés Montes ha realizado bajo la supervisión de nuestro Programa de Doctorado el trabajo titulado "**Natural and pathological aging distinctively impacts the vomeronasal system and social behavior**" conforme a los términos y condiciones definidos en su Plan de Investigación y de acuerdo al Código de Buenas Prácticas de la Universidad Miguel Hernández de Elche, cumpliendo los objetivos previstos de forma satisfactoria para su defensa pública como tesis doctoral.

Lo que firmo para los efectos oportunos, en Sant Joan d´Alacant a ..25.. de ……marzo…….. de 2024

Y para que conste, a los efectos oportunos, firmo el presente certificado.

Dra. Cruz Morenilla Palao

Coordinadora del Programa de Doctorado en Neurociencias

La presente tesis doctoral ha sido financiada por subvenciones del Ministerio de Ciencia e Innovación de España SAF2017-82524-R y PID2020-113878RB-I00, el Programa "Severo Ochoa" para Centros de Excelencia en I+D (SEV-2013-0317 y SEV-2017-0723), la Generalitat Valenciana Prometeo/2019/014 (para Dra. Sandra Jurado), y un contrato FPI (BES-2017-081243) para Adrián Portalés.

AGRADECIMIENTOS

Este trabajo de tesis ha sido posible gracias al apoyo de muchas personas dentro y fuera del IN. Después unos 6 años de momentos buenos y menos buenos, quiero agradecer a todas las personas que han hecho que este trabajo haya llegado a este punto. En primer lugar, mi más profundo agradecimiento va para mi supervisora Sandra Jurado, quien me eligió como estudiante de doctorado para su laboratorio y que ha sido extremadamente alentadora durante todo mi tiempo aquí. Gracias a la libertad intelectual y apoyo que he tenido durante todo este periodo no he perdido nunca la motivación por la investigación.

En segundo lugar, esta tesis se ha beneficiado de todos los miembros del laboratorio: Sonia, María Royo, Bea, María Pérez y Pili. De todas vosotras he aprendido algo. Mi agradecimiento también va para Juan Lerma y los miembros de su laboratorio, que me han proporcionado un ambiente de trabajo cooperativo y con críticas constructivas muy útiles. Gracias también a Pablo Chamero, a la gente del INRAE y sobretodo a las cabras por hacer que mi tiempo en Francia fuese más ameno.

Finalmente, agradezco el apoyo de mis padres y de Rebeca, además de la paciencia de Alberto, Andrés, Cristian, Rubén y Melania, entre otros muchos.

Mira, mira….

TABLE OF CONTENTS

ABBREVIATIONS

Aβ: Amyloid Beta Deposits

ACIII: Adenylate Cyclase III

ACo: Cortical Amygdala

AD: Alzheimer's Disease

AOB: Accessory Olfactory Bulb

AON: Anterior Olfactory Nucleus

APP: Amyloid Beta Precursor Protein

BNST: Bed Nucleus of the Stria Terminalis

Ca2+: Calcium

cAMP: Intracellular Cyclic AMP

Cl-: Chloride Channels

CTF: Corrected Total Fluorescence

Ent: Entorhinal Cortex

EPL: External Plexiform Layer

FFT: Food Finding Test

FPRs: Formylated Peptide Receptors

Gαi2: G protein G(alpha) i2

Gαo: G protein G(alpha) o

Gγ8: G protein G(gamma) 8

gl: glands

GL: Glomerular Layer

Golf: olfactory neuron specific-G protein

HMW: High Molecular Weight

IL-6: Interleukin-6

kDa: Kilodaltons

LPS: Lipopolysaccharide

lx: luxes

MeA: Medial Amygdala

MOB: Main Olfactory Bulb

MOE: Main Olfactory Epithelium

MOP: Medial Preoptic Nucleus

M/T: Mitral/Tufted

MRI: Magnetic Resonance Imaging
MCI: Mild Cognitive Impairment
MOS: Main Olfactory System
MPO: Medial Preoptic Nucleus
MUPs: Major Urinary Proteins
NSE: Non-Sensory Epithelium
OB: Olfactory Bulb
OBPs: Olfactory Binding Proteins
OE: Olfactory Epithelium
OMP: Olfactory Marker Protein
Ors: Olfactory Receptors
OSNs: Olfactory Sensory Neurons
OT: Olfactory Tubercle
PB: Phosphate Buffer
PBS: Phosphate Buffer Saline
PCNA: Proliferative Cell Nuclear Antigen
PCR: Polymerase Chain Reaction
PCx: Piriform Cortex
PFA: Paraformaldehyde
PLCo: Posterolateral cortical amygdaloid nucleus
PMCo: Posteromedial cortical amygdaloid nucleus
PS1, PS2: Presenilin 1, Presenilin 2
RT: Room Temperature
SCL: Supporting Cell Layer
Sox2: SRY-Box Transcription Factor 2
SVZ: Subventricular Zone
TBS: Tris Phosphate Buffer
Trpc2: Transient Receptor Potential Channel Trpc2
VNO: Vomeronasal Organ
VNS: Vomeronasal System
VSE: Vomeronasal Sensory Epithelium
VSNs: Vomeronasal Sensory Neurons
VRs: Vomeronasal Receptors
V1Rs: Type I Vomeronasal Receptors

V2Rs: Type II Vomeronasal Receptors

X-gal: X-Galactosidase

ABSTRACT

The sense of smell, known as olfaction, is greatly affected by age, with older individuals often experiencing a decline in their ability to smell. These deficits are typically permanent and can significantly impact their quality of life, eating habits, and may serve as early indicators of cognitive decline, and dementia. Despite their impact in life quality, we currently lack basic understanding regarding the effects of both natural and pathological aging on the ability to smell. A particularly intriguing category of olfactory information pertains to social odors, the disruption of which could potentially contribute to reduced social interactions and increased health issues.

Our study of the vomeronasal organ, which serves as the primary gateway for pheromone-encoded information, revealed distinct effects of both natural and pathological aging on the neurogenic capacity of the vomeronasal sensory epithelium. In an animal model of Alzheimer´s disease (double mutant APP/PS1 mice), cell proliferation largely remained intact, but naturally aged animals showed significant deficiencies in the number of mature, proliferative, and progenitor cells.

Our findings suggest that aging hinders the processing of social olfactory cues, leading to reduced exploration, discrimination, and habituation to social odors in both wild-type senescent mice (2-year-old) and in 1-year-old APP/PS1 mice. These changes may contribute to age-related difficulties in recognizing social cues and displaying social behaviors. As expected, social novelty was diminished in 1-year-old APP/PS1 mice, indicating that alterations in the processing of social cues occur more rapidly in pathological aging. This study unveils fundamental differences in the cellular processes through which natural and pathological aging disrupt the exploration of social information and social behavior.

RESUMEN

El sentido del olfato se ve afectado por la edad. Estos déficits olfativos suelen ser permanentes y pueden tener un impacto significativo en la calidad de vida y hábitos alimenticios, además de servir como potenciales indicadores tempranos de deterioro cognitivo y demencia. A pesar del impacto en la calidad de vida, actualmente desconocemos como el envejecimiento natural y patológico afectan a la función olfativa. Un tipo particularmente interesante de información olfativa implica la detección de olores sociales, cuya alteración podría afectar a la conducta social agravando otros problemas de salud.

Nuestro estudio ha analizado el efecto del envejecimiento natural y patológico sobre el órgano vomeronasal, un órgano sensorial especializado en la detección de feromonas. Nuestro trabajo ha identificado que los procesos de envejecimiento natural y patológico afectan de manera distinta la capacidad neurogénica del epitelio sensorial del órgano vomeronasal. De manera inesperada, se observó que la proliferación celular en un modelo animal de enfermedad de Alzheimer (EA; línea transgénica doble mutante APP/PS1) presentaba niveles similares a la de animales control, mientras que los animales envejecidos de manera natural mostraban deficiencias significativas tanto en el número de células maduras y en estado proliferativo, así como de células progenitoras.

A pesar de no identificarse efectos en la capacidad proliferativa del órgano vomeronasal, se observó una reducción significativa en el procesamiento de las señales olfativas sociales, indicado por una menor tasa de exploración, discriminación y habituación a los olores sociales en ratones APP/PS1 de 1 año, déficits que se encontraron exacerbados en comparación con la disminución de los mismos parámetros en ratones senescentes (2 años). Estas alteraciones en el reconocimiento de señales sociales podrían contribuir a déficits en la conducta social. Para comprobar esta hipótesis analizamos la sociabilidad y novedad social en animales envejecidos de forma natural y ratones APP/PS1 de un año mediante un test de tres cámaras. Nuestros resultados indican que a pesar de que la sociabilidad general no se encuentra alterada, existe una disminución muy

significativa de la novedad social en el modelo de Alzheimer. Este estudio revela diferencias fundamentales en los procesos celulares a través de los cuales el envejecimiento natural y patológico afectan a la exploración de información social, su procesamiento y, finalmente el comportamiento social.

1. INTRODUCTION

1.1. What importance does olfaction have in human life?

In humans, who mainly use visual signals for navigation, the sense of smell has historically been undervalued. However, olfaction plays an essential role as a defense mechanism and alertness (e.g., to detect harmful gases). In fact, it is reported that nearly 80 % of people with functional impairments in the olfactory system have faced a domestic accident commonly related to fire or spoiled food (Bonfils et al., 2008). Additionally, the sense of smell plays a crucial role in interpersonal relationships exhibiting high inter-individual heterogeneity (Hummel and Nordin, 2005).

Furthermore, olfaction is known to decline with age in humans, during both natural and pathological conditions. These alterations have been correlated with disease advancement in dementia patients, posing a risk factor for mild cognitive impairment (MCI) to progress to Alzheimer´s disease (AD). So, in addition to the contribution to overall quality of life, olfaction has gained attention as a potential predictive tool for neurodegenerative diseases, an aspect that will be discussed in section 1.7. of this Introduction.

1.2. Studying chemical communication in animal models to understand olfactory dysfunction in humans

In rodents, chemosensory systems play a critical role influencing various aspects of their behavior and survival. These sensory systems primarily involve the detection and interpretation of chemical cues from the environment, allowing mice to navigate, communicate, and make decisions essential for survival. Particularly, rodent social and reproductive behaviors heavily rely on communication using pheromones, secreted or excreted signals that commonly trigger innate behaviors in conspecifics (Karlson and Luscher, 1959).

In rodent species, both pheromones and olfactory cues related to social communication are detected mainly by the vomeronasal organ (VNO) (Halpern and Martínez-Marcos, 2003). Numerous studies have demonstrated the fundamental role of pheromonal detection in social and sexual behaviors in mice.

A good example involves the significant reduction of ultrasonic vocalizations in response to either female or female urine presentation in males in which the VNO was ablated (Wysocki et al., 1982).

While the VNO is considered to extend the complexity of chemosignal detection in some mammalian species, a potential functional role of the vestigial VNO-like structure found in humans remains controversial. Nonetheless, the neuronal structure surrounding the vestigial human VNO suggests a function, perhaps related to an enhancement of odor discrimination capabilities (Smith et al., 2014).

In parallel to other sensory systems, olfaction is known to decay with age. Olfactory impairments have been identified as one of the major sources of nutritional deficiencies and eating disorders in the elderly. These effects may be at the root of broader health complications ranging from immune deficits to depression. Importantly, olfactory deficits have been shown exacerbated and to appear early in the context of neurodegenerative disorders, mainly AD (Hummel and Nordin, 2005). Thus, we are in need to further investigate how both natural and pathological aging impact olfaction in order to gain basic knowledge which could lead to early diagnosis and/or therapeutic interventions for ameliorating neurodegenerative disorders.

1.3. Olfactory systems in mice

The olfactory systems in mice can be categorized into different subsystems based on various factors, including the location of their sensory neurons, the types of olfactory receptors, the signaling pathways to transmit chemosensory signals, the specific odors detected, and the connectivity of sensory neurons to the forebrain (Munger et al., 2009a). In rodents, the primary distinction lies between the main olfactory system (MOS) and the vomeronasal system, also called the accessory olfactory system (AOS) (Figure 1).

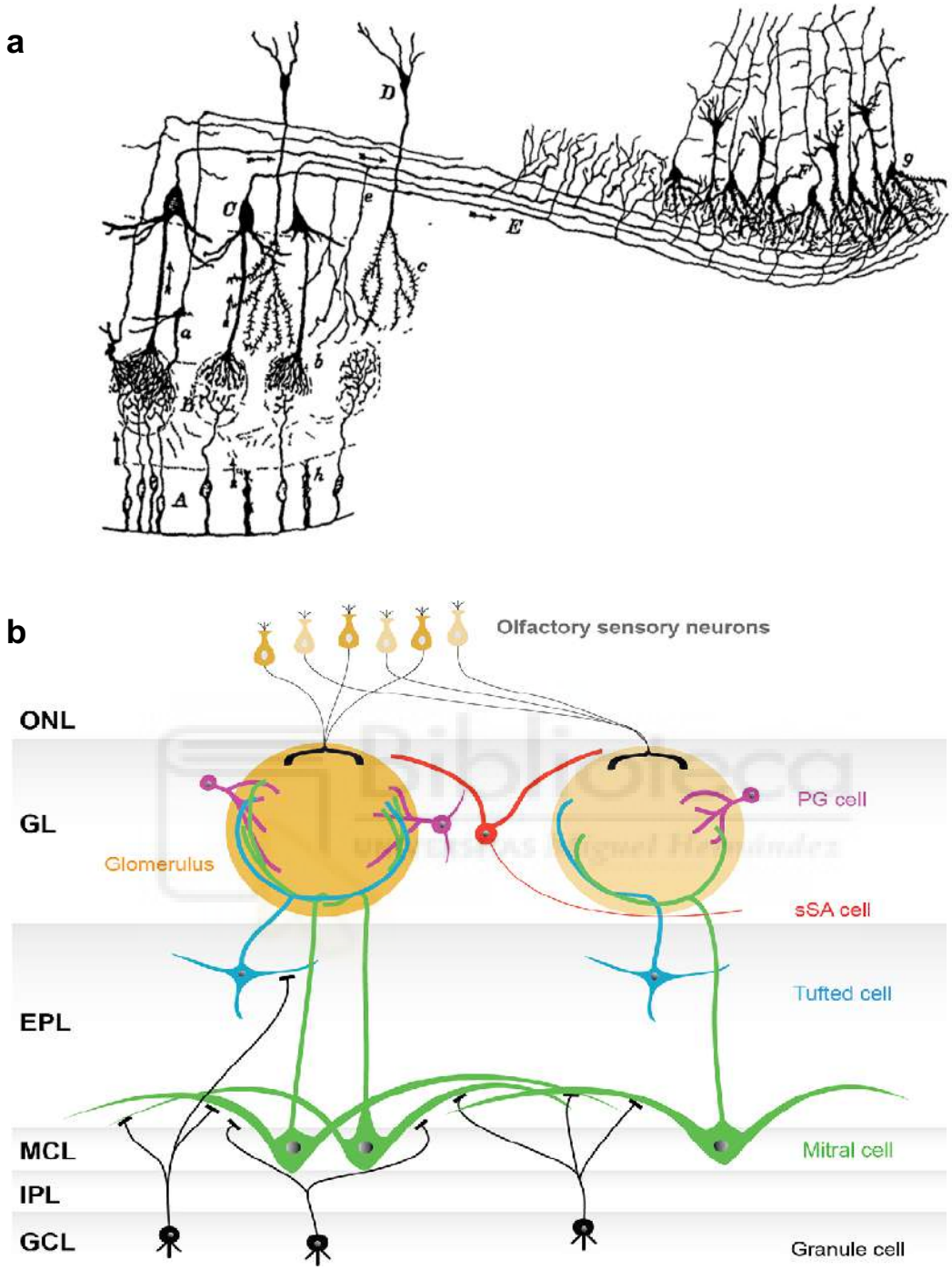

Figure 1. Basic models of the olfactory bulb (OB) network. **a**, Image used by Santiago Ramón y Cajal in his Croonian Lecture in 1894, showing the pathway that the olfactory information would take from the olfactory receptor cells (A), forming the glomeruli in the OB (B), to the mitral cells (C), whose axons would constitute the lateral olfactory tract (E), allowing the olfactory information to reach the olfactory cortex (F; figure adapted from Jones, 1994). **b**, Current basic model of the OB circuitry (adapted from Nagayama et al., 2014).

Throughout the 20th century, our comprehension of the olfactory system made significant advances, primarily driven by the emergence and optimization of molecular biology and physiology techniques. This progress reached a peak with the groundbreaking cloning of the olfactory receptors in the late 20th century. In recognition of their remarkable contributions to the field, professors Richard Axel and Linda Buck were awarded the Nobel Prize in Physiology and Medicine in 2004, for their pioneering research concerning the organization of the olfactory system. Their work led to the characterization of 18 distinct members of a multigene family responsible for encoding seven-transmembrane helical protein domains with highly selective expression in the olfactory epithelium. This discovery marked the identification of the first olfactory receptors (ORs) and provided a crucial step for understanding the intricacies of the olfactory system (Figure 2; Buck and Axel, 1991).

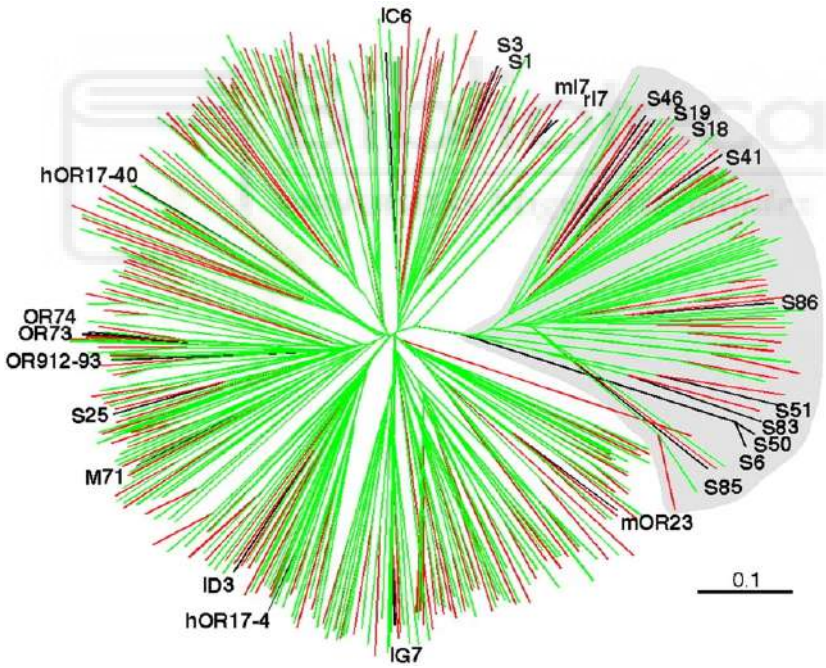

Figure 2. **The olfactory receptor gene family**. Comparison of mouse (green) and human (red) ORs subfamilies represented in a phylogenetic tree (adapted from Godfrey et al., 2004).

Thus, the MOS underlies the sense of smell and the mechanisms responsible for detecting and processing olfactory stimuli, playing a pivotal role in shaping behavior and physiology. It serves as a compass for animal actions, helping them locate food sources, recognize potential mates, and evade predators. Additionally, it exerts an influence on physiological responses, including

hormonal fluctuations and reproductive behaviors. Understanding the olfactory system in mice is essential for studying their behavior, including their food preferences, social interactions, and navigation abilities. Given the similarities between the rodent and human olfactory systems, mouse models of olfactory dysfunction may provide relevant insights for understanding pathological conditions.

1.3.1. Molecular mechanisms of odor perception

The perception of odors relies on the reception and coding by the sensory olfactory epithelium, located in the nasal cavity (Figure 3).

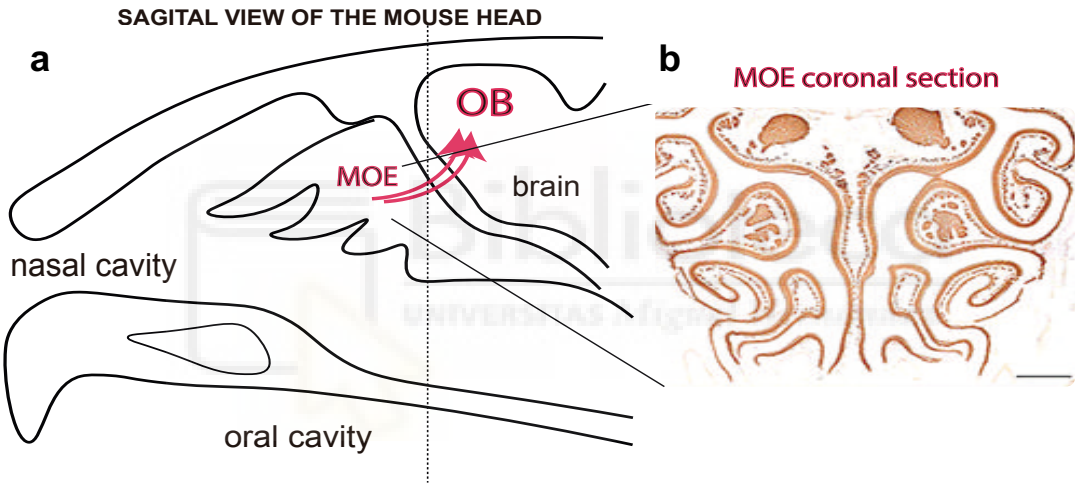

Figure 3. The Main Olfactory Epithelium (MOE). a, Olfactory Sensory Neurons (OSNs) in the olfactory epithelium detect and send their axons encoding sensory information to cells in the OB. **b**, Representative image of a transverse section of a mouse MOE stained with anti-OMP antibody (adapted from Barrios et al., 2014). Scale bar: 500 μm.

Volatile particles traverse the mucus before interacting with the ORs (Buck and Axel, 1991), located in the membrane of the dendrites of OSNs within the olfactory epithelium (Figure 4a). These receptors possess a highly variable region that provides them with substantial structural and functional diversity, constituting the domain where olfactory molecules bind (Katada et al., 2005).

The molecular and cellular machinery necessary for the transduction of olfactory stimuli is localized in the cilia of OSNs (Figure 4b). This process begins with the

specific binding of the olfactory molecule to distinct receptors on the outer surface of the olfactory cilia of OSNs. Due to the hydrophobic nature of most olfactory molecules, the stimulus-receptor interaction can occur directly or through proteins that facilitate the receptor assembly (i.e. OBPs, from Olfactory Binding Proteins) and also act as solubilizing agents (Breer, 2003), among other functions.

In mammals, the main signaling cascade involved in olfactory transduction utilizes cyclic nucleotides as second messengers. Commonly, the odorant molecule binds to the receptor, which is associated with a specific G protein of the olfactory system called G*olf*, activating a specific olfactory processing adenylate cyclase (ACIII), leading to an increase in intracellular cyclic AMP (cAMP) levels within milliseconds (Breer and Boekhoff, 1992). The increased intracellular cAMP activates ion channels, allowing the entry of sodium (Na^+) and calcium (Ca^{2+}), which in turn, activates chloride channels (Cl^-) that reduce the concentration of intracellular Cl^-. The resulting depolarization is passively transmitted from olfactory cilia to the axonal growth cone of OSNs, where action potentials are generated and transmitted to the OB (Figure 4a). The signaling cascade concludes when cAMP production ceases through feedback reactions (Mori and Yoshihara, 1994).

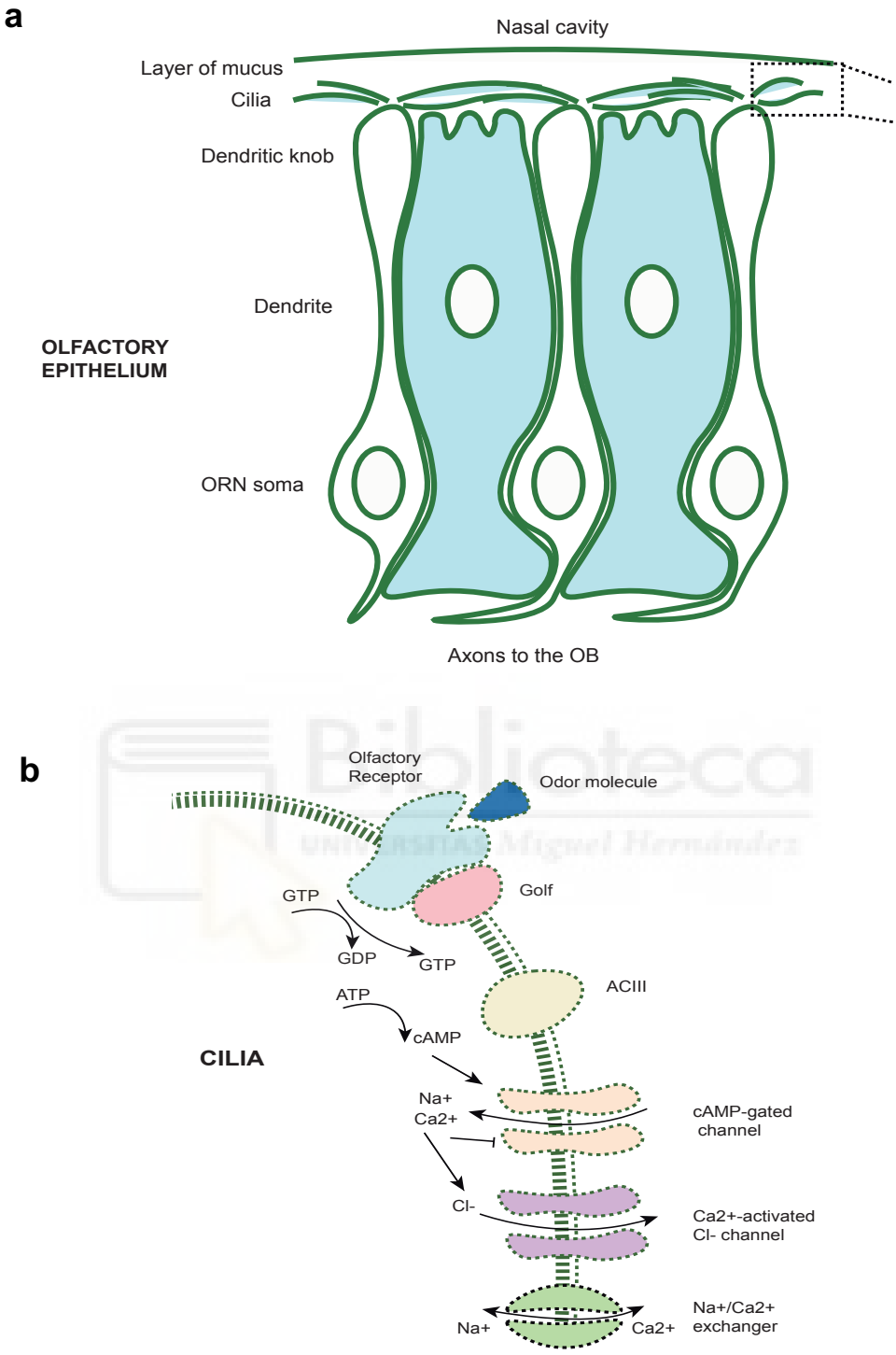

Figure 4. **Mechanism of olfactory transduction. a**, The detection of odorants in mammals is mediated by OSNs that reside in the olfactory epithelium of the nose. **b**, The molecular and cellular machinery necessary for the transduction of olfactory stimuli is localized in the cilia of OSNs.

1.3.2. OSNs enables adaptations to specific olfactory stimuli.

OSNs have mechanisms that enable them to work efficiently under various conditions. For example, these cells possess specialized features that allow them to be selectively triggered in response to olfactory cues, achieved through the precise configuration of cAMP-gated ion channels. Alterations in the concentration of specific odors can lead to changes in the timing, duration, and even the firing rate of OSNs. Consequently, each OSN can process specific information about the environment to higher brain centers, which integrate these diverse inputs to generate appropriate responses in different contexts (Kim et al., 2023).

Additionally, similar to other sensory receptors, OSNs exhibit mechanisms of habituation when continually exposed to the same odorant (Zufall and Leinders-Zufall, 2000). Olfactory adaptation becomes evident when an individual's capacity to identify or discriminate between odors diminishes after prolonged exposure to the same stimulus (Figure 5).

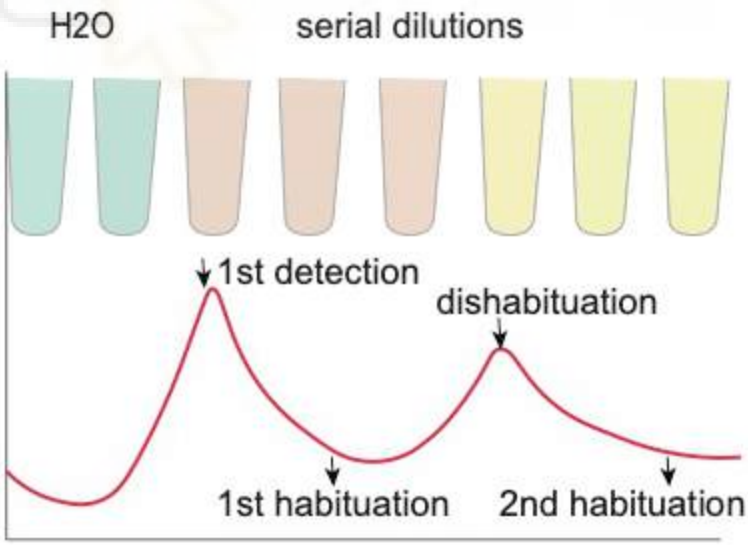

Figure 5. Social odor habituation-dishabituation test. The test is used in this study to evaluate the mice capability to detect and discriminate between similar social cues. Each odor is presented in three consecutive 1-minute trials with 1-minute intervals. An increase of exploration time when a new odor is presented for the first time (1st detection) indicates normal social discrimination. The plot illustrates an idealized response in response to two different social odors.

Physiologically, OSNs adaptation is characterized by a reduction in the frequency of action potential firing, primarily associated with a decrease in the sensitivity of ion channels to cAMP or the removal of Ca^{2+} through the activation of Na^{+}/Ca^{2+} exchange channels, which leads to a decline in receptor efficiency. Additionally, several studies have tested the impact of odor habituation on olfactory responses in mitral/tufted (M/T) cells and in the glomerular layer of the OB, resulting in a reduced M/T and glomerular response outputs (Chaudhury et al., 2010; Ogg et al., 2015), demonstrating that the olfactory system exhibits MOE-independent mechanisms to adapt to persistent olfactory stimuli.

1.3.3. Expression of receptors in the olfactory sensory epithelium

In the human olfactory system, 874 distinct receptors have been described, whereas in rodents, a more extensive repertoire of approximately 1483 receptors have been identified (Barnes et al., 2020). Each OSN exclusively expresses a single receptor, although each receptor exhibits the capability to bind with any odor that shares common molecular characteristics (Figure 6). Consequently, a single neuron can respond to a diverse array of odors, contributing to the intricate nature of smell perception (Duchamp-Viret et al., 1999). Additionally, odors can interact with several different receptors, depending on their molecular features, further amplifying the complexity of olfactory coding (Firestein, 2001).

The implication of an OSN expressing only one receptor type is that, among the roughly 20 million OSNs situated in the mouse's olfactory epithelium, we can distinguish approximately 1500 distinct OSN subpopulations (Barnes et al., 2020). In vertebrates, OSNs expressing a specific receptor are heterogeneously distributed and this distribution adheres to a spatial segregation pattern, with neurons arranged randomly within each zone. Therefore, in mice, approximately 4 or 5 discernible zones along the nasal cavity's anterior-posterior and medio-lateral axes have been identified (Sullivan et al., 1995).

1.3.4. Transfer of olfactory information to the main olfactory bulb

The axons originating from OSNs within the olfactory epithelium, all expressing the same receptor, project to one or two specific glomeruli situated in the main olfactory bulb (MOB). This arrangement gives rise to a highly structured olfactory spatial map, where different odors activate distinct MOB glomeruli (Mombaerts et al., 1996). Within each glomerulus, each OSN forms connections with a unique set of principal neurons responsible for transmitting information to other processing centers, such as the anterior olfactory nucleus (AON) (Miyamichi et al., 2011), the amygdala (Sosulski et al., 2011), and the piriform cortex (PCx) or olfactory cortex (Figure 6; Sosulski et al., 2011). Hence, the same group of principal neurons in the OB can adopt diverse roles in processing olfactory stimuli, contingent upon their postsynaptic targets and the organization of their projections (Kobayakawa et al., 2007).

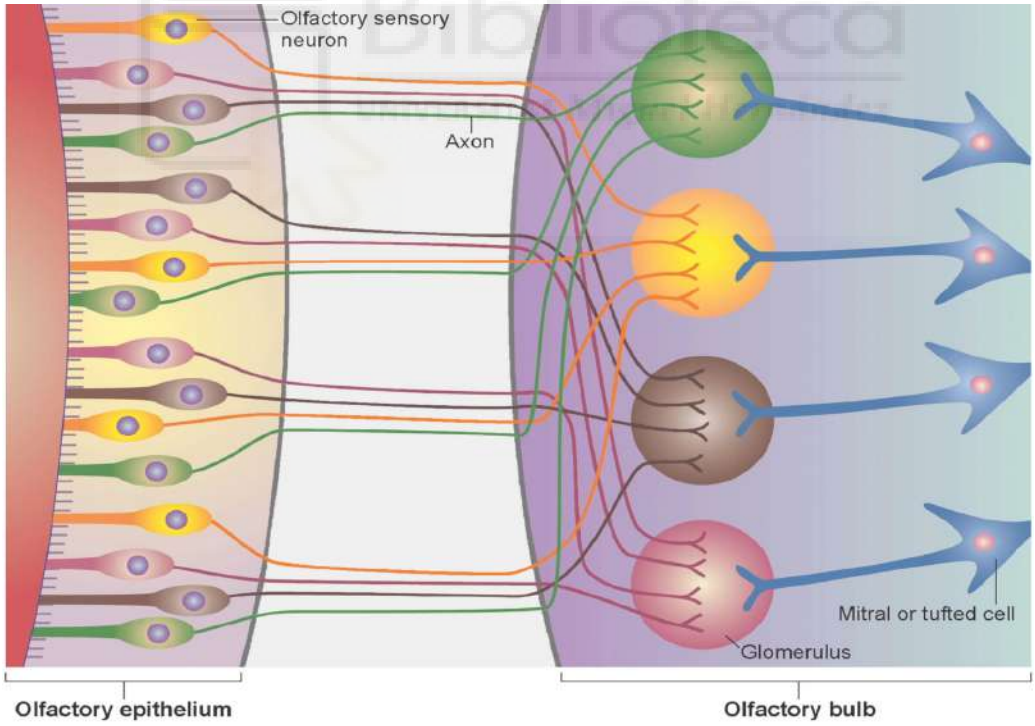

Figure 6. **The wiring scheme of the mouse olfactory system.** OSNs, characterized by the expression of different ORs, that are represented in different colors in the OE. OSNs expressing the same OR converge their axons into specific glomeruli within the olfactory bulb. Within these glomeruli, the axons of OSNs establish synapses with the dendrites of second-order neurons, which then extend their axons to the olfactory cortex (adapted from Mombaerts, 2006).

1.4. The vomeronasal system

In addition to the MOS, many mammals possess an AOS, commonly referred to as the vomeronasal system (VNS) (Brennan and Zufall, 2006; Dulac and Torello, 2003; Halpern and Martinez-Marcos, 2003). The VNS comprises three distinct components (Figure 7):

1. VNO: located at the base of the nasal septum, the VNO is a chemosensory structure containing vomeronasal sensory neurons (VSNs).

2. Accessory Olfactory Bulb (AOB): located within the caudal part of the OB, the AOB serves as the primary processing center for vomeronasal information originating from the VNO.

3. Higher-order olfactory and vomeronasal centers: these regions receive input from the AOB, either directly or indirectly, contributing to further processing of sensory information.

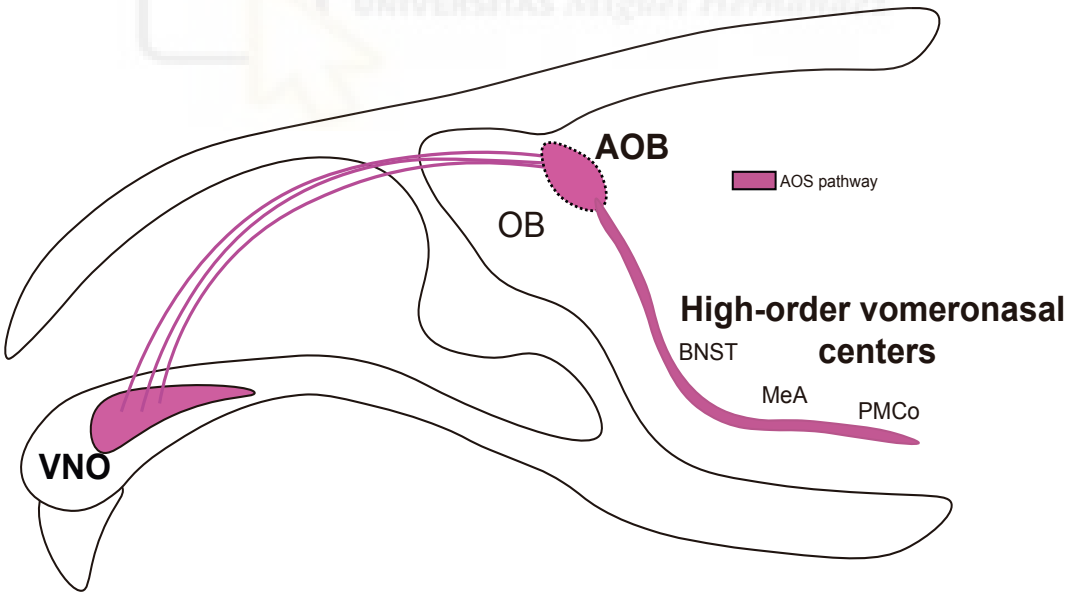

Figure 7. The vomeronasal and accessory olfactory systems. The VNS or AOS are constituted by: the VNO, the AOB and the high-order vomeronasal centers as for example the bed nucleus of the stria terminalis (BNST), the medial amygdala (MeA) and the posteromedial cortical amygdala (PMCo), among other regions.

The dual olfactory system, constituted by MOS and AOS, allows mammals to gather a broader spectrum of sensory information, enhancing their ability to perceive and respond to their environment and social context.

1.4.1. Localization and organization of the VNO

The VNO, first discovered by Ludvig Levis Jacobson in 1813, is a tubular structure located bilaterally and symmetrically in the anterior-ventral region of the nasal septum, situated near the vomer bone (Figure 8a). Along the anterior-posterior axis, the organ exhibits a distinctive vomeronasal duct extending along all its length. This duct terminates at the caudal end and opens into the nasal cavity at the rostral portion. The VNO is constituted by a pseudostratified epithelium containing bipolar sensory neurons, a supporting cell layer (SCL), an upper non-sensory epithelium (NSE), and a sensory epithelium (VSE), containing the VSNs (Figure 8b).

In addition to the vomeronasal duct, the organ possesses a blood capillary network. This vascular network facilitates the entry of chemical signals into the lumen of the vomeronasal duct, where they contact with the VSNs (Figure 8b). The arrangement and morphology of the vomeronasal duct can vary among different species, and in some cases, it may be difficult for chemical signals to gain access. Certain species, such as carnivores, ungulates, and other mammals, employ a mechanism called the Flehmen response to aid with the entry of these signals (Buzek et al., 2022). The Flehmen response is a voluntary reflex that facilitates the access of pheromones into the VNO (Figure 8c), that complements involuntary reactions like salivating when exposed to food.

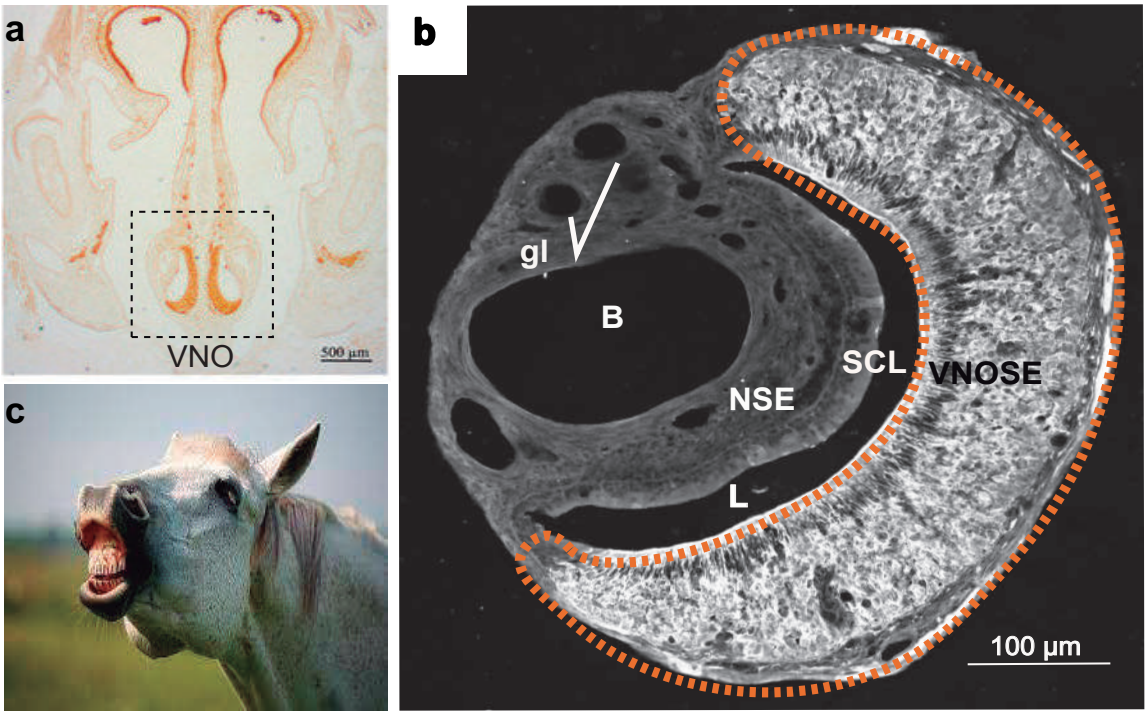

Figure 8. Structure and function of the VNO. **a**, the VNO is a bilateral structure located in the antero-ventral portion of the nasal cavity (adapted from Witt et al., 2018). **b,** The VNO contains a VSE and a NSE, including blood vessels (B) and secretory glands (gl). The VSE contains VSNs and supporting cells located within the SCL. **c**, Some mammals use the Flehmen response that allows a better access to the chemical cues (photo credit to Peter Meade). Scale bars: 500 µm; 100 µm.

1.4.2. Discovery and controversy regarding the VNO function

From a historical perspective, the role of the vomeronasal system has been a subject of controversy from its discovery. While it is believed that the first illustrations of the VNO in humans were made by Frederic Ruysh and Samuel Semmering (Ruysh, 1703; Semmering, 1809), the official discovery is attributed to Ludvig Levis Jacobson in his 1813 article (Jacobson, 1813). This is the reason why the VNO was initially referred as the "Jacobson's Organ." In his original article, Jacobson hypothesized about a possible sensory function of the VNO, which was later supported by morphological studies using Golgi staining techniques that revealed VNO's connections to a specific region in the OB, subsequently named the AOB (McCotter, 1912). The identification of the connection between the VNO and the AOB led to multiple speculative theories about the function of both structures during the first half of the 20th century (Johns

et al., 1986). Furthermore, the morphological similarities across different species indicated an evolutionarily conserved function in olfactory detection.

The controversy surrounding the VNO in humans is ongoing, and researchers continue to investigate its structure, and potential functions. While it is well-established that the VNO is present in the human embryo, it often appears to regress during fetal development, and by adulthood, it is considered to be vestigial. However, the absence of vomeronasal neurons and a vomeronasal nerve, indicates that the vomeronasal epithelium in adult humans is not a sensory organ, unlike in other mammals (Trotier et al., 2000; Meredith, 2001).

1.4.3. The Dual Olfactory Hypothesis

During the years 1955 to 1969, a series of experiments carried out by various research teams unveiled that specific cues present in urine could influence the reproductive physiology of mice (Lee and Boot, 1955; Whitten, 1956; Bruce, 1959; Vandenbergh, 1969). These findings sparked the hypothesis that the VNO might play a pivotal role in detecting these chemical signals collectively referred to as "pheromones". A prominent example of the role of pheromones is the drastic changes in female reproductive state and sexual behavior upon the detection of certain chemical signals. As such, male pheromones trigger stereotyped responses in females, such as lordosis, facilitating sexual contact. These signals also have enduring effects on endocrine physiology such as the Whitten and the Bruce Effects.

The Whitten Effect, observed primarily in certain mammalian species, particularly rodents like mice and rats, entails the synchronization or induction of the estrous phase in a group of previously non-estrus females when they are exposed to male pheromones. This phenomenon is believed to be an adaptation that enhances the reproductive success of males by increasing the likelihood of successful mating (Whitten, 1956). Conversely, the Bruce Effect describes the tendency of female animals to either terminate their pregnancies or delay implantation when exposed to the scent or pheromones of a new, unfamiliar male during the early stages of pregnancy. This adaptation is thought to have evolved

as a strategy for females to maximize their reproductive fitness by ensuring that their offspring are fathered by the dominant or resident male, rather than a newcomer (Figure 9; Bruce, 1959).

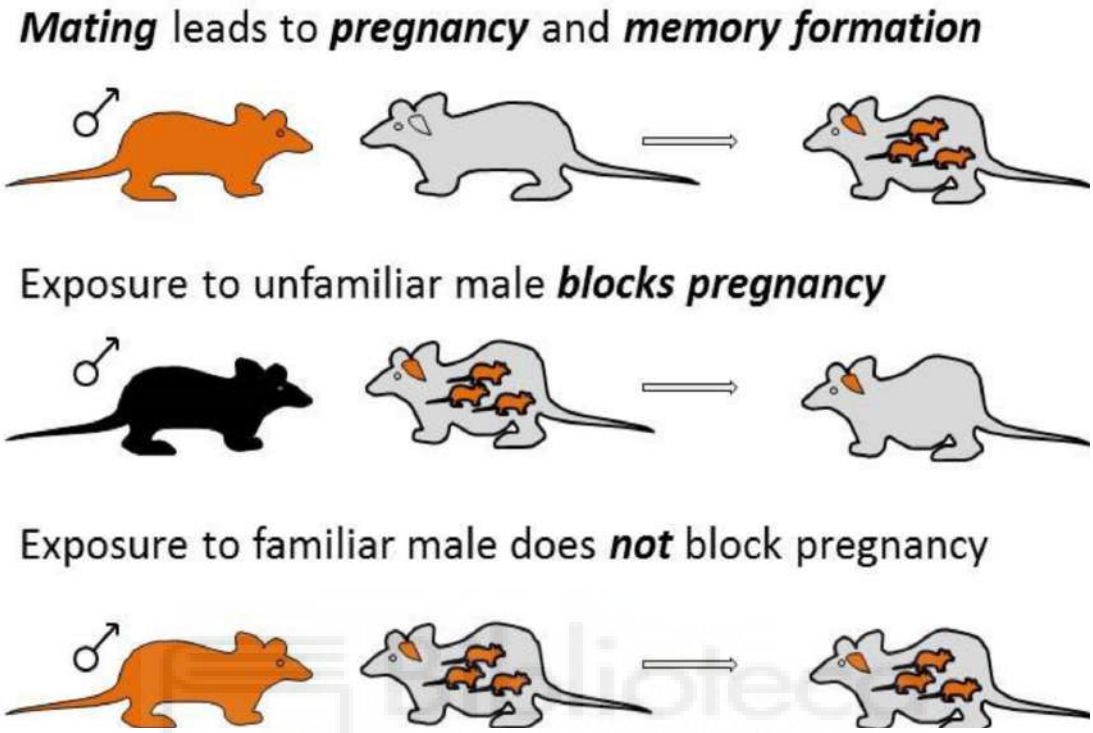

Figure 9. The Bruce Effect. If a pregnant mouse encounters an unfamiliar male, the likelihood of the pregnancy ending prematurely becomes significant (credit to Yoram Ben-Shaul).

Subsequent studies demonstrated that the male signals responsible for initiating both the female's ovarian cycles and preventing pregnancy were pheromones (Bronson, 1971; Gangrade and Dominic, 1984) secreted in the urine (Marchlewska-Koj, 1977). The relationship between the VNO, pheromone detection and socio-sexual behavior was further strengthen by the discovery of the VNO's role in the reproductive behavior of hamsters (Power and Winans, 1975) and its involvement in the ovulatory reflex mediated by signals in the urine of anovulatory rats (Johns et al., 1978).

By the end of the 20th century, the connection between the VNO and sexual as well as reproductive behaviors became increasingly evident (Wysocki, 1979; Halpern, 1987). Surgical lesions in the VNO removed essential olfactory-dependent neuroendocrine functions in female mice, including mate recognition, pregnancy block, facilitation of lordosis, puberty acceleration, and induction of

estrus (Kaneko et al., 1980; Lomas and Keverne, 1982; Jakupovic et al., 2008; Kelliher et al., 2006). Additionally, it was shown that the genetic inactivation of the transient receptor potential channel 2 (Trpc2), the primary sensory ion channel of the VNO, leads to various alterations in female reproductive behaviors, such as the absence of puberty acceleration, maternal aggression, lordosis, and an increase in male-like sex behaviors (Haga et al., 2010; Leypold et al., 2002; Kimchi et al., 2007; Hasen and Gammie, 2009). However, studies involving surgical VNO removal or Trpc2 elimination resulted in some discrepancies, including unusual mounting levels towards males, altered ultrasonic vocalizations, and sex behavior towards females (Pankevich et al., 2004). These studies helped to establish a functional link between the pheromone detection by the VNO and sexual behavior. However, this association was believed to be exclusive of the VNS, thought to be solely responsible for processing the sexual behavior of mammals (Belluscio et al., 1999; Buck, 2000; Dulac, 2000).

However, in the 1970s, it was first documented that the AOB formed connections with adjacent regions of the amygdala, previously considered exclusively olfactory (Winans and Scalia, 1970; Raisman, 1972; Scalia and Winans, 1975). These discoveries led to the proposal of the "dual olfactory hypothesis," positing the existence of two distinct pathways from the olfactory and vomeronasal epithelia to the forebrain. Each pathway was believed to be responsible for exclusive functions: the olfactory system for detecting odors and the vomeronasal system for pheromones.

1.4.4. Revision of the Dual Olfactory Hypothesis

The VNS has gained attention through a series of recent studies that have shown its pivotal role in chemical signal-based communication and social behaviors. However, the conventional dichotomy proposed by the Dual Olfactory Hypothesis, which once delineated the MOS as the main structure responsible for detecting volatile odors and the VNS for non-volatile pheromones, has had to be reconsidered (Kelliher, 2007).

Both of these systems exhibit significant overlap and complementarity in their functions, from the range of stimuli they can discern to the subsequent behavioral or physiological effects they can elicit (Brennan and Zufall, 2006; Zufall and Leinders-Zufall, 2007). Furthermore, VNO's function is orchestrated by independent subsystems that originate in specific subpopulations of the VSNs, which stand apart in their molecular and functional attributes (Ackels et al., 2014; Akiyoshi et al., 2018).

1.4.5. Vomeronasal Receptors

In 1995, Catherine Dulac and Richard Axel marked a pivotal moment in our understanding of the VNS by describing a family of genes encoding vomeronasal receptors (VRs; Dulac and Axel, 1995). Two years later, three separate research groups independently identified a second family of these receptors (Herrada and Dulac, 1997; Matsunami and Buck, 1997; Ryba and Tirindelli, 1997). The gene families code for receptors characterized by seven transmembrane domains coupled with G proteins and were named as type I vomeronasal receptors (V1Rs) and type II vomeronasal receptors (V2Rs). Within the last decade, an additional family of vomeronasal receptors has emerged, specifically represented by five out of the seven members of the formylated peptide receptor (FPRs) family expressed in the VSE (Figure 10; Liberles et al., 2009).

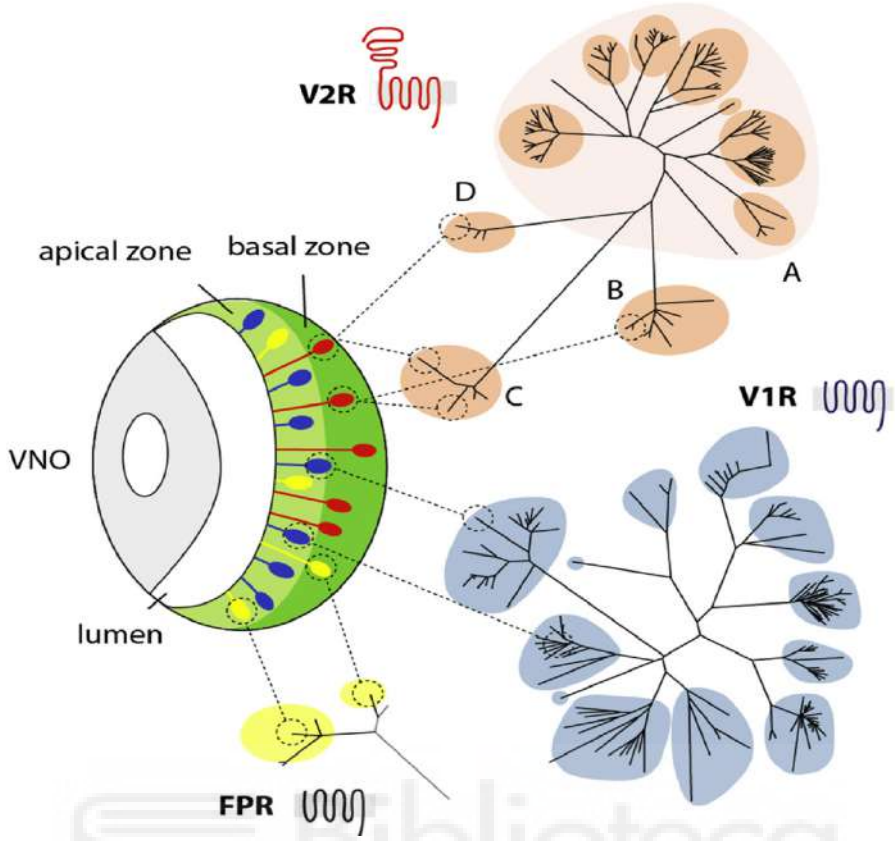

Figure 10. The vomeronasal receptor family. Each sensory neuron expresses a sole V1R or FPR gene, and conversely, two V2R genes that can be transcribed in every cell (adapted from Rodríguez, 2016).

The structural and functional features of the VNO in various species are linked to the distribution and heterogeneity of these VRs. Interestingly, in rodents, lagomorphs, and didelphimorphs, the VSE is divided into two distinct neuronal layers based on the expression of specific receptors and G proteins. The VSNs situated in the apical region of the epithelium express Gαi2 proteins, while those in the basal region express Gαo (Figure 11; Dulac and Axel, 1995; Riviere et al., 2009). These two primary populations of VSNs may concurrently express all three families of VRs together with Gαi2 and/or Gαo. Typically, VSNs in the apical zone express V1Rs in conjunction with Gαi2, while VSNs in the basal layer express V2Rs and Gαo (Halpern and Martinez-Marcos, 2003).

Conversely, FPRs interact with both types of G proteins: FPR-rs3, FPR-rs4, FPR-rs6, and FPR-rs7, primarily act through Gαi2, while FPR3 primarily couples with Gαo (Liberles et al., 2009; Riviere et al., 2009). Additionally, VSNs express G

proteins consisting of gamma (γ) subunits in a differential manner: neurons in the apical layer express G proteins with various types of gamma subunits, while basal VSNs exclusively express Gγ8 proteins (Sathyanesan et al., 2013).

Furthermore, this distinct regionalization within the vomeronasal epithelium is mirrored in the AOB: the apical sensory neurons of the VNO project their axons to the glomeruli in the rostral half of the AOB, while the basal neurons do so in the caudal portion (Figure 11). While the functional implications of this spatial segregation remain elusive, certain mammalian species, including wallabies, tamarins, and goats, possess a uniform VSE (Takigami et al., 2000; Takigami et al., 2004; Schneider et al., 2012). Recently, significant progress has been made in identifying specific ligands that bind to each of these zones, bringing us closer to unveiling the molecular and functional mechanisms that underlie this anatomical division in the VSE (Fu et al., 2015).

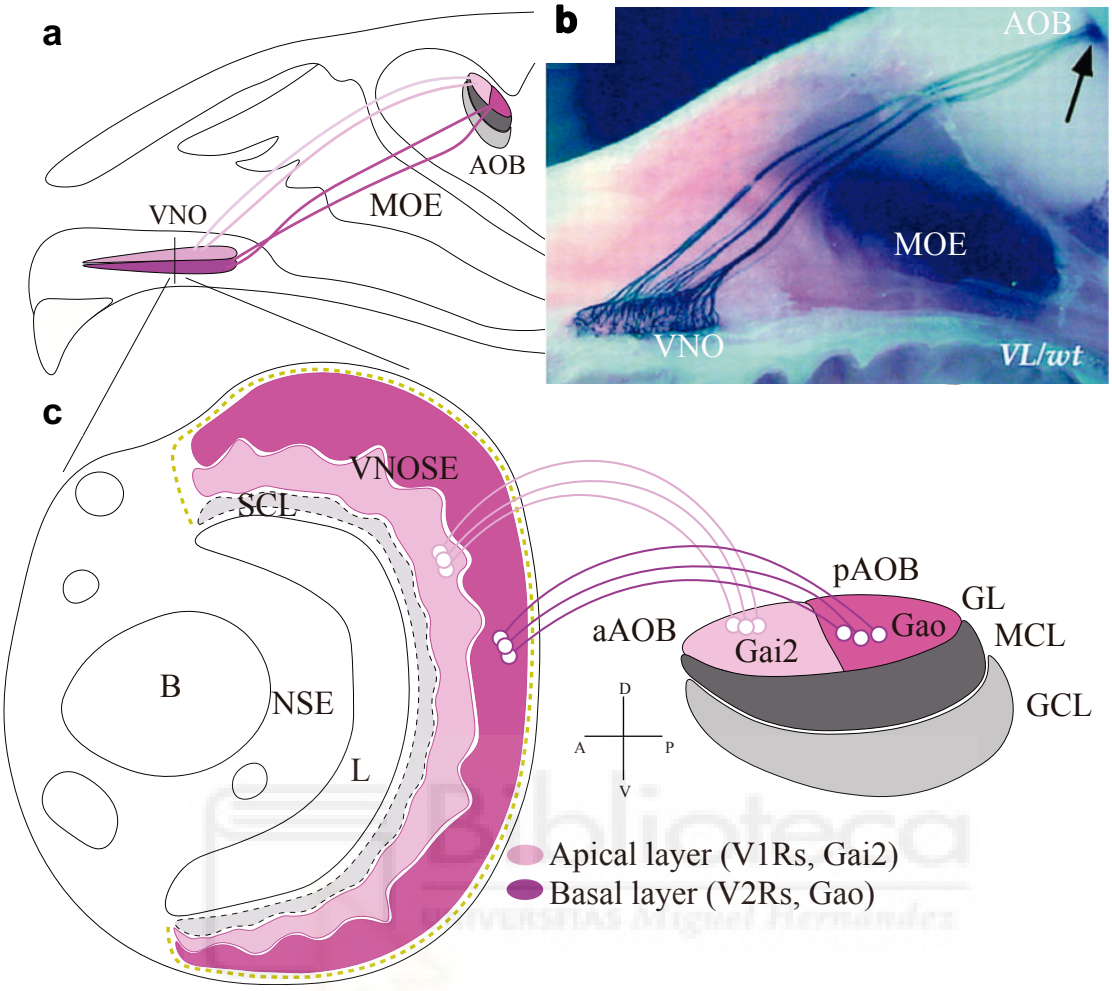

Figure 11. **The VNO exhibits specialized regions**. **a**, diagram depicting a parasagittal view of a mouse's nose, highlighting the VNO and its connection to the AOB. **b**, parasagittal section displaying the VNO's projection to the AOB using X-gal staining (adapted from Rodríguez et al., 1999). **c**, distinct neural circuitry composed of VSNs expressing V1R and V2R.

1.4.6. The functions of the VNO arise from the specificity of its VRs.

VRs exhibit specificity for certain ligands: V1Rs recognize volatile molecules and steroids, while V2Rs preferentially bind to peptides and proteins (Fu et al., 2015). This VRs specificity suggests that they could be involved in the encoding of different information (Isogai et al., 2011; Pérez-Gómez et al., 2014).

However, the majority of pheromone-mediated behaviors are not solely dependent on the sensory transduction initiated by either V1Rs or V2Rs. Instead,

these behaviors often emerge from cooperative or complementary interactions between both pathways, and frequently involving the MOS. This intricate interplay complicates the assignment of specific functions to V1Rs and V2Rs.

In addition to their role in regulating social interactions with conspecifics, V1Rs and V2Rs have been implicated in mediating aversive behaviors such as predator recognition and the detection of toxic substances (Chandrashekar et al., 2000). Interestingly, the VNO plays an important role in triggering aversive responses to infected individuals by detecting molecules associated with pathogenic microorganisms (Boillat et al., 2015). These functions are mediated by the FPRs, that are also found in the immune system, contributing to innate immunity by recognizing molecules involved in inflammatory processes (Riviere et al., 2009; Bufe et al., 2012; Weiss and Kretschmer, 2018). Furthermore, it has been observed that this response can be exceptionally specific, as VSNs expressing the FPR3 receptor only respond to signal peptides from bacterial proteins, which alone are sufficient to trigger aversive behaviors in mice (Bufe et al., 2019).

1.4.7. VSNs exhibit a strong preference for the molecules found in urine.

In numerous studies of the MOS, diluted urine is commonly used as a stimulus to study the activation of VSNs (Leinders-Zufall et al., 2000; Spehr et al., 2002; Stowers et al., 2002; Cichy et al., 2015), resulting in activation of approximately 30-40 % of VSNs (Figure 12; Chamero et al., 2017).

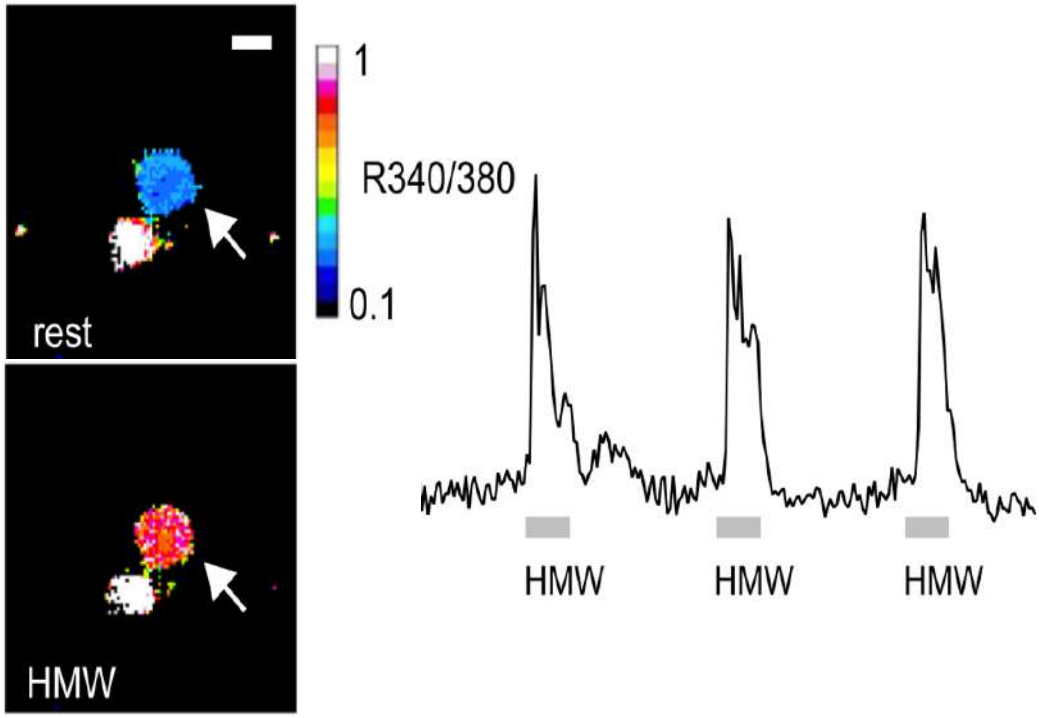

Figure 12. Fura-2 calcium imaging performed on *in vivo* dissociated VSNs. Examples of VSNs using fura-2 (left; R340/380 ratio images), along with time sequences illustrating cytosolic calcium transients induced by a high molecular weight (right; HMW) urine fraction (diluted at 1:300; adapted from Chamero et al., 2017).

At the beginning of this century, the urine molecules capable of activate VSNs *in vitro* were identified (Leinders-Zufall et al., 2000; Novotny, 2003) and tested behaviorally to elicit robust physiological responses, including the induction of estrus and the acceleration or delay of puberty (Sam et al., 2001). More recently, it has come to light that a specific subset of VSNs exhibits a preference for molecules of molecular weight exceeding 10 kDa, such as Major Urinary Proteins (MUPs), which, in turn, activate distinct VSNs subpopulations (Chamero et al., 2007; Chamero et al., 2011). Additionally, it has been noted that distinct VSNs subpopulations exhibit selective responses depending on the sex and individual characteristics of the animal whom the urine sample originates, potentially serving as a molecular mechanism for individual recognition (He et al., 2008; Wyatt, 2017).

The present study relies on this well-documented evidence, and has implemented urine presentation to elicit VNO stimulation.

1.4.8. Transmission of olfactory and pheromonal information to higher-order processing centers

The OSNs and VSNs in the MOE and VSE send sensory information to the MOB and to the AOB, respectively. OBs serve as intermediaries for transmitting sensory information to higher-level processing centers through at least two separate pathways. Principal neurons in the MOB, including mitral and tufted cells, project their axons to various cortical and limbic areas, encompassing the PCx, cortical amygdala (ACo), and olfactory tubercle (OT). In contrast, principal neurons in the AOB convey information to limbic system regions, such as the vomeronasal amygdala and the BNST, as well as to PMCo (Figure 13; Bellver et al., 2017). Notably, despite these anatomical distinctions, both olfactory systems contribute to mediating and processing olfactory and social behaviors in rodents.

1.4.9. Convergence between the MOS and VNS

While the MOS and VNS are two distinct sensory systems with different pathways, they exhibit convergence within specific brain nuclei, such as the BNST and the MeA, along with other hypothalamic regions like the medial preoptic nucleus (MPO) and paraventricular areas (Figure 13; Pérez-Gómez et al., 2015). It is known that several behaviors mediated by pheromonal stimuli, which are typically altered by genetic deletion of vomeronasal genes, are also abolished by the deletion of olfactory genes (Stowers et al., 2002; Mandiyan et al., 2005). These findings indicate that the processing of chemical cues exhibits redundancy, particularly in the integration of aversive signals from predators (Liberles, 2015; Brechbuhl et al., 2008; Pérez-Gómez et al., 2015; Moine et al., 2018).

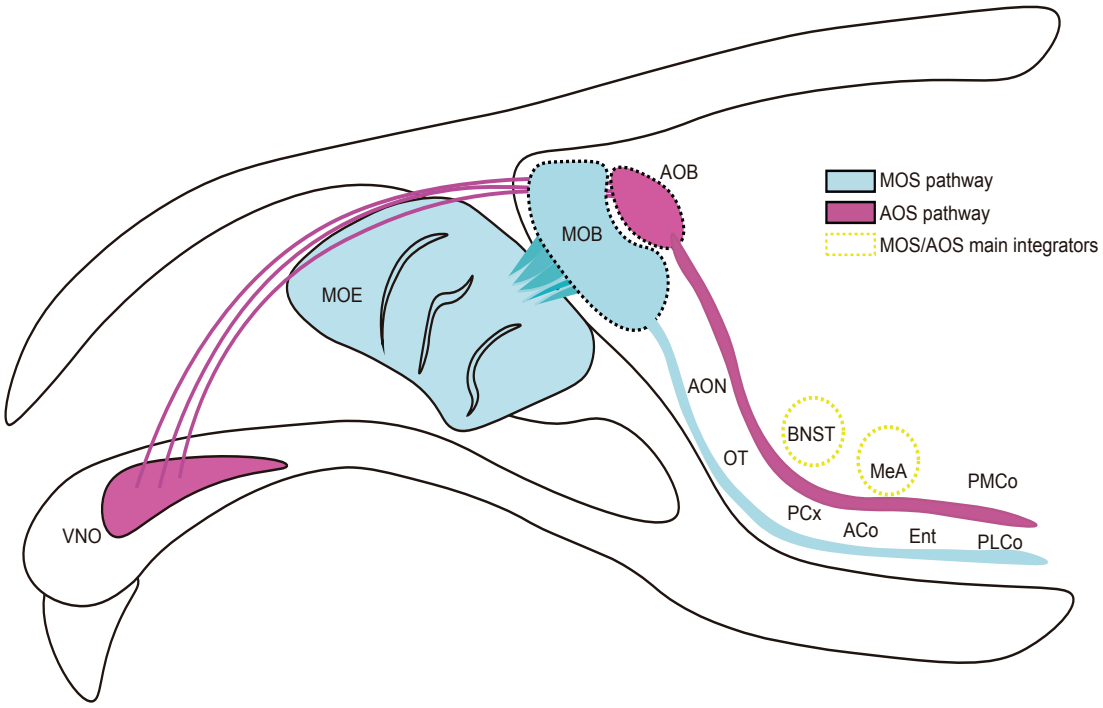

Figure 13. **Neuronal pathways mediating learned and innate olfactory behaviors**. Olfactory information (in blue) from the MOE is transmitted to the MOB and then is further processed in higher brain regions, including the AON, PCx, Ent, OT, PLCo and ACo. Information reaching the vomeronasal system (in purple) is relayed from the vomeronasal organ to the AOB and from there to the medial amygdala MeA, the BNST and the PMCo. Both pathways predominantly converge in the BNST and MeA (in yellow).

1.5. Pathology of the olfactory systems

Olfactory function impairments are a prevalent symptom in the elderly population, and their frequency and intensity notably rise with age. However, there is a limited understanding of the fundamental cellular and molecular mechanisms responsible for this phenomenon (Mobley et al., 2014). Given that olfactory dysfunction is closely linked with various neurodegenerative conditions, it has been explored as a clinical marker for AD, MCI, Lewy body diseases (including Parkinson's disease) frontotemporal dementia, Huntington's disease and a wide group of neurological disorders (Doty, 2014; Doty and Kamath, 2014; Hawkes, 2006). Disturbances in the sense of smell are not uncommon: approximately 4-6 % of the general population experience a complete loss of smell, referred as anosmia, with prevalence rates reaching 14 % in individuals over 65 years-old

(Schubert et al., 2012). In those aged between 65 and 80, the prevalence exceeds 50 %, and it skyrockets to 80 % in those over 80 years-old (Doty and Kamath, 2014).

As olfactory dysfunction can manifest early in neurodegenerative diseases, it serves as an early clinical sign indicating the onset of neurodegenerative disorders and cognitive decline (Doty et al., 1991; Devanand et al., 2000; Doty, 2012; Gallarda and Lledo, 2012). Olfactory impairment significantly affects quality of life by influencing the physical and psychological health and is linked to the development of anxiety, depression, and a higher mortality rate (Wilson et al., 2011). Multiple underlying causes of olfactory dysfunction have been identified, including several structural and functional alterations at various levels of the olfactory system, from the olfactory epithelium to the entire olfactory system (Doty and Kamath, 2014). Declined ability to identify odors in old age has practical implications for daily activities, as it has been correlated with diminished cognitive function and a decline in episodic memory (Wilson et al., 2006). Consequently, olfactory function may serve as a valuable indicator of the overall health of the aging brain. Regrettably, many clinicians often overlook the symptomatic significance and potential preclinical value of olfactory dysfunction (Alves et al., 2014).

1.5.1. Natural olfactory dysfunction in aged humans

A significant proportion of the elderly population, exceeding 75 % among those aged over 80 years, exhibit symptoms or signs indicative of pronounced olfactory dysfunction (Boyce and Shone, 2006), with approximately 5 % experiencing anosmia (Figure 14; Landis et al., 2004). These olfactory alterations often give rise to various challenges, adversely affecting overall quality of life for many individuals (Hummel and Nordin, 2005).

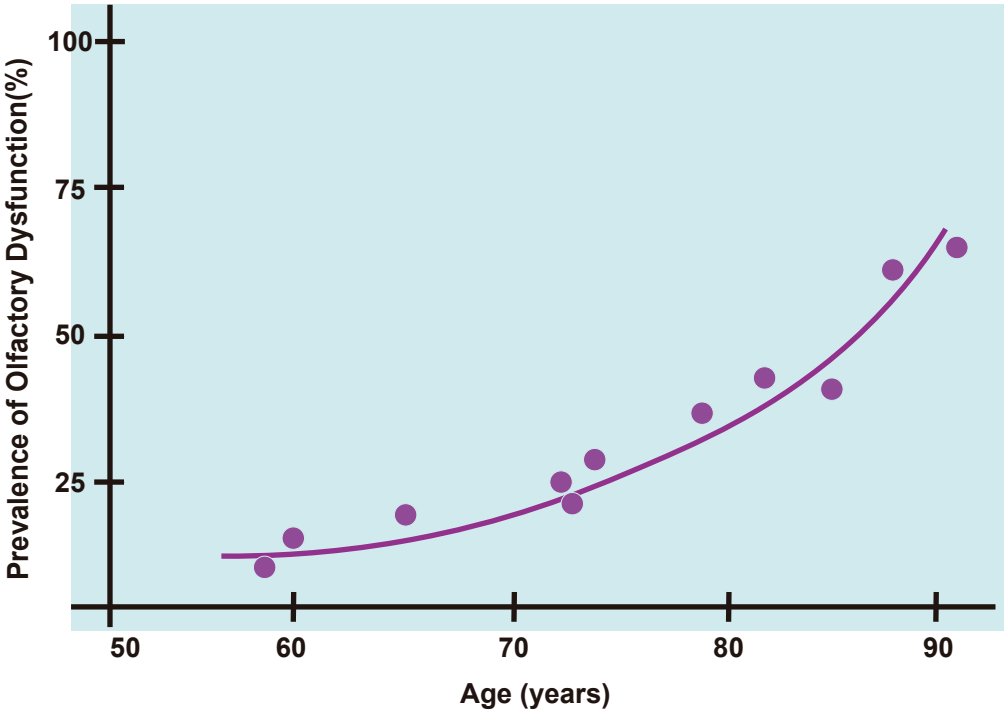

Figure 14. Prevalence of olfactory dysfunction in healthy individuals aged 60 years-old and older (adapted from Dan et al., 2021**).**

Concretely, age-dependent olfactory impairment alters the capacity of detection, perception, discrimination, and memory:

1.5.2. Olfactory detection deficits

The olfactory detection threshold represents the lowest concentration of an odorant required for an individual to perceive a scent. Studies indicate that this threshold for specific non-social odors, such as isoamylacetate, rose oil, and eugenol, begins to increase after the age of 60 and further escalates in individuals over 80 years-old (Figure 15; Kaneda et al., 2000). Aging also leads to a reduced perception of odor intensity at concentrations above the detection threshold (Stevens et al., 1982). However, these changes are contingent on the specificity of odor stimulus (Wysocki and Gilbert, 1989) and may vary among individuals (Stevens and Cain, 1987).

1.5.3. Olfactory discrimination deficits

Olfactory discrimination tests assess an individual's ability to differentiate between various odors. These evaluations typically involve presenting odors sequentially to determine if individuals perceive them as matching scents. When employing very similar odors, the test becomes more demanding. Consequently, in its most complex form, a decline in olfactory discrimination performance becomes evident with advancing age, particularly in individuals aged 60 and older (Figure 15; Kaneda et al., 2000).

Moreover, the capacity of humans to discriminate odors is notably superior in young adults (up to approximately 25 years-old) compared to children under 15 years-old. This suggests that olfactory discrimination skills may undergo a maturation process influenced by experience. These abilities undergo a modest decline until the age of 55, after which a more pronounced deterioration becomes apparent (Hummel and Welge-Luessen, 2006).

1.5.4. Olfactory identification deficits

The UPSIT (University of Pennsylvania Smell Identification Test), recognized as the worldwide benchmark for olfactory assessments, consists of presenting and identifying approximately 40 distinct scents. For each sample presented, there are multiple-choice response options (Doty et al., 1984). This test offers insights into the extent of olfactory loss, covering a spectrum from total anosmia to mild hyposmia or microsmia (Figure 15).

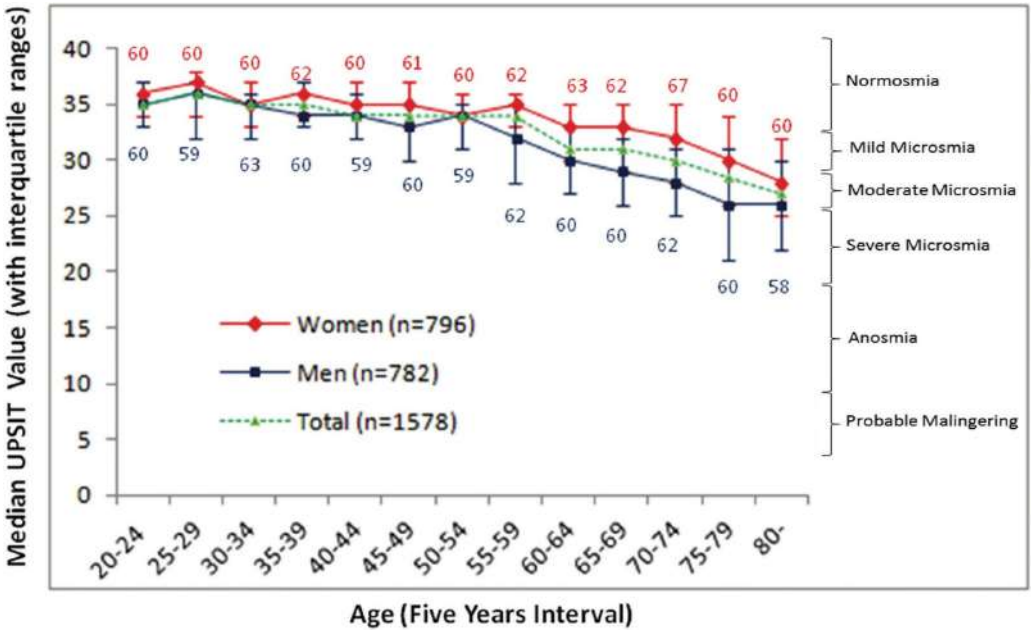

Figure 15. **Representation of the scores obtained in the UPSIT test and their relationship with the age and sex of the participants** (adapted from Fornazieri et al., 2014).

This assessment has revealed that the ability to identify odors peaks between the ages of 20 and 40, but then declines after the age of 60 (Figure 16). Additionally, there are subtle sex differences, with women generally outperforming men. Furthermore, it has been noted that olfactory dysfunction may not be detected in response to unpleasant or aversive odors (Konstantinidis et al., 2006), indicating a critical role of the odor's perceived valence.

1.5.5. Olfactory memory deficits

Olfactory memory involves the recall of a particular odor or a sequence of odors over time. Methods to assay this particular type of memory typically involve initially presenting a group of odors, and after a specified time interval, reintroducing these odors along with others that were not previously presented.

In the most commonly used version of this test, individuals must name an odor they had previously perceived. As people age, their performance in this test tends to decline (Murphy et al., 1991). To successfully complete the test, individuals must not only have well-preserved episodic olfactory memory but also rely on

semantic memory to verbally identify the odor (Murphy et al., 1997). Experiments conducted in the late 1990s examined the short-term and long-term retention of a series of odors paired with verbal descriptors. These studies revealed that older individuals exhibited less accurate recall of both odors and associated words, with a more noticeable decline in odor memory (Murphy et al., 1997). The deficits observed in odor identification with age might result from a dual cognitive decline affecting both semantic memory and olfactory sensory memory (Choudhury et al., 2003).

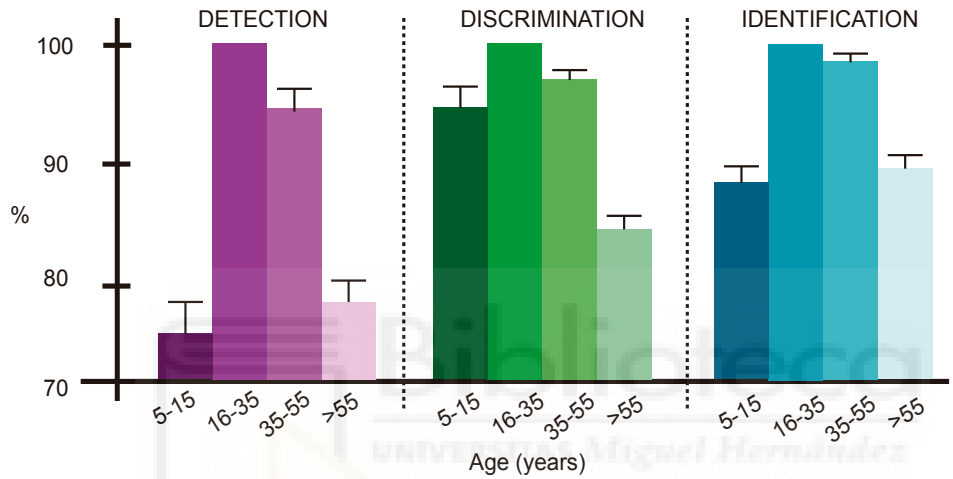

Figure 16. Olfactory detection, discrimination, and identification abilities are altered during natural aging in humans. Data is expressed as percentages relative to the values of the group with the best performance (16-35 years-old) (adapted from Hummel et al., 2006).

1.6. Animal models to study AD: the APP/PS1 transgenic mice

Some of the insights gained from studying olfactory dysfunction come from research in AD patients, that have also been replicated in animal models of AD. Interestingly, early-onset AD is primarily triggered by mutations in the presenilin (PS1, PS2) and/or Amyloid Precursor Protein (APP) genes. In contrast, late-onset AD may be linked to apolipoprotein E alleles (Ferencz and Gerritsen, 2015). However, both forms of AD exhibit similar neuropathological features involving the accumulation of amyloid beta deposits (Aβ; Huang and Mucke, 2012). Diverse transgenic mice models have been generated to explore specific aspects of AD progression (Braidy et al., 2012; Webster et al., 2014).

Among these models, the APP/PS1 double transgenic mouse line has been widely utilized to explore the cognitive deficits associated with AD, displaying a gradual age-related progression of Aβ accumulation (Jankowsky et al., 2001; Janus et al., 2015), due to the overexpression of amyloid APP and PS1 genes. The APP/PS1 mouse model was shown to exhibit notable cognitive impairments (Huang et al., 2016). Impaired spatial memory and reduced cognitive flexibility are commonly observed in this animal model, reflecting the impact of amyloid pathology on neural circuits associated with memory and cognition (Huang et al., 2016).

Interestingly, few studies have explored social behavior in this animal model with some evidence pointing to social deficits and disrupted social recognition, suggesting a correlation between the accumulation of amyloid plaques and alterations in social behavior. Thus, understanding the social deficits in the APP/PS1 mouse model not only provides insights into the progression of AD but also offers a new perspective to explore the emotional symptoms of the disease.

1.7. Causes of olfactory dysfunction

Olfactory dysfunction is a heterogeneous condition with a wide spectrum of severity, ranging from the mildest form called hyposmia to the complete loss of smell (Daramola and Becker, 2015). In some cases, olfactory impairment can manifest as the perception of odors in the absence of any stimulus (phantosmia) or as a distorted perception of odors when a stimulus is present (parosmia) (Scangas and Bleier, 2017). The fact that olfactory dysfunction is a common symptom in various mental diseases suggests that it likely arises from a combination of genetic and environmental factors including exposure to pathogens and lifestyle habits (Daramola and Becker, 2015).

The decline in olfactory function seen in older individuals may be associated with structural changes of the nasal cavity and the associated brain regions (Doty and Kamath, 2014). In addition to general challenges, such as infections, age-related deterioration of nasal epithelium, reduced blood flow in the nasal mucosa, decreased foramina in the cribriform plate, and cilia function impairment, there

are specific alterations that specifically target the olfactory system such as: (1) alterations in the OE, (2) alterations in the OB, (3) changes in the brain regions responsible for processing olfactory information and (4) chronic brain inflammation.

1.7.1. Age-related OE alterations

Age-related alterations involve a reduction and adjustments in the number of ORs, thinning of the sensory epithelium and the substitution of olfactory tissue with respiratory tissue. These changes are driven by shifts in cell turnover, the necrosis of OSNs due to an age-related decrease in the size and quantity of holes in the cribriform plate, as well as the impairment of critical immunological and enzymatic defense mechanisms essential for maintaining the integrity of the OE. Additionally, age-related decreases in the specificity of OSNs and exposure to airborne environmental agents, including air pollution or cigarette smoke, may contribute to these modifications. Both environmental factors and genetic predispositions may influence the extent of olfactory function in aged individuals (Doty et al., 2011).

Immunohistochemical examinations of the OE have revealed the presence of Aβ and tau pathology within OE cells, as well as dystrophic neurites, which are observed in both neurologically normal elderly individuals and those with AD (Arnold et al., 2010). Finally, one of the prominent features of the OE is its remarkable ability to regenerate OSNs through the differentiation of neural stem cells situated in the basal part of the epithelium (Sultan-Styne et al., 2009). As individuals age, some authors have demonstrated a substantial decline in its regenerative capacity, which correlates with the typical age-related decline in the sense of smell (Doty and Kamath, 2014; Mobley et al., 2014).

1.7.2 Age-related OB alterations

With advancing age, both humans and rodents experience a reduction in the size of the OB and a decrease in the volume of its layers. This phenomenon is a result of overall atrophy, neuronal loss, and an increase in glial cells. Age-related

decrease in OB volume has been detected using magnetic resonance imaging (MRI) in living subjects (Buschhuter et al., 2008). Interestingly, these reductions are not exclusive to aging but can occur under various conditions, including smoking, chronic sinusitis, multiple sclerosis, head trauma, and schizophrenia (Doty and Kamath, 2014).

In APP/PS1 transgenic mice, a significant decrease in the labeling of somatostatin and calretinin interneurons has been described in the OB (Saiz-Sanchez et al., 2013). Moreover, recent studies demonstrated an increased susceptibility to cellular apoptosis in the OE compared to control littermates in the APP/PS1 mice (Cheng et al., 2011). Altogether, these data indicate that elevated Aβ production leads to reduced neurogenesis in the subventricular zone (SVZ) in APP/PS1 mice (Haughey et al., 2002), further suggesting that neural replacement and migration to olfactory areas might be impaired in AD.

Interestingly, a study employing an early transgenic mouse model of AD (Tg2576/APP mice that overexpress a mutated form of human APP), revealed a clear correlation between the decline in olfactory perception and the accumulation of Aβ in the olfactory system (Wesson et al., 2010). This study showed that the deposition of Aβ peptides in the OB was observed before it occurred in any other region, a fact that supports the notion that the damage of the OB may precede the effect over other brain regions (Wesson et al., 2010).

A remarkable property of the OB is the presence of active adult neurogenesis. OB interneurons originate from neural stem cells within the SVZ and migrate as neuroblasts to reach the OB, where they predominantly differentiate into granule cells and periglomerular neurons, becoming part of pre-existing mature circuits (Mobley et al., 2014). In mice, it has been suggested that the decline in olfactory function could be attributed to a reduction in these OB interneurons, possibly due to errors in the cell division cycle or a decrease in the production of neuroblast in the SVZ (Seo et al., 2018). Nevertheless, despite a decrease in OB neurogenesis, the density of granule interneurons appears to remain unaffected by natural aging (Richard et al., 2010). Consequently, while the rate of replacing new interneurons seems to diminish with age, the existing ones might extend

their lifespan to compensate for the reduced rate of replacement. Nonetheless, the failure to incorporate new neurons could lead to reduced adaptability of mature olfactory circuits to respond to new olfactory stimuli, resulting in diminished sensitivity to odors (Kondo et al., 2020).

Though widespread neuronal loss is not a characteristic feature of OB aging, subtle and specific adjustments in synaptic density have been detected. For instance, there is a loss of synapses in the glomerular layer of the MOB (GL), while the external plexiform layer (EPl) remains unaffected. These subtle imbalances in OB circuitry may contribute to aged-related olfactory impairments (Richard et al., 2010).

1.7.3. Alterations in brain regions responsible for olfactory processing

These changes involve a decrease in the volume of specific brain regions, including the hippocampus, amygdala, PCx, and AON (Segura et al., 2013). Age-related decrease in the quantity, size, and distribution of islands of Calleja within the OT, a cortical structure that receives direct input from the OB, may also contribute to pathological changes in olfactory cortex function and olfactory perception (Adjei et al., 2013). Additionally, anosmia is associated with changes in various brain structures involved in olfaction, including the PCx and insular cortices, the orbitofrontal cortex, the medial prefrontal cortex, the hippocampus, the parahippocampal gyrus, the nucleus accumbens, the subcallosal gyrus, and the medial and dorsolateral prefrontal cortices (Bitter et al., 2010).

1.7.4. Chronic inflammation

Aged-related chronic inflammation has been recently associated with olfactory dysfunction. In humans, elevated levels of the pro-inflammatory cytokine IL-6 have been detected in individuals with hyposmia (Henkin et al., 2013). In mice, repeated intranasal administration of lipopolysaccharide (LPS) has been shown to induce nasal inflammation, atrophy of the OB, and impaired regeneration of the MOE (Hasegawa-Ishii et al., 2019).

Hence, in addition to changes in EO and OB structure, neurogenesis, variations in ORs expression and abnormal synaptic reorganization, inflammation may also play a pivotal role in olfactory dysfunction. The combination of all these factors could constitute the cellular and molecular mechanisms contributing to the age-related decline in the sense of smell.

2. OBJECTIVES

In humans, olfactory dysfunction is one of the early symptoms in neurodegenerative diseases, as well as during natural aging. However, the processes underlying these deficits are unknown, and it is unclear if there are differences between natural and pathological aging. Identifying the cellular mechanisms associated with these processes and its impact on olfactory and social behaviors would contribute to understand the circuital adaptations associated with aging, a basic knowledge that could serve for the development of new biomarkers for the early diagnosis of neurodegenerative diseases. For this purpose, we defined the following objectives:

1. Characterization of potential structural alterations of the vomeronasal organ as a consequence of natural and pathological aging.

2. Analysis of cell specific changes in the vomeronasal system during both natural and pathological aging.

3. Study the impact of natural and pathological aging on the detection and processing of social olfactory information.

4. Exploring the impact of natural and pathological aging on social behavior

3. MATERIALS AND METHODS

3.1. Animals

The experiments involved two sets of mice: wild type and heterozygous APP/PS1 mice (APP/PS1^{Het}) on a C57/BL6 genetic background. Wild type mice were divided into young adults (2–4 months old), middle-aged (6–8 months old), old (12–14 months old), and senescent (20–24 months old) groups. On the other hand, the APP/PS1 mice were either young adults (2–4 months old) or old (12–14 months old). APP/PS1 mice were obtained from Jackson Labs (Stock No. 004462, MMRRC Stock No. 34829).

Each experiment utilized separate groups of animals. The APP/PS1^{Het} mice carried a chimeric mouse/human amyloid precursor protein (Mo/HuAPP695swe) and a mutant human presenilin 1 (PS1-dE9), which caused them to develop Aβ deposits at approximately 6 months of age. These mice also displayed early-onset cognitive impairments (Jankowsky et al., 2004; Jankowsky et al., 2001; Reiserer et al., 2007) and had a reduced life expectancy of around 14–16 months old compared to littermate APP/PS1 controls (APP/PS1^{WT}). This reduced life expectancy limited our ability to extend the study to a comparable age range as naturally aged animals (20–24 months old).

All mice were housed in groups and had no prior exposure to experimental conditions throughout their lives. They were kept in pathogen-free conditions, living in ventilated cages with unrestricted access to food and water and a 12-hour light/dark cycle. All the experimental procedures were conducted in accordance with Spanish and European Union regulations governing animal research (2010/63/EU). The Bioethical Committee at the Instituto de Neurociencias and the Consejo Superior de Investigaciones Científicas (CSIC) approved all experimental procedures.

3.2. APP/PS1 genotyping

DNA from tail biopsies was extracted and genotyped through polymerase chain reaction (PCR). The primers for APP transgene are (sigma; 5'-GAC TGA CCA CTC GAC CAG GTT CTG-3') and (sigma; 5'-CTT GTA AGT TGG ATT CTC ATA TCC-3') which gives a band at ~ 400 bp in APP transgenic mice. The primers for PS1 transgene are (sigma; 5'-GCC ATG AGG GCA CTA ATC AT-3') and (sigma; 5'-ATT AGA GAA CGG CAG GAG CA-3') which gives a band at ~ 600 bp in PS1 transgenic mice (Figure 17).

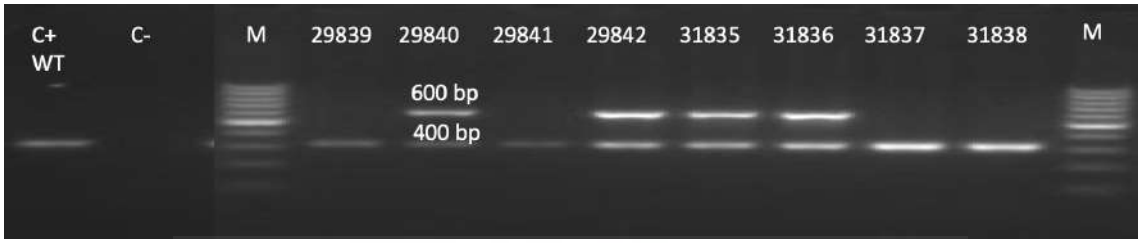

Figure 17. APP/PS1 double-transgenic mice genotyping. Bands 29839, 29841, 31837 and 31838 are the WT representative mice. Bands 29840, 29842, 31835, 31836 are the transgenic mice. M: BioDL100 DNA mark. C: control.

3.3. VNO dissection

Mice underwent transcardial perfusion using phosphate buffer saline (PBS) at a pH of 7.4, followed by fixation using a solution of 4% paraformaldehyde (PFA) in 0.1 M phosphate buffer (PB) with a pH of 7.4. After fixing the mouse head, it was positioned under a microscope, and the lower jaw was excised to enable a view of the palate. In order to extract the VNO, the palate and nasal septum were both removed, and the bilateral VNOs were separated into two sections. Finally, the bone covering each section was meticulously removed to extract the VNOs. The tissue was then immersed in a 30% sucrose solution for cryoprotection and stored at -4 °C until the sectioning process. Subsequently, the samples were embedded in OCT and frozen at -80 °C for the cryosectioning procedure (Figure 18).

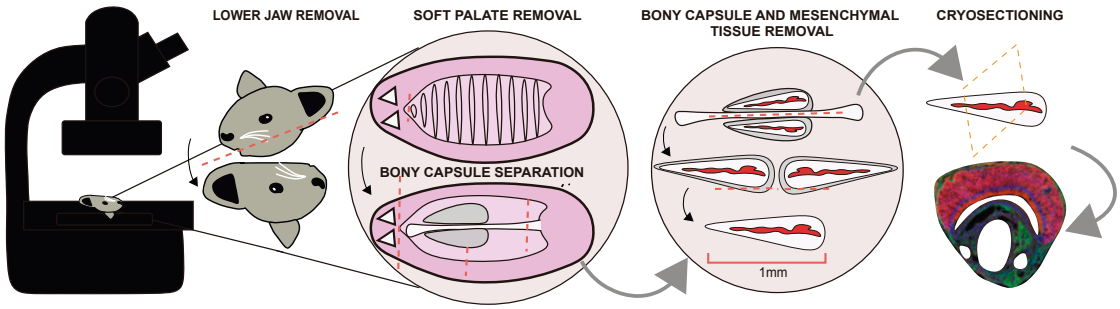

Figure 18. VNO dissection procedure. The VNO is responsible for pheromone detection in mice. Here, we have analyzed its morphological properties, cellular composition and neurogenic capacity during natural and pathological aging by directly dissecting the organ after fixation with PFA.

3.4. Immunohistochemistry

VNOs embedded in OCT medium were sliced in 16 µm thick sections in a cryostat apparatus (Leica CM 3050S). Slices were incubated in blocking solution containing 0.5% Triton X-100 and 5% normal horse serum in 0.1 M tris phosphate buffer (TBS) for 2 h at room temperature (RT). Primary antibody incubation was performed overnight (o/n) at 4 °C with anti-OMP (Wako goat polyclonal; 1:2000), anti-PCNA (Sigma, rabbit monoclonal; 1:2000), and anti- Sox2 (R&D Systems, goat polyclonal; 1:300) (Table 1). For PCNA immunostaining, slices were incubated in 10 mM citrate buffer (100 °C; pH, 6.0) for 5 min prior staining. Sections were incubated with Alexa Fluor 488 or 594-conjugated secondary antibodies (Table 2; Jackson Laboratories, 1:500) for 2h at RT and Hoechst (Sigma, 1:10,000) was added during 5 min after the secondary antibody incubation for nuclei visualization. Imaging was performed using a vertical confocal microscope Leica SPEII. Final images were assembled in Adobe Illustrator.

ANTIBODY	DILUTION	REFERENCE
Anti-OMP	1:2000	Wako
Anti-PCNA	1:2000	Sigma – P8825
Anti-Sox2	1:300	R&D Systems – MAB2018

Table 1. List of primary antibodies used.

ANTIBODY	DILUTION	REFERENCE
anti-Rabbit ALEXA 488	1:500	Invitrogen – A11034
anti-Mouse ALEXA 594	1:500	Invitrogen – A11032

Table 2. List of secondary antibodies used.

3.5. Sox2 fluorescence intensity at the VNO-SCL

For determining the expression of Sox2 in the VNO-SCL where single-cell quantification was limited by the densely packed disposition of the cells, we calculated the corrected total fluorescence (CTF) of the area of interest employing the Freehand ROI tool of Image J. CTF was calculated by subtracting the background fluorescence from a minimum of 3 sections, 16 μm thick, from at least 4 animals per condition.

3.6. Stereology, cell quantification, and AOB volume estimation

The total number of olfactory mature neurons (OMP^+ neurons) in the entire VSE was estimated using stereology (optical fractionator method (Wong et al., 2018) employing Stereo Investigator (MBF Bioscience). Two different tools are combined in this unbiased quantification method: a 3D optical dissector for cell counting and a fractionator, based on a systematic, uniform, and random sampling over a known area (Parrish-Aungst et al., 2007). The number of neurons was estimated as:

$$N = (1/h \times 1/ssf \times 1/asf \times \sum Q - t)$$

In this context, ∑ Q represents the total cell count within the region of interest, determined using the optical dissector method. The variable "t" signifies the average thickness of the mounted sections, "h" denotes the height of the optical dissector, "asf" corresponds to the area sampling fraction, and "ssf" refers to the section sampling fraction.

For the stereological analysis of the VSE, we conducted sampling using a 20 × objective lens (Leica, NA 0.6). The counting frame area measured 2500 μm2, while the sampling grid area covered 22,500 μm2. In VSE stereology, "H" was set at 8 μm, with upper and lower guard zones each measuring 1 μm, and "t" was established at 10 μm. Cell quantifications were carried out in the marginal regions of the VSE, where the area was divided into segments of equal length, as previously outlined (Brann and Firestein, 2010; Giacobini et al., 2000). To quantify cells in the anterior–posterior regions, the VSE was divided into 10 sections per animal. The results were normalized by area to yield the cell count per square millimeter within each subdivision. Quantification of cell numbers in the marginal area was conducted in three slices from each animal, demarcated using a 50 × 50 dissector with the assistance of Stereo Investigator (MBF Bioscience).

To calculate the VSE volume, we multiplied the sampled area by the slice thickness (16 μm) and the number of series (10 slices per animal). This approach enabled us to estimate the VSE area and volume in young adults (4 months old), senescent (24 months old), and old (12 months old) APP/PS1^{WT} mice, as well as old APP/PS1^{Het} mice.

The volume of the AOB was estimated by measuring the AOB area and multiplying the sampled area by the section thickness (50 μm) and the number of analyzed sections.

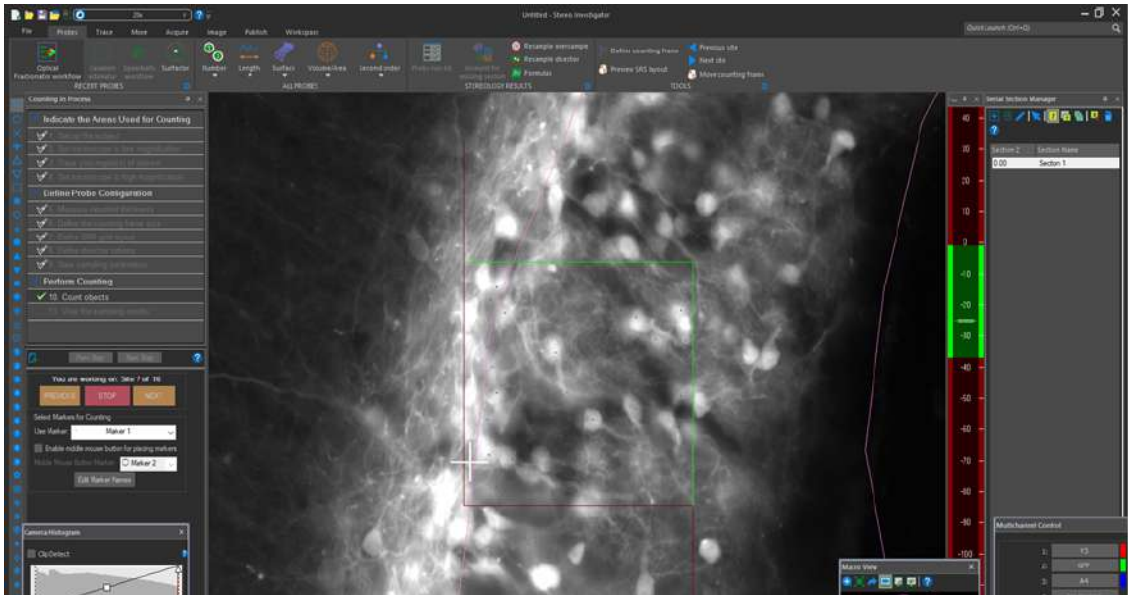

Figure 19. Example of cell number estimation using stereological approaches. The optical dissector method (Stereo Investigator – MBF Bioscience) was used to quantify OMP^+ neurons within the VSE.

3.7. Odorants

To investigate the impact of aging on social odor perception, we utilized both social and non-social scents. For non-social scents, we employed two substances: (1) IA, a banana-like odor (Sigma), known to be primarily detected at the level of the MOE (Xu et al., 2005). This odor possesses a neutral valence and is effective across a wide range of dilutions (Fortes-Marco et al., 2015). (2) Additionally, we utilized food pellets as part of a food finding test (FFT; see below).

As for the social scent, we employed urine from conspecifics, which is known to trigger significant VNO activity (Chamero et al., 2017). The urine samples were collected following established protocols (Kurien et al., 2004). In habituation-dishabituation tests, we used frozen urine samples obtained from young cage mates to assess fine odor discrimination. For sensitivity tests, urine samples were pooled into a stock sample, which was used for each round of odor presentations until the experiment was concluded.

3.8. Behavioral evaluation

All behavioral experiments involving both social and non-social stimuli were conducted within a dedicated room, which maintained a continuous airflow and was illuminated with low-intensity indirect lighting (20 lx). The preparation of odor dilutions took place in a separate room outside of the animal housing area.

For odor presentation, a custom-made methacrylate box with removable walls for cleaning was utilized. This chamber had dimensions of 15 cm in width, 15 cm in length, and 30 cm in height. A small hole, measuring 1 cm in diameter, was positioned in the middle of one of the sides, situated 5 cm above the box's floor. This hole was designed to accommodate standard cotton sticks that had been impregnated with 1 µL of the odorant, enabling direct contact with the sticks (Figure 20). Prior to the presentation of odorants, the animals underwent a habituation phase to acclimate them to the testing conditions. This consisted of a 5-minute period of handling, followed by free exploratory activity in the box and familiarization with the movement of the cotton stick, also lasting for 5 minutes. To ensure the preservation of non-volatile pheromones and mimic the natural method of physical contact between conspecifics, urine samples were presented by embedding them within a cotton stick. In order to minimize variability stemming from the intensity of volatile urine components, only instances of direct nose contact with the tip of the cotton stick were considered as exploratory behavior, specifically measuring sniffing and exploration time.

The experiments were monitored through video recording, with a camera fixed 15 cm above the testing box. Subsequently, the collected videos were analyzed offline using BORIS (Friard and Gamba, 2016) and SMART video-tracking softwares (PanLab S.L.).

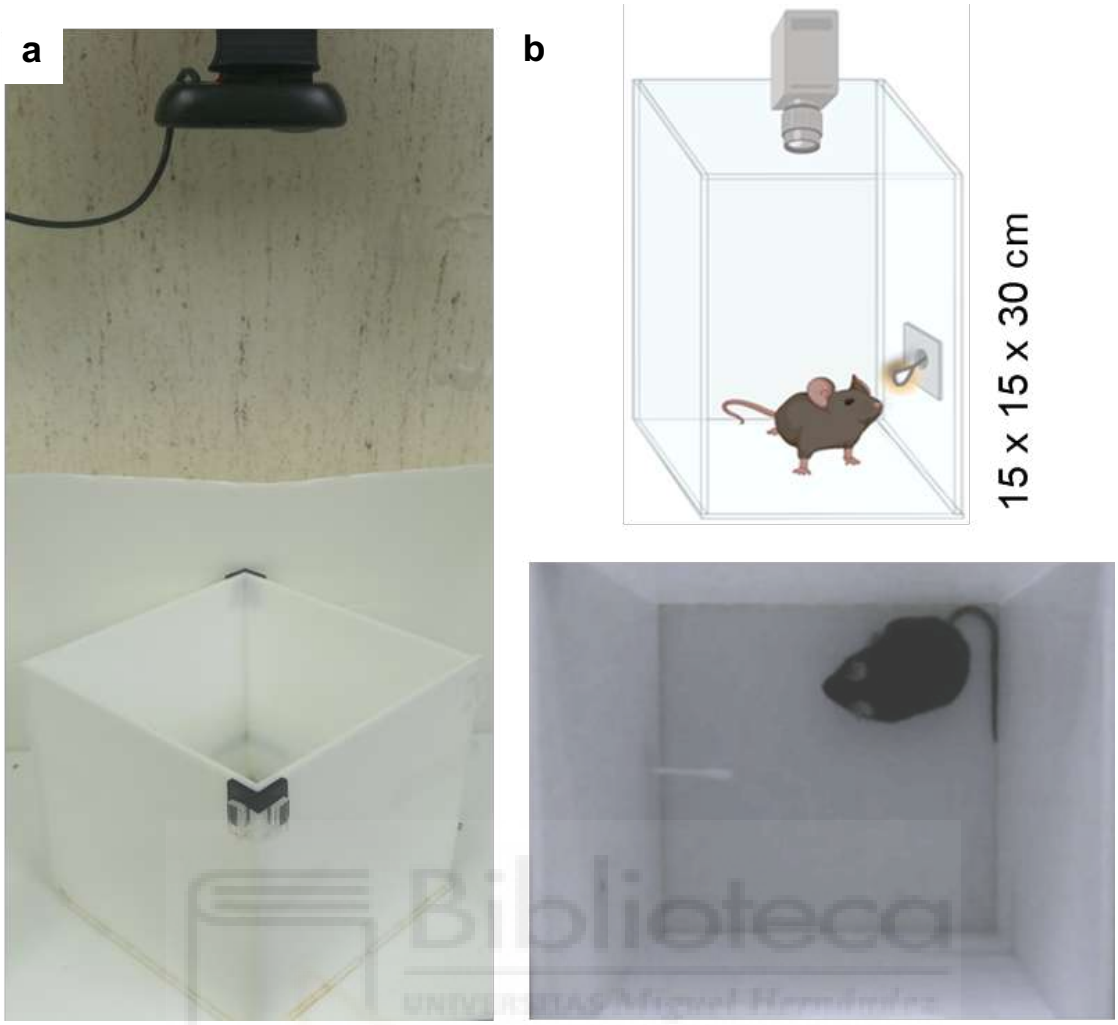

Figure 20. Image illustrating the setup for the olfactory experiments. a, A video-camera was located 30 cm above the testing box during the experiment. **b,** Schematic (top) and a representative image (below) of a mouse during a trial. Successful olfactory exploration will be considered when the mouse makes nasal contact with the cotton stick.

3.8.1. Odor exploration test

After a period of habituation (10 min), mice were exposed to two control trials (mineral oil for IA assays or water for urine tests) during 1 min separated by intervals of 1 min to avoid odor habituation (Breton-Provencher et al., 2009; Sanderson and Bannerman, 2011). Subsequent presentations consisted on serial dilutions of either urine samples (diluted in water: 1:1.000, 1:500, 1:250, 1:100, 1:50, 1:10, and non-diluted (nd)) or IA were tested in ascending order (diluted in mineral oil: 1:5 × 105, 1:100.000, 1:10.000, 1:1.000, 1:100). Animals were considered to detect the olfactory stimulus when spent more time investigating the odors than the vehicles (water or mineral oil).

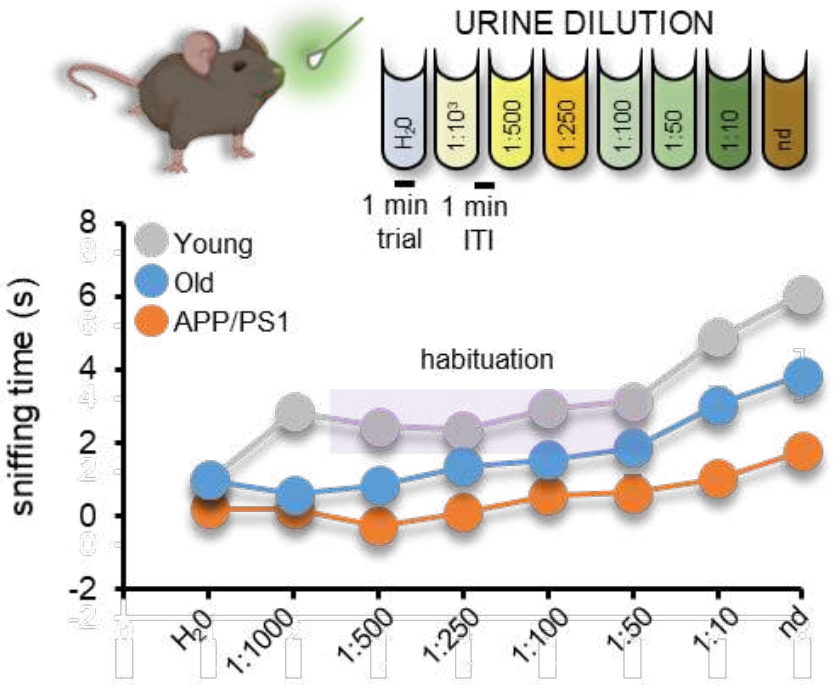

Figure 21. **Social odor detection test to evaluate sensitivity to social cues**. Social odors (urine) are diluted and presented serially ranging from the lowest dilution (1:1000) to the non-diluted sample during 1-minute trials in 1-minute intervals. An increase of exploration time compared to the vehicle (water) indicates effective olfactory detection. The plot illustrates an idealized response in which deficits in social odor sensitivity are apparent in old and APP/PS1 mice. ITI: Inter-trial interval.

3.8.2. Food finding test

The FFT was conducted following established protocols (Figure 22; Deacon et al., 2009). Prior to the test, mice underwent a 24-hour period of food deprivation. In a designated corner, five food pellets (~ 35 g) were placed and covered with 5 cm of bedding. Animals were considered to have detected the food pellet when they engaged in digging, touching, and holding the food pellet for more than 5 seconds.

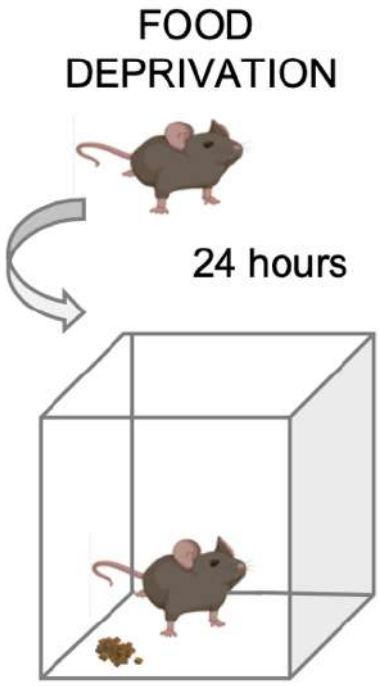

Figure 22. Food-finding test. To additionally evaluate olfactory capabilities, a buried food-seeking assay was implemented. This test determines whether food-deprived mice can successfully locate a buried food pellet.

3.8.3. Social odor habituation-dishabituation test

An examination of the impact of aging on social odor discrimination and habituation was carried out using a modified habituation-dishabituation test (Gheusi et al., 2000). After a 10-minute period of acclimatization to the cage, two control trials were conducted using cotton sticks soaked with 1 µL of water (vehicle). Three consecutive presentations of urine from an animal of the opposite sex (S1a-c) were succeeded by three presentations of urine from a different subject of the opposite sex (S2a-c) to assess fine chemo-olfactory discrimination and habituation. The urine samples were obtained from young animals of the opposite sex to enhance approaching behavior (Garratt et al., 2011). Each presentation of the sample lasted 1 minute, with 1-minute intervals in between. Habituation was quantified by observing a decrease in exploration time (sniffing) over the cotton stick tip after the initial exposure to urine from the same animal (S1a). Dishabituation (discrimination) manifested as a measurable increase in exploration time in response to a new odor presentation (S2a). The test enabled the exploration of two consecutive phases of discrimination (H2OB-S1a and S1c-S2a) and habituation (S1a-S1b and S2a-S2b). Trend lines between H2OB-S1a,

S1c-S2a, S1a-S1b, and S2a-S2b were fitted to derive slope values indicating the amplitude of the discrimination and habituation effects for each tested condition. Higher positive values indicated more pronounced social discrimination, while higher negative values corresponded to more robust habituation.

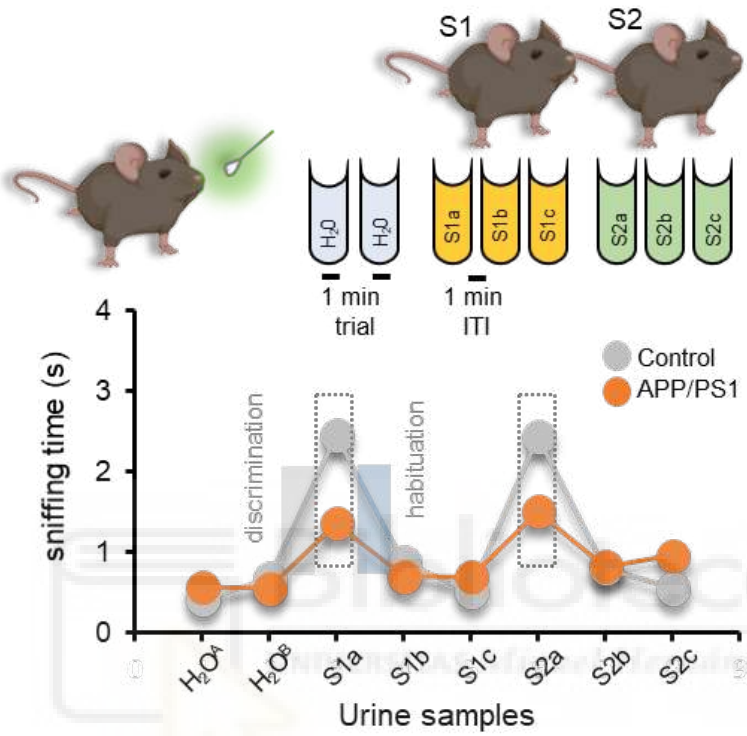

Figure 23. The social odor habituation-dishabituation test. The test allows to evaluate the mice capability to detect and discriminate between similar social cues, including odors from animals of the same age (S1, S2). Each odor is presented in three consecutive 1-minute trials in 1-minute intervals. An increase of exploration time when a new odor is presented for the first time (S1a or S2a) indicates normal social discrimination. The plot illustrates an idealized response in which deficits in social odor discrimination are apparent in APP/PS1 mice. ITI: Inter-trial interval.

3.8.4. Long-term social habituation-dishabituation test

The previously mentioned social odor habituation task underwent modification to assess social cue memory by reintroducing the urine sample used in S1a, 24 hours after the initial test. Intact social odor memory was evidenced by a reduction in sniffing time during the second presentation of S1a, a phenomenon particularly noticeable in young animals.

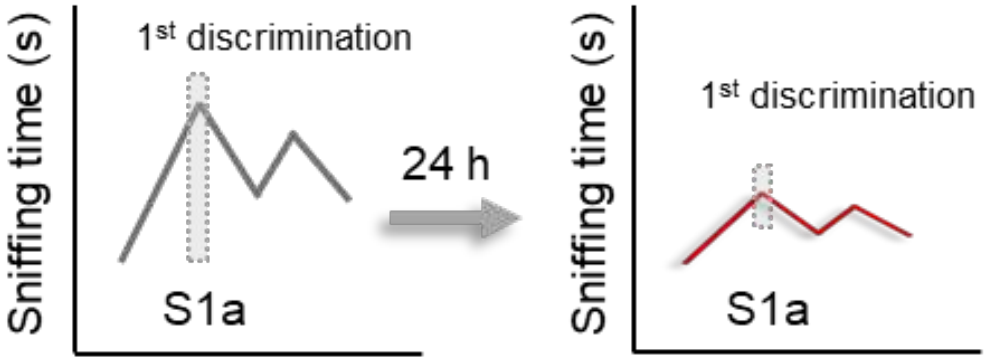

Figure 24. Long-term social discrimination. The social odor habituation-dishabituation test can be adapted to study long-term olfactory memory. Impairments in long-term olfactory memory can be detected at Day 1 by measuring the exploration time of the same odor presented the day before (Day 0). The plots show an idealized response in which transgenic animals show similar sniffing time of S1a in Day 0 and Day 1.

3.8.5. Three-chamber test

Social assessments were conducted in a cage measuring 60 × 40 × 22 cm, following established protocols (Nadler et al., 2004). Dividing walls, crafted from clear Plexiglas, featured openings allowing entry into each chamber. The test mouse was initially placed in the middle chamber and given 10 minutes to explore. Following the habituation period, an unfamiliar subject of the same sex (mouse 1, M1A) was positioned in one of the side chambers. The unfamiliar mouse was contained within a small, circular wire cage, facilitating nose contact through the bars. In the first session (sociability), the test mouse had the option to spend time in either the empty chamber (E) or the chamber occupied by M1A. After the sociability session, each mouse underwent a second 10-minute session to assess social preference for a new subject. Another unfamiliar mouse (mouse 2, M2) of the same sex was placed in the chamber that had remained empty during the first session. This second unfamiliar mouse was also enclosed in an identical wire cage to M1A. The test mouse had a choice between the first, already-investigated mouse (M1B) and the novel unfamiliar mouse (M2), indicating their social preference or response to social novelty (Nadler et al., 2004). Continuous video recordings were captured and subsequently analyzed

offline using BORIS (Friard and Gamba, 2016) and SMART video-tracking software (PanLab S.L.). Measures of time spent sniffing E, M1A−B, and M2 were quantified for each session.

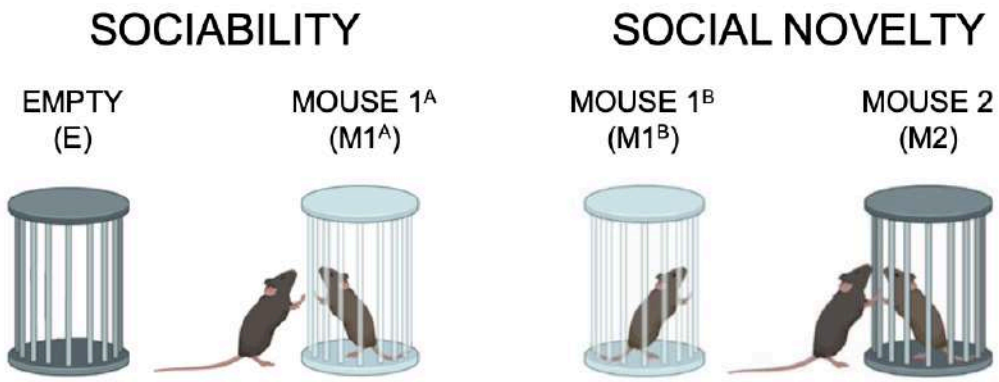

Figure 25. The Three-chamber test evaluates sociability and social novelty in rodents. Typically, rodents exhibit a preference for spending more time with another rodent (sociability) and show greater interest in exploring a new intruder compared to a familiar one (social novelty). Thus, the Three-chamber test can identify impairments in both sociability and/or social novelty.

3.9. Data analysis

All data underwent statistical testing for significance using GraphPad Prism 8. Data normality was assessed using the Shapiro–Wilk test. For cell quantifications and anatomical data, a one-way ANOVA with Tukey's test for multiple comparisons with a single variable was employed. Behavioral analysis utilized a two-way ANOVA with Tukey's test for multiple comparisons involving more than one variable. P values for statistical significance are indicated in all figures above the corresponding comparisons, with $P \leq 0.05$ considered statistically significant. Furthermore, a two-way ANOVA incorporating the interaction of age vs. genotype was applied to all datasets that included these variables. Detailed results of these statistical analyses can be found in ANNEX I.

4. RESULTS

4.1. Structural modifications of the mouse VSE during natural and pathological aging

Our first goal was to explore the changes in the VSE structure during both natural and pathological aging, as the VSE serves as the primary entry site for pheromone-encoded social information (Cheetham et al., 2007; Ferrero et al., 2013). Through stereological analysis, we discovered notably smaller VSE volumes in 2-year-old (senescent) mice (Figure 26a). This finding was corroborated by a decrease in the number of olfactory marker protein (OMP^+ cells) along the rostrocaudal axis of the VSE (Figure 26b, c).

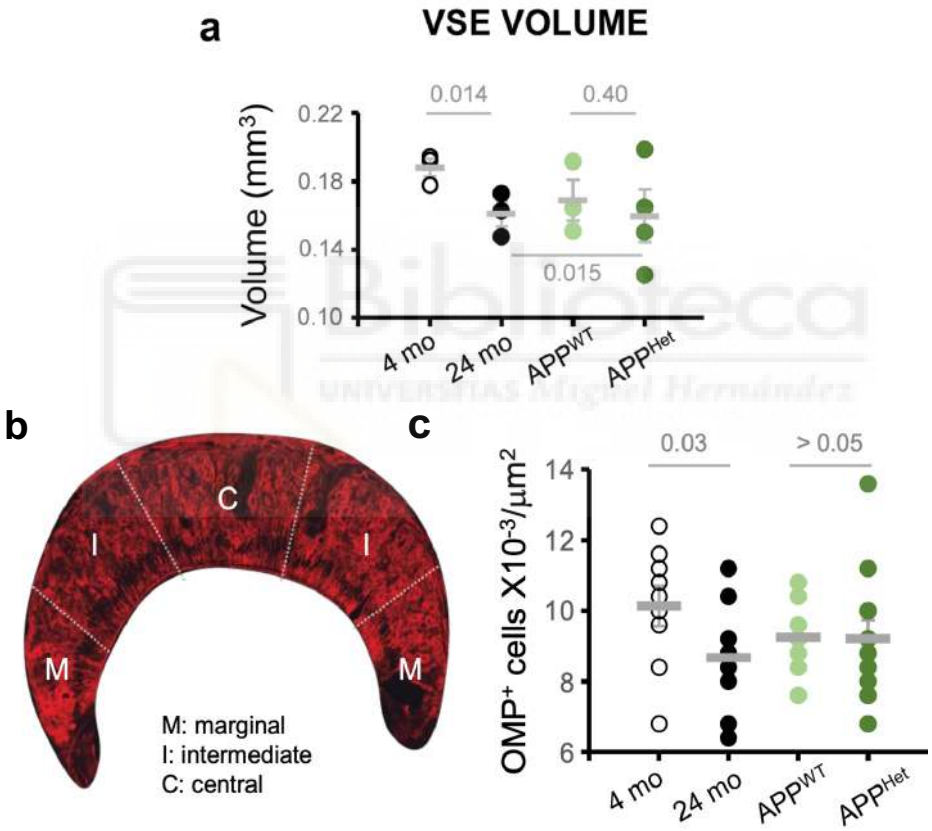

Figure 26. Structural modifications of the mouse VSE during natural and pathological aging. a, Dispersion plot of the VSE volume indicates a significant reduction during natural but not pathological aging. **b,** Representative image of the VSE stained with the OMP. **c,** Dispersion plot indicating the total estimation of OMP^+ cells in the VSE. Thick lines indicate the mean ± SEM. Data were obtained from 4 animals per condition. M: marginal zone; I: intermediate zone; C: central zone.

We also analyzed the VSE along the antero-posterior axis, obtaining significate differences in the anterior and medial portions when comparing young with naturally aged mice stained with OMP, suggesting that aging impacts differently on the VSE axis (Figure 27a, c). Next, we expanded our study to the Sox2+ cells in the SCL, a neural stem cell marker that also marks mature differentiated sustentacular cells (Guo et al., 2010; Taroc et al., 2020; Katreddi and Forni, 2012). The assessment of Sox2 labeling intensity in the SCL revealed a significant reduction in senescent mice but not in APP/PS1^{Het} mice (Figure 27b, d). These findings indicate that natural aging disrupts the VSE structure by diminishing the number of sensory (OMP^{+}) and SCL sustentacular (Sox2^{+}) cells, although this might not necessarily imply a complete elimination of proliferative capacities (Brann and Firestein, 2010).

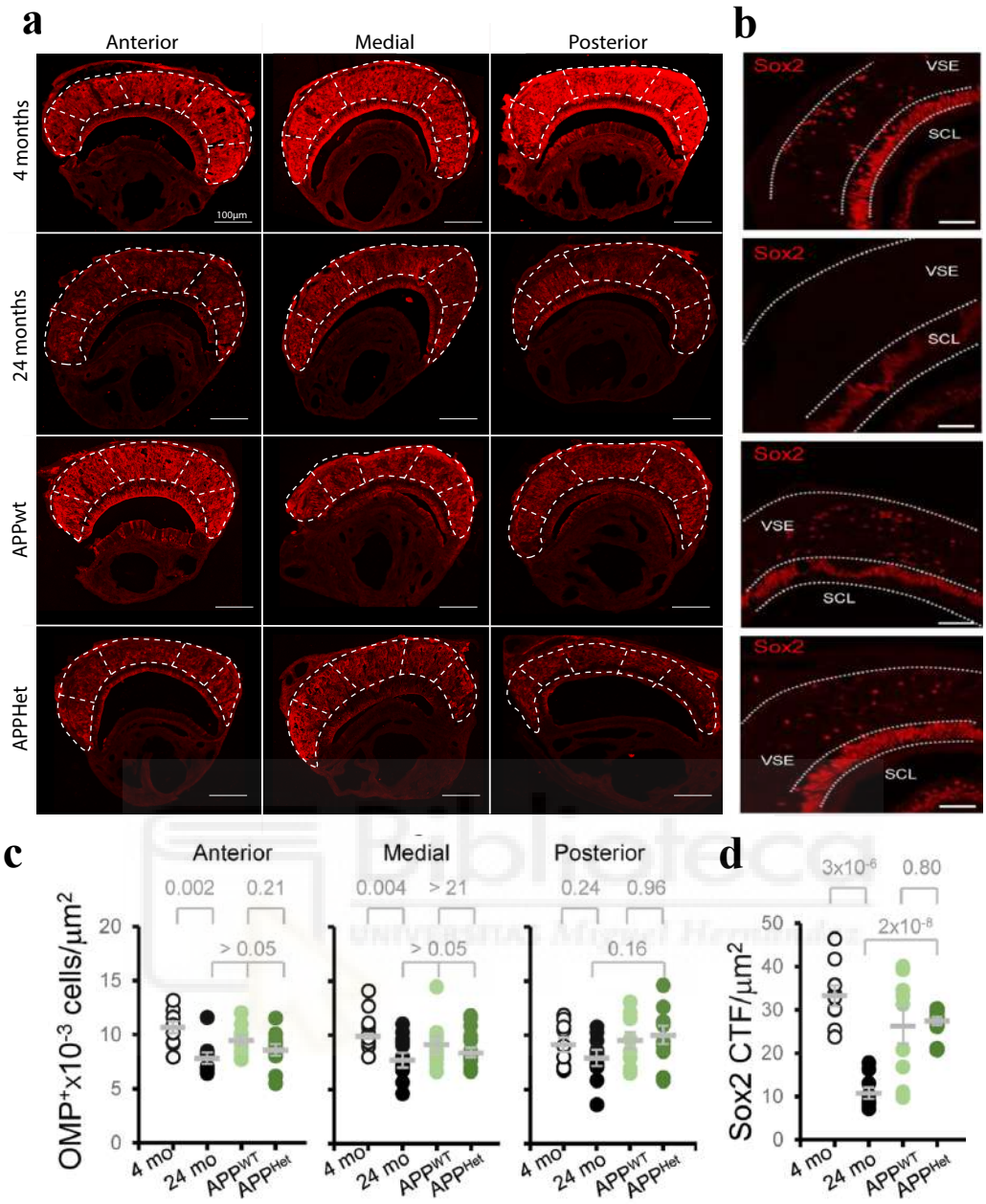

Figure 27. Natural aging disrupts VSE structure differently in the VSE rostro-caudal axis. a, Representative images of OMP staining in the VSE antero-posterior axis during natural and pathological aging. Scale bar indicates 100 µm. **b,** Representative images of Sox2 staining in the VSE and the supporting cell layer. Scale bar indicates 20 µm. SCL: supporting cell layer. **c**, **d,** Dispersion plots represent the number of OMP^+ cells along the VSE axis (number of cells × $10^{-3}/\mu m^2$) and the intensity of Sox2 fluorescence in the SCL (Sox2 CTF/μm^2). Thick lines indicate the mean ± SEM. Data were obtained from slices from at least 4 animals per condition. Statistical comparisons were calculated by two-way ANOVA with Tukey's test. $P \leq 0.05$ was considered statistically significant. *P* values are indicated above the corresponding comparisons.

We then hypothesized that the decline in OMP$^+$ cells in senescent mice could lead to a diminished axonal projection to the AOB, the primary target region of the VNO, resulting in reduced AOB volumes. As expected, we noted a decrease in AOB size without evident histopathological changes in 2-year-old mice (Figure 28), signifying that natural aging impacts fundamental structural aspects of the VNO-AOB axis.

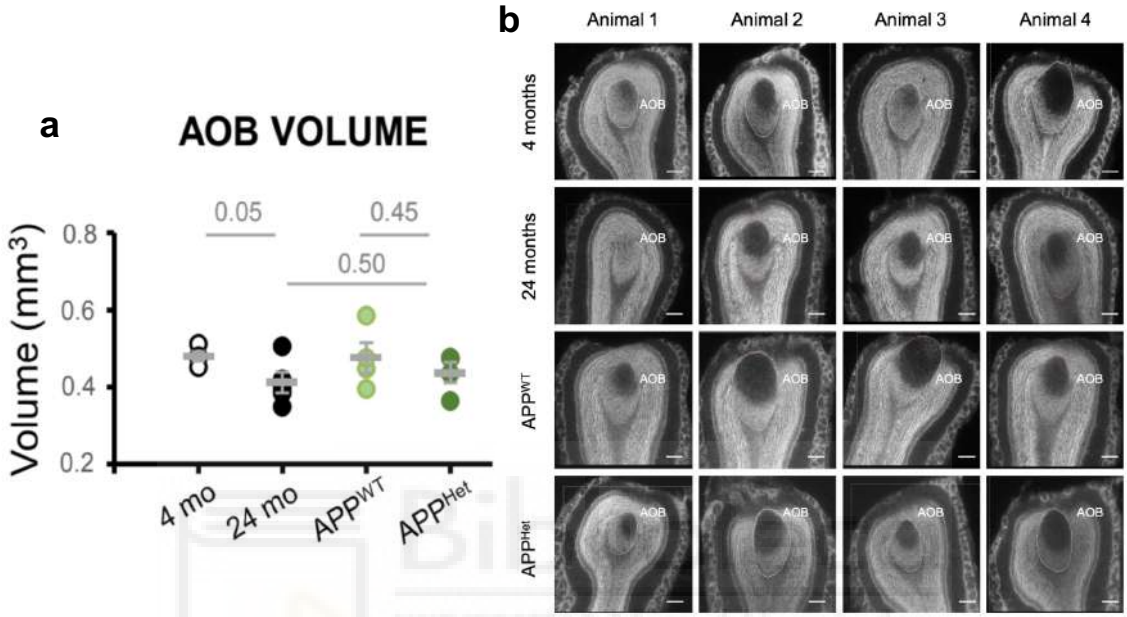

Figure 28. The decline in OMP$^+$ cells during natural aging leads to a reduced AOB volume. a, Dispersion plot of AOB volume. **b**, Representative images of the AOB during the volume estimations. Thick lines indicate the mean ± SEM.

4.2. Natural and pathological aging differentially impacts VSE cell proliferation

Due to the limited information available regarding the neurogenic capability of the VSE in animal models of neurodegeneration, we conducted an analysis to investigate the presence of proliferative cell nuclear antigen (PCNA)-positive cells (PCNA$^+$ cells) in the anterior, medial, and posterior VSE of aged mice and those with the APP/PS1^{Het} mutation. In alignment with prior studies, young animals exhibited abundant cell proliferation in the marginal zone of the anterior and medial VSE (Brann and Firestein, 2010; Giacobini et al., 2000) (Figure 29a, b). However, senescent mice displayed a notable decrease in PCNA$^+$ cells in the marginal VSE (Figure 29a, b), indicating diminished cell proliferation. Interestingly, APP/PS1^{Het} mice demonstrated a significant increase in PCNA+

cells in the anterior VSE, with a declining trend in the posterior VSE (Figure 29a, b), suggesting a region-specific elevation in cell proliferation in these animals. Crucially, no substantial overlap between OMP and PCNA staining was observed, indicating that these markers identify cell populations at distinct maturation stages (Figure 29).

We then investigated whether the reduced number of proliferative $PCNA^{+}$ cells in senescent mice might be attributed to a decrease in stem cell generation by examining the quantity of $Sox2^{+}$ neural precursor cells in the VSE (Tucker et al., 2010; Panaliappan et al., 2018). We noted a significant reduction in the number of Sox2+ cells in 2-year-old mice, but no such decline was observed in $APP/PS1^{Het}$ animals, indicating a diminished neurogenic capacity in the naturally aged VSE (Figure 29c). In summary, these findings highlight a fundamental distinction in how natural aging and disease-related aging impact the structure and proliferative capacity of the VSE.

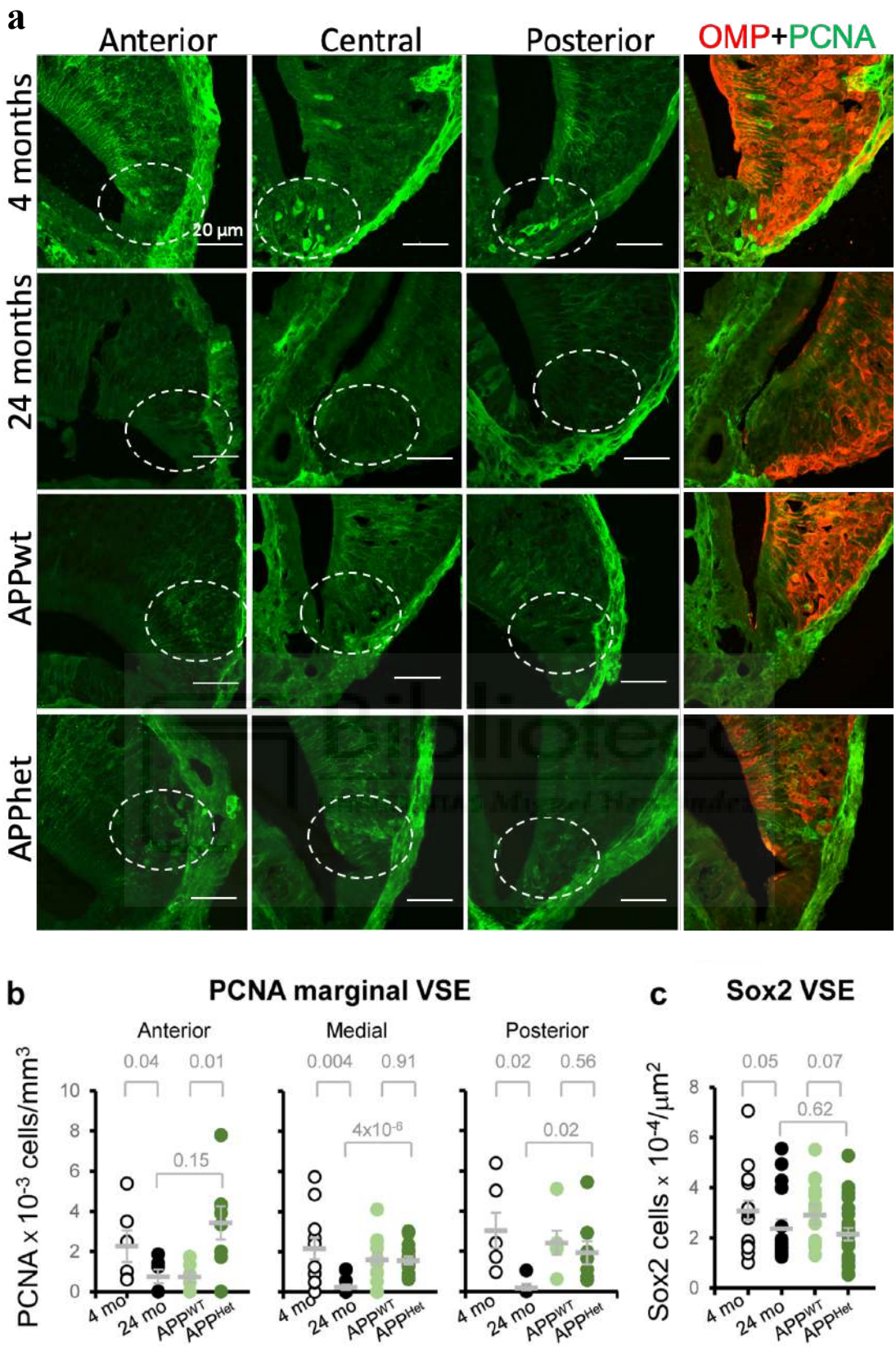

Figure 29. **Natural and pathological aging differentially impacts cell proliferation in the marginal VSE. a**, Representative confocal images of PCNA staining in the VSE proliferative niche during natural and pathological aging. Panels on the right show confocal images of OMP and PCNA double staining in the VSE. To note, there is no overlapping signal between the two markers

indicating the identification of cells at different maturation stages. Circles indicate active proliferative marginal region of the VSE. Scale bar represents 20µm. **b, c,** Dispersion plots represent the number of $PCNA^+$ cells (number of cells × $10^{-3}/mm^3$) and the number of $Sox2^+$ cells (number of cell × $10^{-4}/\mu m^2$) in the marginal VSE. Thick lines indicate the mean ± SEM. Data were obtained from slices from at least three animals per condition. Statistical analysis was calculated by two-way ANOVA with Tukey's test for multiple comparisons. $P \leq 0.05$ was considered statistically significant. P values are indicated above the corresponding comparisons.

4.3. Late onset of social exploration deficits during natural aging

Our findings suggest that natural aging brings substantial changes in the structure, proliferative capacity, and cellular composition of the VSE. Consequently, we delved into whether these adaptations could result in impairments in processing socio-sexual information. Existing evidence indicates that olfactory decline is a prevalent symptom of both natural and pathological aging (Murphy et al., 2002; Doty and Kamath, 2014; Rawson et al., 2012; Roberts et al., 2016). However, many of these studies and diagnostic tests utilized synthetic odors. Therefore, the temporal progression and severity of the age-related decline in the recognition of social cues, predominantly processed by the VNO-AOB axis, remain uncertain.

To assess the impact of natural aging on social odor detection, we implemented an odor-evoked sniffing test. In this test, serial dilutions of urine from young conspecifics of the opposite sex were presented to either male or female subjects across various age groups: young adults (2–4 months), middle-aged (6–8 months), old (12–14 months), and senescent mice (20–24 months) (Figure 30a, see also Materials and Methods section for details). Our results revealed a notable decrease in exploration time across different urine dilutions compared to adult wild-type mice (Figure 30b, c; ANNEX I).

Moreover, senescent mice exhibited a progressive increase in exploration time corresponding to odor concentration. In contrast, young adults, middle-aged, and old animals displayed a habituation phase at intermediate dilutions (1:500, 1:250,

1:100, and 1:50), suggesting effective odor detection and recognition capabilities (Yang and Crawley, 2009).

4.4. Reduction in the exploration of social information is accelerated in an animal model of neurodegeneration

Subsequently, we explored whether pathological aging would impact the investigation of social olfactory cues, despite no apparent effects on VSE structure or proliferative capacity. Social odor sensitivity tests conducted on 1-year-old APP/PS1^{Het} mice unveiled decreased sniffing times for low urine dilutions compared to age-matched APP/PS1^{WT} control mice. This implies that pathological aging expedites the decline in exploration time for social odors (Figure 30d, e; ANNEX I). Comparable to senescent mice, these findings were consistent when examining raw sniffing time data (ANNEX I).

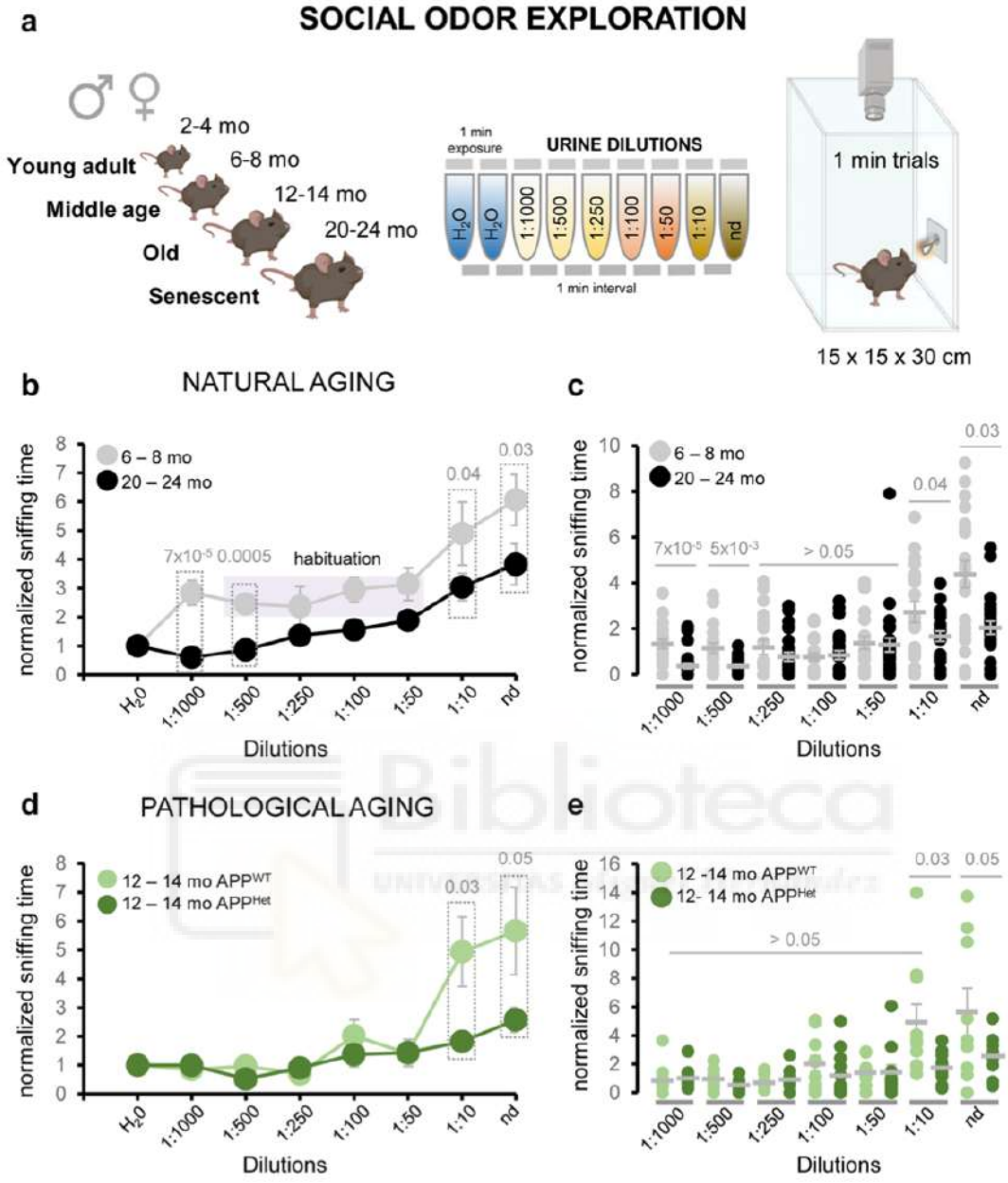

Figure 30. Natural and pathological aging reduces exploration to social odors. **a,** Schematics of the olfactory test used in this study in which urine dilutions are presented as a social signal. **b,** Average of the sniffing time of urine serial dilutions normalized to the exploration time of the vehicle (water) of adult and aged wild-type mice. A typical habituation indicated by a purple box was observed in adult mice at intermediate dilutions (1:500, 1:250, 1:100; 1:50). **c,** Dispersion plot of the normalized sniffing time of each urine dilution (nd (non-diluted); 1:10; 1:50; 1:100; 1:250; 1:500; 1:1000) for adult and aged wild-type mice. **d,** Average of the sniffing time of urine dilutions normalized to the exploration time of the vehicle (water) of middle-aged APP^{WT} controls and middle-aged APP/ $PS1^{Het}$ mice. **e,** Dispersion plots of normalized sniffing time of middle-aged APP^{WT} controls and $APP/PS1^{Het}$ mice. Grey lines in the dispersion plots

indicate mean ± SEM. Data were analyzed by a one-way ANOVA with Tukey's test to test multiple comparisons with more than one variable. $P \leq 0.05$ was considered statistically significant. *P* values are indicated above the corresponding comparisons.

Finally, when examining data based on gender, there were no discernible differences between sexes in the decrease of time spent exploring urine (Figure 31).

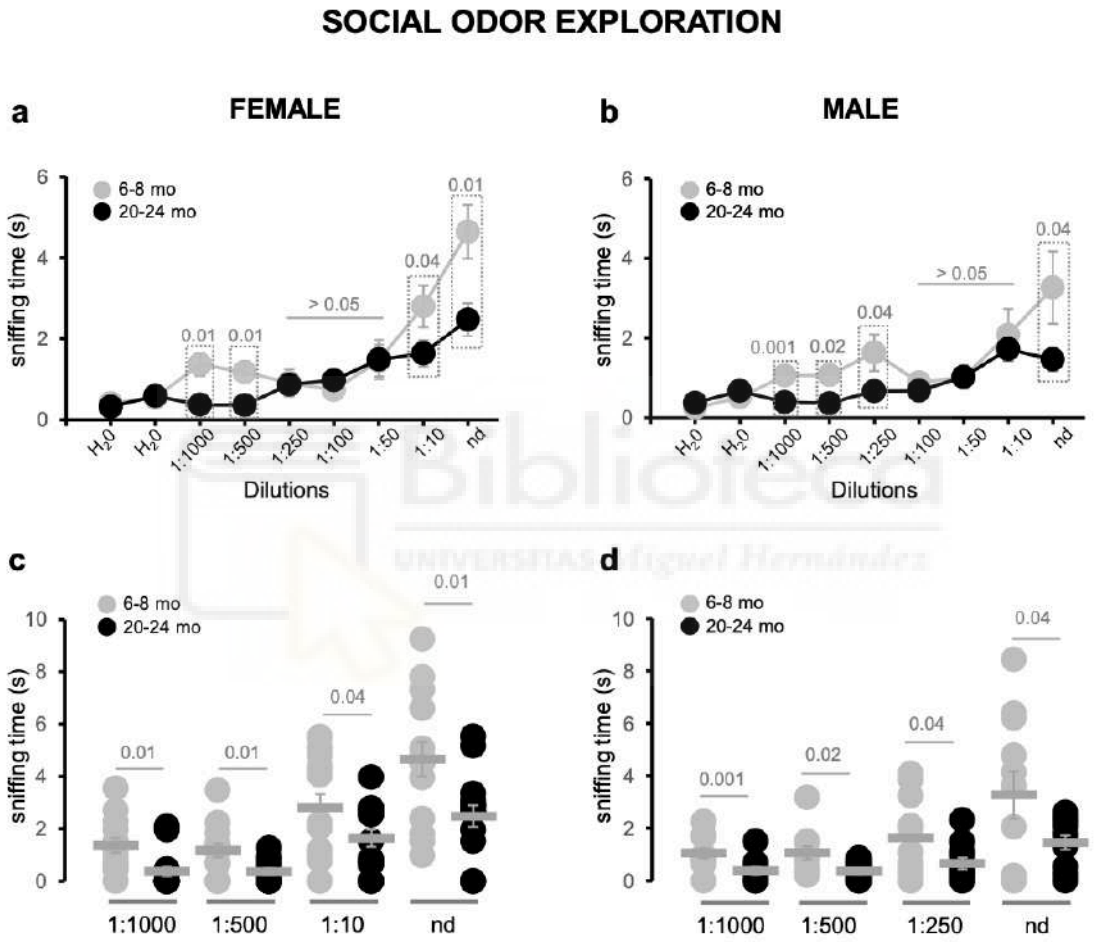

Figure 31. Similar decrease in the exploration of social odors in senescent males and females across different dilutions. a, b, Average of the sniffing time of urine serial dilutions normalized to the exploration time of the vehicle (water) of adult and aged wild-type female and male mice, respectively. **c, d,** Dispersion plots of the normalized sniffing times of some representative urine dilutions for adult and aged wild-type female and male mice. Grey lines in the dispersion plots indicate mean ± SEM. Data were analyzed by a one-way ANOVA with Tukey's test to test multiple comparisons with more than one variable. $P \leq 0.05$ was considered statistically significant. *P* values are indicated above the corresponding comparisons.

4.5. Natural aging mildly reduces neutral odor exploration

We then inquired whether non-social odor experiences were similarly influenced in senescent and APP/PS1^{Het} animals. To address this question, we assessed the exploration time for both food and synthetic neutral odors. Initially, we exposed naturally aged and APP/PS1^{Het} mice to varying concentrations of IA, a synthetic banana-like odor with neutral valence at higher dilutions (Fortes-Marco et al., 2015). In line with previous research, mice across all conditions exhibited significantly reduced responses to the neutral odor compared to urine (Figure 32a–d), reflecting the higher valence of urine over a synthetic odor (Saraiva et al., 2016; Kobayakawa et al., 2007; Jagetia et al., 2018). Our results indicated no significant differences in the exploration times of IA in senescent mice, while there was a modest but noteworthy increase in the sniffing time for the 1:10^4 and 1:100 IA dilutions in APP/PS1^{Het} animals (Figure 32a–d; ANNEX I). Similarly, FFT analysis revealed no significant differences in the latency to find food pellets after 24 hours of food deprivation in either naturally aged or middle-aged APP/PS1^{Het} mice (Figure 32e; ANNEX I). These results imply that deficits in social exploration time at advanced stages of natural aging and in an animal model of AD are more pronounced than in response to other olfactory-encoded information.

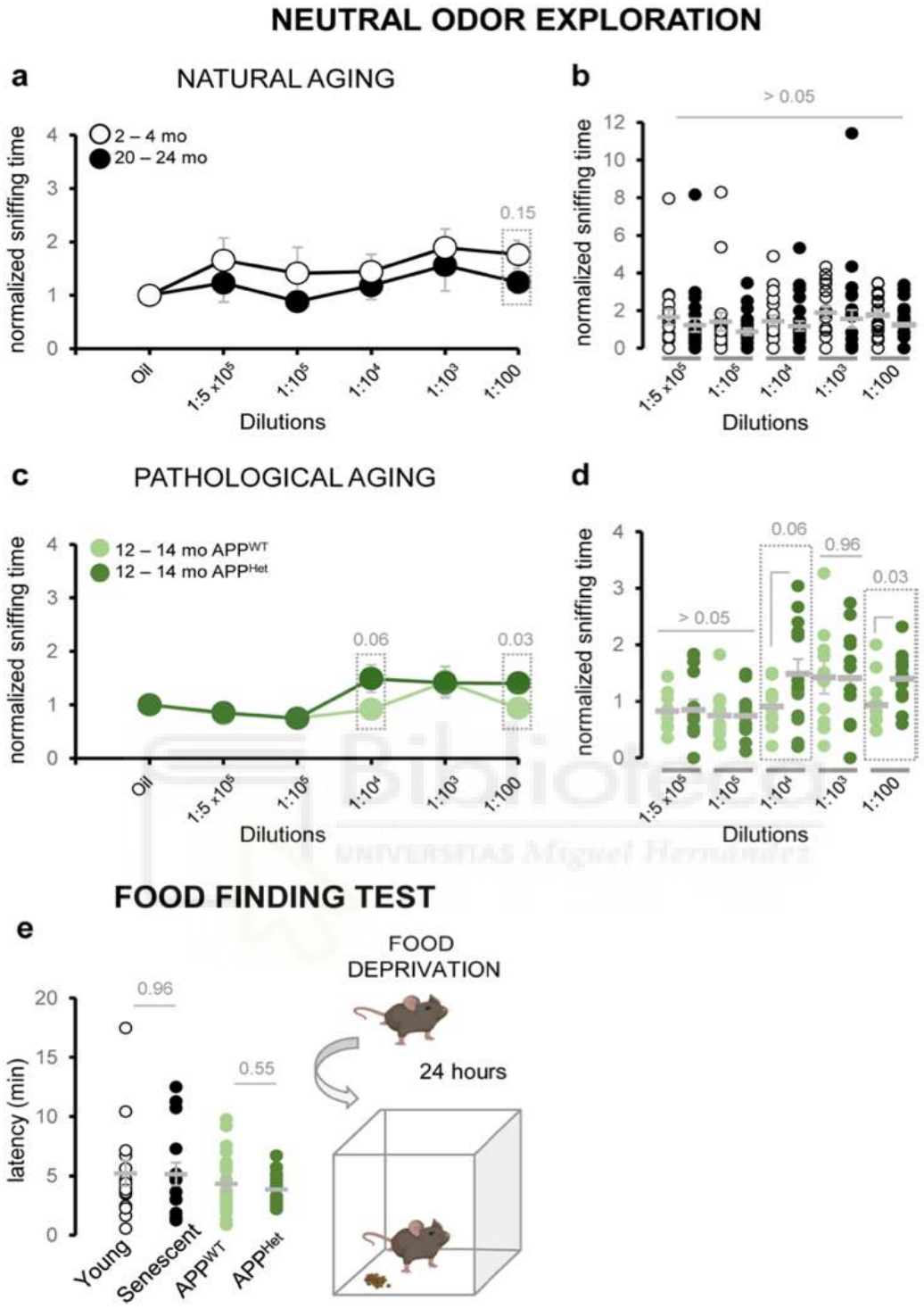

Figure 32. Aging and neurodegeneration impact social odor recognition more severely than other odor modalities. **a**, Average of the sniffing time of young and aged mice in response to a neutral synthetic odor (IA) normalized to the vehicle (mineral oil). **b**, Dispersion plots of the normalized sniffing time of young and aged mice in response to various IA dilutions. **c**, Average of the sniffing time of middle-aged APP/PS1^{WT} and APP/PS1^{Het} mice in response to IA samples normalized to the vehicle (mineral oil). **d**, Dispersion plots of normalized sniffing time of APP/PS1^{WT} and APP/PS1^{Het} mice in response to various IA

dilutions. Note that APP/PS1^{Het} mice showed higher exploration times for the 1:104 and 1:100 IA dilutions. **e**, Food- deprived animals performed a food finding test (schematics on the right) which revealed equivalent latencies to find hidden food pellets as shown in the dispersion data plot (left panel). Thick grey lines in the dispersion plot indicate mean ± SEM. Data were analyzed by a one-way ANOVA with Tukey's test to test multiple comparisons with more than one variable. $P \leq 0.05$ was considered statistically significant. P values are indicated above the corresponding comparisons.

4.6. Social odor discrimination and habituation are reduced in naturally aged and AD mouse model

To further investigate the impact of aging and neurodegeneration in the detection of social information, we performed a habituation–dishabituation test, which relies on the animal's ability to discriminate novel smells (Yang and Crawley, 2009). For these experiments, young (2–4 mo.) and aged (20–24 mo.) wild-type animals were presented three consecutive replicates of urine samples from two different animals (S1a-c and S2a-c) (Figure 33a). Aged animals were able to discriminate between urine sources, but showed reduced sniffing times during the first and second discrimination and habituation phases (Figure 33b, c). Similarly, middle-aged APP/PS1^{Het} mice also exhibited reduced sniffing times in comparison to aged-matched APP/PS1^{WT} controls (Figure 33d). Analysis of the slope values of the first and second discrimination and habituation phases revealed that senescent mice exhibited significant deficits during both rounds of social habituation–dishabituation, whereas APP/PS1^{Het} mouse impairments were apparent during the second phase of discrimination (Figure 33; ANNEX I).

Then, we adapted the habituation-dishabituation test to assay potential changes in long-term social odor memory (Figure 33f). Thus, animals were exposed to the same S1a urine sample 24h after the first presentation. A reduction of the sniffing time during the first discrimination phase was interpreted as an indicator of memory. This reduction was clearly observed in young adults, but absent in naturally aged and 1-year-old APP/PS1^{Het} mice (Figure 34g; ANNEX 1), suggesting long-term social odor memory impairments during both natural and pathological aging.

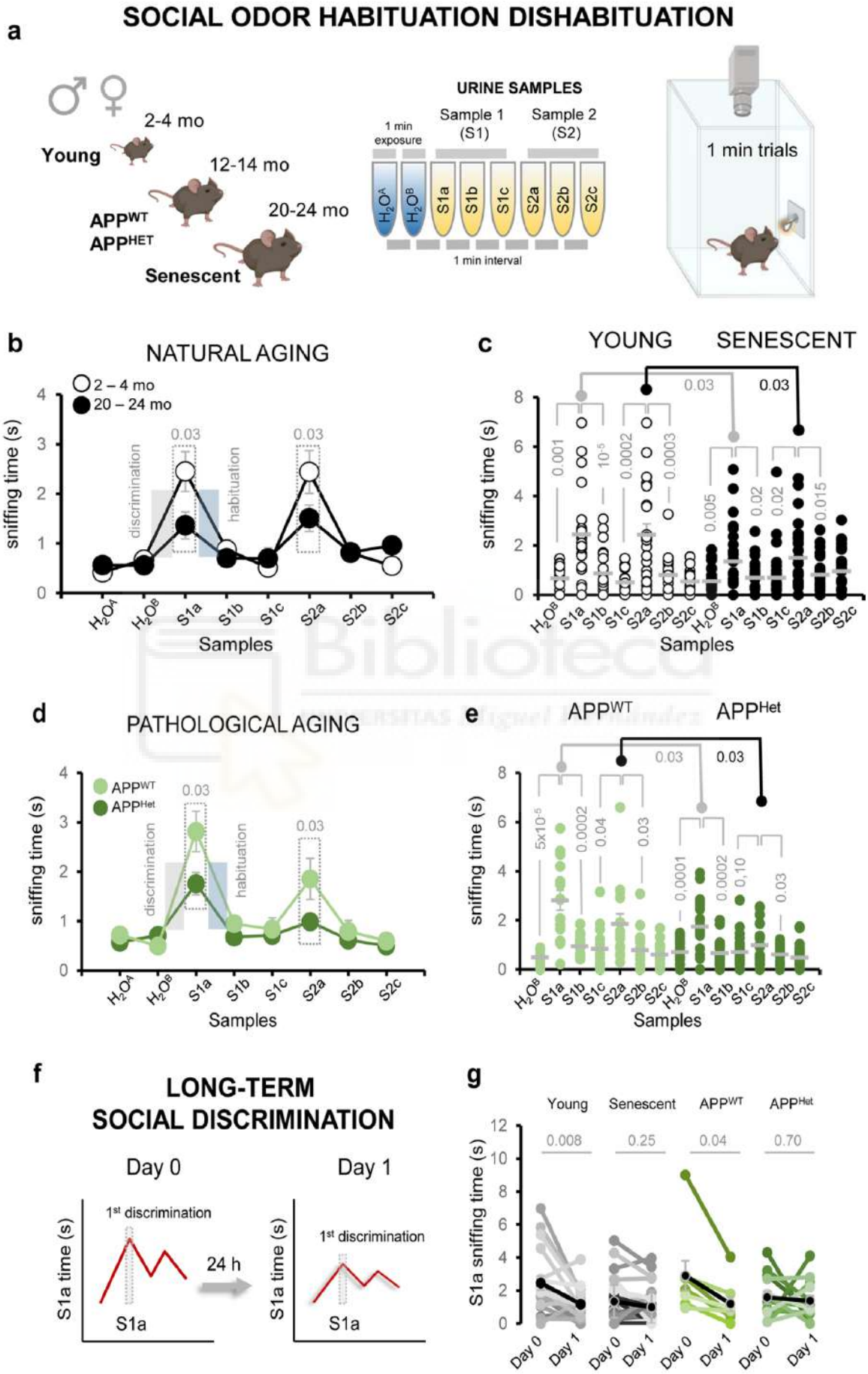
a
SOCIAL ODOR HABITUATION DISHABITUATION
2-4 mo
Young
12-14 mo
APPWT
APPHET
20-24 mo
Senescent
URINE SAMPLES
1 min exposure
Sample 1 (S1)
Sample 2 (S2)
H2OA
H2OB
S1a
S1b
S1c
S2a
S2b
S2c
1 min interval
1 min trials
b
NATURAL AGING
2 – 4 mo
20 – 24 mo
sniffing time (s)
discrimination
habituation
0.03
0.03
Samples
c
YOUNG
SENESCENT
0.03
0.03
0.001
10-5
0.0002
0.0003
0.005
0.02
0.02
0.015
d
PATHOLOGICAL AGING
APPWT
APPHet
e
APPWT
APPHet
5x10-5
0.0002
0.04
0.03
0.0001
0.0002
0,10
0.03
f
LONG-TERM
SOCIAL DISCRIMINATION
Day 0
Day 1
1st discrimination
24 h
S1a time (s)
S1a
g
Young
Senescent
APPWT
APPHet
0.008
0.25
0.04
0.70
S1a sniffing time (s)
Day 0
Day 1

Figure 33. Social odor discrimination and habituation are reduced in naturally aged and APP/PS1^{Het} mice. a, Schematics of the social habituation-dishabituation test used in this study: after habituation to the experimental cage, the animal was exposed to the same urine sample three times (S1a-c) which induces a typical increase in exploration time (1st discrimination) to be followed by a reduction in the sniffing time (1st habituation). Dishabituation induced by a urine sample from a new subject (S2a) elicits a second round of habituation–habituation (see "Materials and Methods" for details). **b,** Average sniffing time of the social habituation-dishabituation test performed by young and aged wild-type mice. **c,** Dispersion plot of the sniffing time of young and aged animals during the social habituation-dishabituation test. **d,** Average sniffing time of the social habituation-dishabituation test performed by middle-aged APP/PS1^{WT} controls and age-matched APP/ PS1^{Het} mice. **e,** Dispersion plot of the sniffing time of middle-aged APP/PS1^{WT} controls and APP/PS1^{Het} mice during the social habituation-dishabituation test. **f,** The habituation-dishabituation test was modified to assess potential deficits in long-term discrimination due to natural or pathological aging by presenting the same S1a sample 24h after. **g,** Paired data corresponding to the sniffing time during the first and second S1a presentation (24h later) is plotted for each condition. Thick lines in dispersion plots and black dots in g, indicate mean ± SEM. Data were analyzed by a one-way ANOVA with Tukey's test to test multiple comparisons with more than one variable. $P \leq 0.05$ was considered statistically significant. *P* values are indicated above the corresponding comparisons.

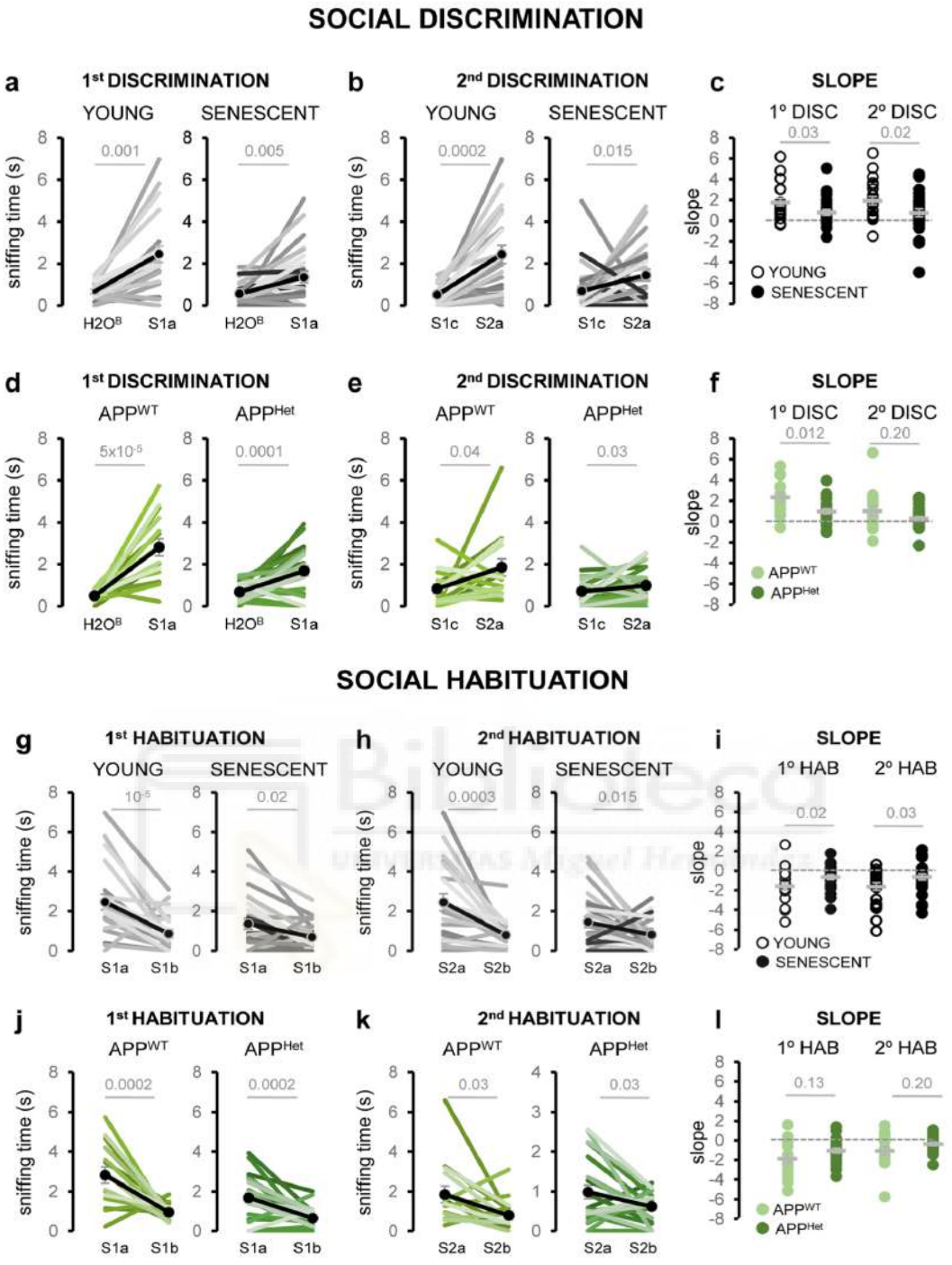

Figure 34. Analysis of the social discrimination and habituation decay during natural and pathological aging. **a,** Paired data of the sniffing time of young and aged wild-type animals corresponding to the first discrimination phase (H_2O-S1a). **b,** Paired data of the sniffing time of young and aged wild-type animals corresponding to the second discrimination phase (S1c-S2a). **c,** Dispersion plots of the slope values corresponding to the first and second discrimination phases of young and aged mice. **d,** Paired data of the sniffing time of APP^{WT} and APP^{Het} mice corresponding to the first discrimination phase (H_2O-

S1a). **e,** Paired data of the sniffing time of APP^{WT} and APP^{Het} mice corresponding to the second discrimination phase (S1c-S2a). **f,** Dispersion plots of APP^{WT} and APP^{Het} mice corresponding to the slope values of the first and second discrimination phases. **g,** Paired data of the sniffing time of young and aged wild-type animals corresponding to the first habituation phase (S1a-S1b). **h,** Paired data of the sniffing time of the young and aged wild-type animals corresponding to the second habituation phase (S2a-S2b). **I,** Dispersion plots of the slope values of young and aged mice corresponding to the first and second habituation phases. **j** Paired data of the sniffing time of APP^{WT} and APP^{Het} mice corresponding to the first habituation phase (S1a-S1b). **k,** Paired data of the sniffing time of APP^{WT} and APP^{Het} mice corresponding to the second habituation phase (S2a-S2b). **l** Dispersion plots of the slope values of APP^{WT} and APP^{Het} mice corresponding to the first and second habituation phases. Black dots in **a**, **b**, **d**, **e**, **g**, **h**, **j**, **k** and thick lines in **c**, **f**, **i**, **l** indicate mean ± SEM. Data were analyzed by one-way ANOVA with Tukey's test. $P \leq 0.05$ was considered statistically significant. *P* values are indicated above the corresponding comparisons

4.7. Age-related deficits in social discrimination and habituation are not influenced by previous experience

Subsequently, we conducted an experiment involving animals exposed to either familiar (littermate urine, L) or novel social odors (novel urine, N) in the habituation-dishabituation test (Figure 35a). Aged animals exhibited a poor performance in the L-N dishabituation task, with no significant increase in sniffing time. This implies that the decline in social odor discrimination and habituation is not influenced by prior experience.

Given that the deficiencies in social odor discrimination were more pronounced in naturally aged mice, we inquired whether these deficits extended to the recognition of the animal's own odors. Loss of self-awareness is a commonly occurring disruptive symptom in senescent subjects (La Joie et al., 2016; Valech et al., 2018). For this purpose, animals were presented with samples of their own urine (O) during the second discrimination phase of the habituation-dishabituation test (Figure 35c, d). Our findings indicated that the animal's own urine effectively triggered a typical discrimination (dishabituation) response (Figure 35; ANNEX I).

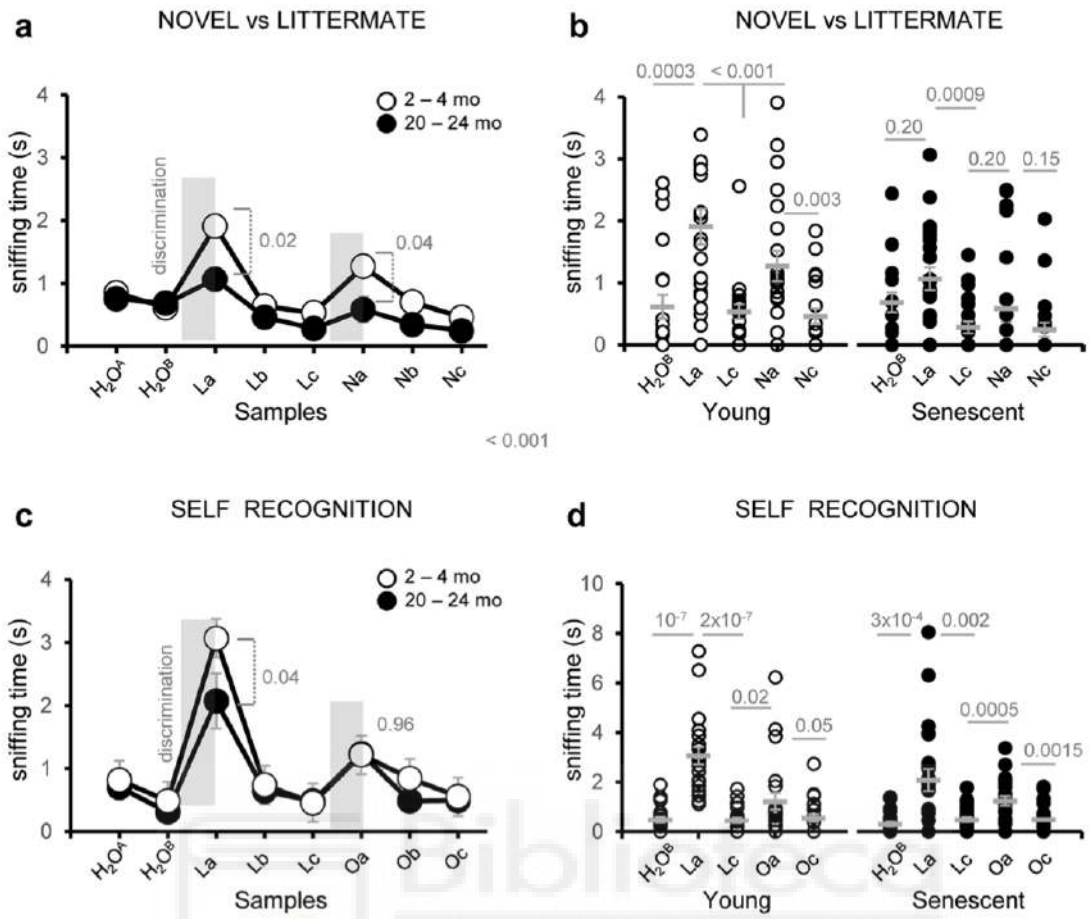

Figure 35. Age-related deficits in social discrimination and habituation are not influenced by previous experience. **a,** Average sniffing time of social habituation-dishabituation test in response to odors from novel (N) or littermate (L) subjects of young and naturally aged mice. **b,** Dispersion plot of the exploration time of young and senescent animals in response to novel or littermate urine samples. **c,** Average sniffing time of social habituation-dishabituation test in response to littermate and animal's own urine (O). **d,** Dispersion plot of exploration time of young and naturally aged animals in response to their own or littermate urine samples. Thick grey lines in dispersion plots indicate mean ± SEM. Data were analyzed by a one-way ANOVA with Tukey's test to test multiple comparisons with more than one variable. $P \leq 0.05$ was considered statistically significant. *P* values are indicated above the corresponding comparisons.

4.8. Social novelty is disrupted during pathological aging

Finally, we investigated whether the identified impairments in social odor exploration and discrimination might adversely affect social interaction in both naturally aged and APP/PS1^{Het} mice. For this purpose, we conducted a three-chamber test (Nadler et al., 2004) (Figure 36a) to evaluate general sociability and social novelty in senescent and APP/PS1^{Het} animals. Our data revealed a decrease in social novelty in middle-aged APP1/PS1^{Het} mice, a trend not observed in 2-year-old animals (Fig. 36b–e; ANNEX I).

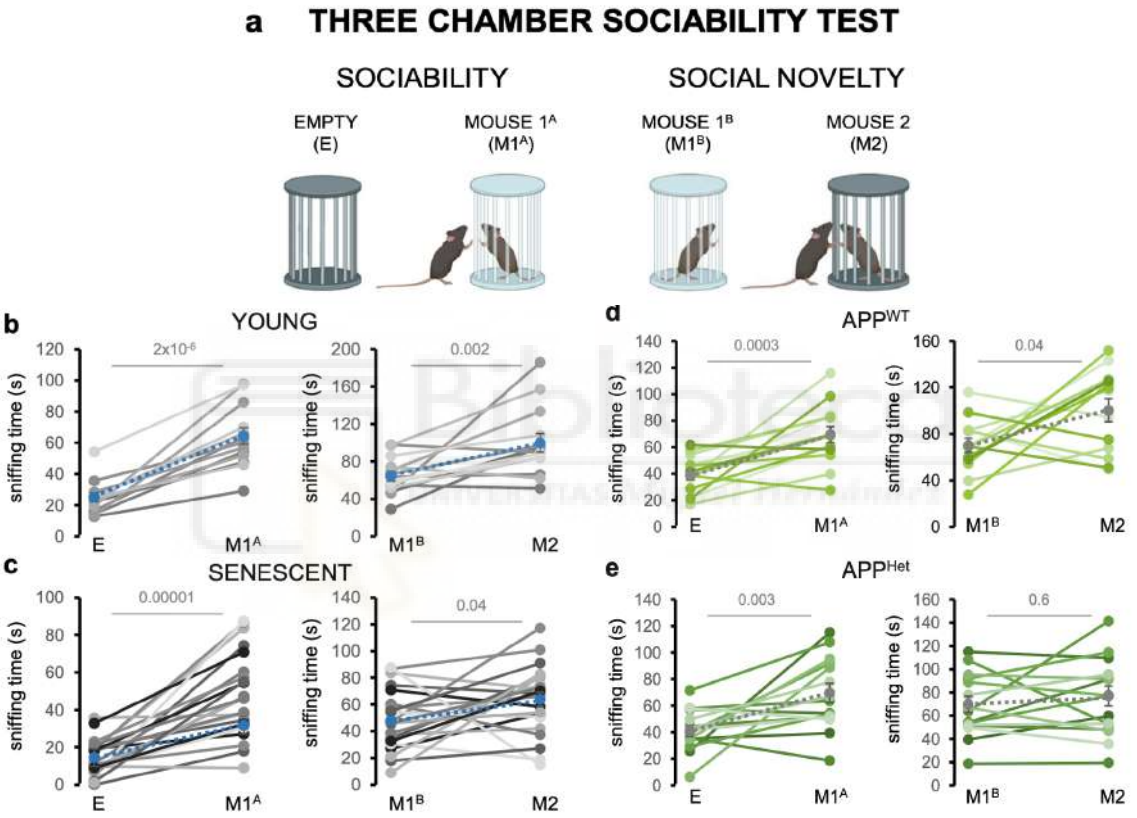

Figure 36. Social novelty is disrupted during pathological aging. a, Schematics of the three-chamber test used in this study to test sociability and social novelty. In the sociability phase, the sniffing time of E and M1^{A} is compared. Social novelty is estimated by quantifying the sniffing time of exploring M1^{B} versus M2 (see "Materials and Methods section"). **b,** Paired data of the sniffing times of young wild-type mice during the sociability (E-M1^{A}) and social novelty (M1^{B}-M2) phases. **c,** Paired data of the sniffing times of aged wild-type mice during sociability and social novelty. **d,** Paired data of the sniffing times of middle-aged APP^{WT} mice during sociability and social novelty. **e,** Paired data of the sniffing times of middle-aged APP^{Het} mice during sociability and social novelty. Colored dots in the paired plots indicate mean ± SEM. Data were analyzed by a one-way ANOVA with Tukey's test to test multiple

comparisons with more than one variable. $P \leq 0.05$ was considered statistically significant. *P* values are indicated above the corresponding comparisons.

Although senescent mice did not exhibit significant impairments in either sociability or social novelty, there was a slight increase in the latency to approach M1 during the social novelty phase (Figure 37), aligning with the overall decrease in exploration time of social odors.

Altogether, these findings unveiled exacerbated deficits in an animal model of AD, suggesting a distinct impact of natural and pathological aging on the manifestation of social behavior.

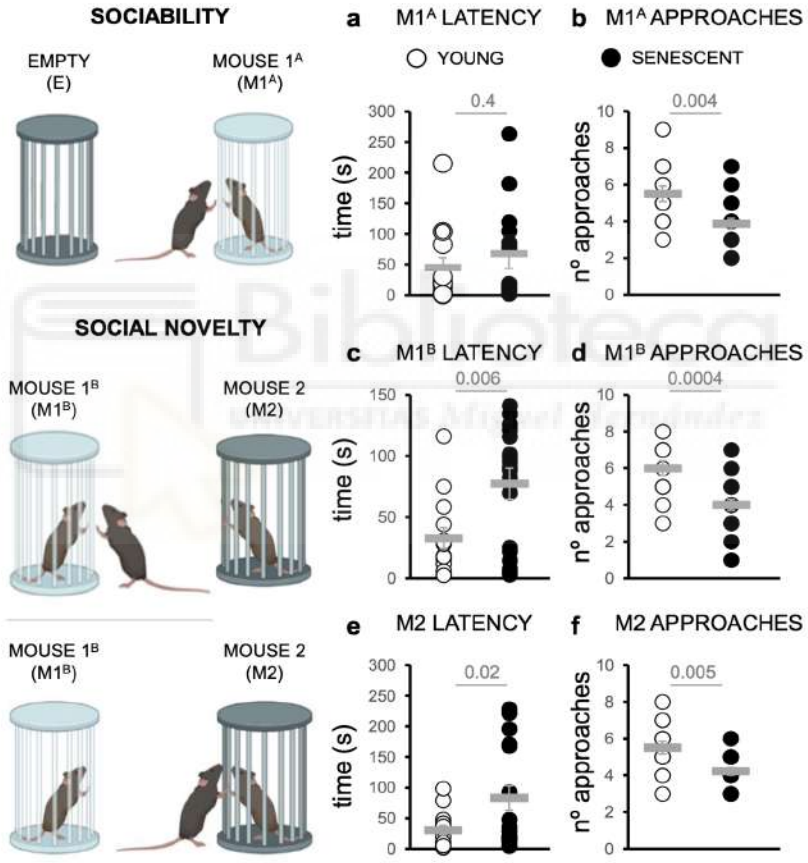

Figure 37. Senescent mice exhibit an increased latency to approach a familiar mouse during the social novelty phase. a, c, e, Latencies to approach a familiar ($M1^a$ and $M1^b$) and a novel mouse (M2) during the sociability and social novelty phases of the test. **b, d, f,** number of approaches to familiar and novel mouse in each test phase.

5. DISCUSSION

1. Natural and pathological aging impact distinctly on the VSE

We observed distinct effects of healthy and pathological aging on the VNO. Consequently, we developed and implemented a series of olfactory tests designed to assess pheromonal-encoded behaviors in mice. We chose these tests as they evaluate various aspects of general olfaction (e.g., detection of food odors) and social behavior (e.g., detection of social and non-social odors). These assessments have proven effective in delineating olfactory abilities in both healthy and pathological mouse models of aging, providing insights that could help develop novel therapies aimed at alleviating age-related diseases such as AD.

Our research provides new insights into the process of pathological aging from a widely used AD animal model. Arguably, the most unexpected result from our work is the unforeseen preservation of the VSE's proliferative capabilities in middle-aged APP/PS1^{Het} mice. These results stand in contrast to the diminished rate of neurogenesis within the SVZ observed in similar AD animal models (Verret et al., 2007; Zhang et al., 2007; Zeng et al., 2016; Scopa et al., 2020), indicating that VSE neurogenesis may be less vulnerable to damage (Brann and Firestein, 2010) and pathological conditions compared to other areas of cell proliferation such as the SVZ.

Furthermore, our data unveiled significant alterations in the VSE during natural aging, contrasting with the results in APP/PS1^{Het} mice. While the VSE of APP/PS1^{Het} mice exhibits unaltered neurogenic abilities, aged wild-type animals displayed a decline in both proliferative and stem cells (PCNA^{+} and Sox2^{+}-positive cells) within the VSE, as opposed to their younger counterparts (Figure 29). This decline may account for the observed reduction in mature OMP^{+} neurons, SCL-Sox2^{+} cells, and overall organ volume (Figure 26). Our findings align with two previous studies, reporting an overall thinning of the VSE (Mechin et al., 2021) and decreased VSE neurogenesis of 2-year-old animals (Brann and Firestein, 2010). It is worth noting that this reduction might not imply a complete elimination of proliferative capacities in older mice (Brann and Firestein, 2010),

but just a reduction with high interindividual variability (*experimental observations*).

2. Natural and pathological aging impair the exploration of socio-sexual cues and social discrimination-habituation

Surprisingly, the exploration of aging and its effects on olfactory capacities in rodents has been relatively neglected in the literature. One contributing factor to this gap of information is the methodologies employed for assessing olfactory abilities in rodents, predominantly relying on tests based in associative learning (Mandairon et al., 2006e). These tests evaluate the mice ability in associating certain odors with rewards or punishments, offering insights into their olfactory learning and memory. However, they may not necessarily unveil the unique dynamics of olfactory function. Associative learning tests involve training animals to execute specific behavioral responses, such as locating a hidden food pellet or avoiding a predator, based on their previous experiences as well as in their ability to detect and recognize specific odors. While valuable in understanding olfactory capabilities, these tests might overlook the subtle changes that specifically occur in the olfactory system as rodents age.

In addition, a noteworthy aspect of our research is that most prior studies addressing olfactory decline utilized synthetic or neutral odors, leaving understudied the specific impact of both healthy and diseased aging on the recognition of social cues. To advance into this question, we examined the exploration time and the habituation-dishabituation response to urine (Figures 30, 33, 34). Our discoveries demonstrated that despite the distinct effects of natural and pathological aging on the structure of the VSE, both processes hindered the exploration of socio-sexual cues, social discrimination-habituation, and social behavior. This suggests fundamental differences in how healthy and diseased aging affect social information processing.

3. The disruption observed in the VSE in aged mice could explain the behavioral deficits in processing social cues.

Additional experiments are required to establish a causal relationship, but our findings propose that the observed changes in the VSE in aging mice may contribute to deficiencies in urine exploration time (Figure 30 and ANNEX I). Such deficits could potentially hinder the processing of social information. Analysis of VSE volume data from middle-aged APP/PS1^{WT} control animals suggests that structural alterations in the VSE may manifest around the age of 12 months (Figure 26). However, the functional consequences of these changes might not become evident until the later stages of aging.

This scenario implies a gradual decline in the VNO that aligns with the aging process observed in other olfactory areas like the OB. Various studies have indicated that certain symptoms of OB aging, such as a reduced regeneration rate of OSNs, a decreased number of synaptic contacts (Richard et al., 2010), loss of expression of odorant receptor genes (Lee et al., 2009; Khan et al., 2013), or alterations in OSN dynamic range (Kass et al., 2018), are distinctly noticeable only in 2-year-old mice. This evidence suggests that although age-related changes may initiate earlier in the olfactory system (Mobley et al., 2014), functional and behavioral deficits may have a delayed onset, implying compensatory mechanisms to safeguard the processing of olfactory cues crucial for the survival of aged animals (Tikhonova et al., 2015).

In contrast to the natural gradual decline, pathological conditions may accelerate functional deficits, even in the absence of modifications in peripheral organs. This acceleration suggests disruptions in the central processing of social information. Notably, defects in the exploration of social odors were found to be exacerbated in middle-aged APP/PS1^{Het} mice (Figure 30), a condition likely to intensify frailty and diminish life expectancy in these animals, as observed in APP/PSEN1^{Het} under our experimental conditions.

4. The recognition of social cues may be altered during both natural and pathological aging

Data obtained from the long-term social habituation-dishabituation test indicated notable impairments in both 2-year-old wild-type animals and middle-aged APP/PS1^{Het} mice. This suggests that, in parallel with sensory decline, the downstream pathways responsible for social cue recognition may be influenced during both natural and pathological aging. To address the potential influence of novelty in the social habituation-dishabituation test, we introduced urine samples from littermate and novel animals, revealing similar deficits in discrimination (Figure 35a, b). Interestingly, while senescent animals displayed significant discrimination deficits, they retained the ability to distinguish between urine from a novel subject and their own. This prevented further exploration of the underlying mechanisms of subjective perception loss, a disruptive symptom of senescence and dementia that currently lacks suitable animal models for preclinical studies (Jessen et al., 2020).

The decline in olfactory detection associated with aging is likely due to alterations in both the MOE and the VNO (Lee et al., 2009; Ueha et al., 2018), potentially impacting various odor modalities. We explored this question by conducting odor-evoked sniffing tests using social and neutral synthetic odors (Figure 32). Quantifying the exploration time across various IA dilutions revealed no significant differences between senescent and young mice, and even increased responses in APP/PS1^{Het} mice. Furthermore, results from the FFT showed no changes in the latency time to find hidden food pellets (Figure 32e). This indicates that defects in social odor detection related to natural and pathological aging might be more severe than those in other odor modalities, such as food odors, which drive vital behaviors like foraging and feeding, reported to be mainly preserved in old age (Harb et al., 2014).

Moreover, the decline in detecting specific odors may result from alterations in the number of sensory neurons and synaptic connections specifically related to the discrimination of conspecifics (Li and Liberles, 2015; Iurilli and Datta, 2017), and heterospecific social cues (e.g., predators) (Iurilli and Datta, 2017).

Alternatively, discrimination of conspecifics, involving repetitive exposure and learning, may be processed by circuits different from those recognizing innate cues like reproductive or predator odors. Notably, impairments in social odor exploration and discrimination may arise from maladaptation of the VNO-AOB axis, consistent with the observed decrease in AOB volume (Figure 28).

5. Natural and pathological aging impacts differently on social behaviors

Social interactions and social support contribute to cognitive reserve, or resilience, which refers to the brain's ability to cope with age-related changes or neurological damage (Livingston et al., 2020). Active social engagement may enhance cognitive function and provide a protective effect against the onset of dementia. Additionally, social support networks can buffer against stress, which is a significant risk factor for mental illness (Herbert, 1997). Biological factors, such as genetics or neurobiology, interact with psychological and social factors to influence disease development. For example, genetic predispositions for certain mental illnesses may be triggered or influenced by adverse social environments or limited social support. Understanding the relationship between social life, aging and dementia requires basic studies in animal models.

In our research, we aimed to understand how age-related deficiencies in social odor sensitivity, discrimination, and memory influence social behavior. The results of a three-chamber test (Figure 36) indicated that sociability was generally maintained in naturally aged and APP/PS1^{Het} animals. However, social novelty was significantly impaired in APP/PS1^{Het} mice, consistent with previous studies (Locci et al., 2021).

The deficits in social novelty observed in APP/PS1^{Het} mice could be associated with the impaired social discrimination observed in the habituation-dishabituation test (Figures 33d, e and 34d, f), potentially hindering the recognition of M2 as a novel subject (Enwere et al., 2004; Moreno et al., 2014). Despite the overall decrease in exploration time for social odors (Figure 30 and ANNEX I), aged animals exhibited an increase in latency to approach novel or familiar mice (M1^{A}, M1^{B}, M2) and a reduced number of approaches (Figure 37). These findings

suggest potential locomotion deficits, although they were not sufficient to impede the adequate performance of the social novelty test. In summary, despite the decline in social odor exploration and discrimination, overall sociability and novelty are largely preserved in naturally aged mice.

It is crucial to note that in contrast, the APP/PS1 neurodegenerative model displays a measurable impairment in social novelty, possibly stemming from a broader issue in learning and memory, a hallmark of AD. This evidence suggests that neuronal circuits governing specific social functions (sociability vs social memory) may be particularly vulnerable to pathological aging.

6. The olfactory and vomeronasal systems as biomarkers for healthy and pathological aging

Our research indicates that the olfactory and vomeronasal systems are distinctively impacted, both anatomically and functionally, by natural and pathological aging. These distinctive effects could be exploited to develop novel tests for early detection of neurodegenerative processes, as well as expanding the basic knowledge of neuronal circuit adaptation in response to aging.

In addition to the normal aging process, certain pathological conditions or diseases can further impair olfactory function. The AD mouse model used in this study exhibits olfactory dysfunction as an early symptom, demonstrating its value to further explore the underlying mechanisms of neurodegenerative disease progression and potential identification of diagnostic markers.

Understanding how the olfactory system changes with age can provide insights into the mechanisms of neuroplasticity and how it may be influenced by both normal and pathological aging. By examining changes in olfactory function, neurobiological markers, and behavioral responses to odors in aged animals. Thus, with this study, we have gained a better understanding of the molecular and cellular mechanisms underlying olfactory natural and pathological aging.

As olfactory deficits can serve as a marker for neurodegeneration and pathological conditions, its implementation in the clinic should be further tested and promoted in parallel to exploring novel neuroprotective strategies. Therefore, investigating the kinetics of olfactory impairments in rodents may contribute to the development of interventions or treatments to mitigate age-related olfactory decline in humans.

Finally, an additional benefit of the tests employed in this work is that they mimic the innate exploratory activity, inherent in mouse´s natural behavior, avoiding associative conditioning approaches. The data derived from mice can be compared to human impairments as the behavioral assays we implemented closely mirror the paradigms utilized in behavioral tasks explored in humans. The selected tests enabled us to differentiate between discrimination and recognition deficits in the context of both healthy and pathological aging. Furthermore, they made possible to unveil that these two types of aging impact olfactory perception with distinct temporal dynamics. Additionally, these olfactory tests provide an ideal framework to further investigate the effects of aging in social cue perception at both the molecular and behavioral level

In summary, by studying the VNS and its changes with aging, we can gain insights into the broader processes of normal and pathological aging in the brain. The olfactory system's unique characteristics make it a valuable model for understanding age-related adaptations, neuroplasticity, and the role of olfactory dysfunction in age-related diseases.

6. CONCLUSIONS

Olfactory deficits are present in nearly 90 % of AD patients, an impairment believed to appear during early stages of the disease, and thus with great potential as a biomarker not only for AD but also for other neurodegenerative disorders such as Parkinson's and Huntington's disease. **Our research provides a novel characterization of the cellular adaptations of the vomeronasal system during natural and pathological aging.** This work has revealed natural and pathological aging have distinct effects at the cellular level which surprisingly resulted in similar outcomes regarding social odor perception and social behavior. The main conclusions of this study can be summarized as follows:

1. Natural and pathological aging distinctly impact the VSE cell population and structure.

2. Unexpectedly, pathological aging assayed in a common animal model of AD (APP/PS1 mice) was associated with normal VNO structure and intact neurogenic capabilities.

3. Naturally-aged mice showed a significant decline in cell proliferation, number of mature OSNs, and reduced AOB volume.

4. Despite the distinctive impact of healthy and pathological aging onto the VNO, both aging processes impaired the sensitivity to social odors (urine).

5. APP/PS1 mice exhibited a more significant impairment in the sensitivity to social odors compared to naturally-aged mice. These impairments were already detected in middle-age animals.

6. Both natural and pathological aging significantly impaired the processing of social odors compared to other smell types, such as food or synthetic odors.

7. Impairments in social odor habituation-dishabituation test during natural aging are independent of previous experience.

8. Despite severe deficits in social odor sensitivity and discrimination, overall sociability is preserved during both natural and pathological aging.

9. Social novelty is significantly impaired in an animal model of AD (APP/PS1 mice) in contrast to senescent animals that exhibit a milder reduction.

General conclusion

While natural aging and AD mice display distinct effects at the cellular level in the VSE, both scenarios disrupt the detection of social odors more severely than other odor modalities. Notably, social detection and behavior impairments are exacerbated in the AD model, suggesting that pathological aging affects the downstream processing of social information even in the absence of observable alterations in the VSE.

CONCLUSIONES

Los déficits olfatorios están presentes en casi el 90 % de los pacientes con enfermedad de Alzheimer (EA), un deterioro que se cree que aparece durante las primeras etapas de la enfermedad, y por lo tanto, con un gran potencial como biomarcador no solo para la EA, sino también para otros trastornos neurodegenerativos como el Parkinson y la enfermedad de Huntington. **Nuestra investigación proporciona una nueva caracterización de las adaptaciones celulares del sistema vomeronasal durante el envejecimiento natural y patológico**. Este trabajo ha revelado que el envejecimiento natural y patológico tienen efectos distintos a nivel celular. A pesar de estas diferencias, ambos procesos de envejecimiento se encuentran asociados a resultados similares en cuanto a resultados similares en cuanto a la percepción de olores sociales y el comportamiento social. Las principales conclusiones de este estudio se pueden resumir de la siguiente manera:

1. El envejecimiento natural y patológico afecta de manera distinta a la población y estructura celular de las células del VSE.

2. Sorprendentemente, el envejecimiento patológico evaluado en un modelo animal de EA (línea transgénica APP/PS1) no afectó a la estructura y capacidades neurogénicas intactas del VNO.

3. Los ratones envejecidos de forma natural mostraron una disminución significativa en la proliferación celular, el número de neuronas sensoriales olfativas maduras y un volumen reducido del AOB.

4. A pesar del impacto distintivo del envejecimiento saludable y patológico en el VNO, ambos procesos de envejecimiento afectaron la sensibilidad a olores sociales (orina).

5. Los ratones APP/PS1 mostraron un deterioro más significativo en la sensibilidad a los olores sociales en comparación con los ratones

envejecidos de forma natural. Estos déficits se detectaron en animales de mediana edad.

6. Tanto el envejecimiento natural como el patológico afectaron significativamente al procesamiento de olores sociales en comparación con otros tipos de olores, como alimentos u olores sintéticos.

7. Los deterioros en la prueba de habituación-deshabituación al olor social durante el envejecimiento natural son independientes de la experiencia previa.

8. A pesar de los déficits significativos en la sensibilidad y discriminación de los olores sociales, la sociabilidad general se encuentra preservada durante el envejecimiento natural y patológico.

9. La novedad social está significativamente deteriorada en un modelo animal de EA (ratones APP/PS1), en contraste con los animales senescentes que muestran una reducción más leve.

Conclusión general

Mientras que el envejecimiento natural y los ratones modelo de EA muestran efectos distintos a nivel celular en el VSE, ambos escenarios reducen la detección de olores sociales de manera más severa que otras modalidades olfativas. Notablemente, los deterioros en la detección social y el comportamiento social se agravan en el modelo animal de EA, lo que sugiere que el envejecimiento patológico afecta el procesamiento de la información social incluso en ausencia de alteraciones observables en el VSE.

Future perspectives

Our research revealed that natural aging impacts the structure and cellular composition of the VSE. Due to the role of this organ, these changes may affect the mice chemical communication capabilities, and, consequently, its behavior. However, these hypotheses should be confirmed by further functional studies, for example taking advantage of genetically-targeted optogenetics to modulate the activity of the VNS in old and APP/PS1 animals to assess behavioral responses upon social odor stimulation. Furthermore, future studies should delve into the anatomical and functional properties of the VNO-AOB circuit to gain a comprehensive understanding of how healthy and pathological aging impact social information processing. The influence of pathological aging on pheromone-encoded behaviors has the potential to disturb various aspects of social communication, possibly causing alterations in mating, social hierarchies, territorial behaviors, and other responses triggered by pheromones. Additional research is necessary to investigate these behavioral adaptations caused by AD-related mutations.

Additionally, conducting longitudinal studies that monitor olfactory capabilities in rodents over their entire lifespan would be highly informative. Such studies could offer valuable insights into the progression of olfactory impairments over time and help determine whether the decline in olfactory function follows a gradual or abrupt pattern at specific stages of aging. This type of information will be crucial in order to determine the predictive value of olfactory tests to identify the optimal time window for therapeutic interventions.

7. BIBLIOGRAPHY

Ackels T, von der Weid B, Rodriguez I, Spehr M. (2014) Physiological characterization of formyl peptide receptor expressing cells in the mouse vomeronasal organ. Front Neuroanat, 8, 134.

Adjei S, Houck AL, Ma K, Wesson DW. (2013) Age-dependent alterations in the number, volume, and localization of islands of Calleja within the olfactory tubercle. Neurobiol Aging, 34(11), 2676-2682.

Akiyoshi S, Ishii T, Bai Z, Mombaerts P. (2018) Subpopulations of vomeronasal sensory neurons with coordinated coexpression of type 2 vomeronasal receptor genes are differentially dependent on Vmn2r1. Eur J Neurosci, 47(7), 887-900.

Alves J, Petrosyan A, Magalhães R. (2014) Olfactory dysfunction in dementia. World J Clin Cases, 2(11), 661-667.

Arnold SE, Lee EB, Moberg PJ, Stutzbach L, Kazi H, Han LY, Lee VM, Trojanowski JQ. (2010) Olfactory epithelium amyloid-beta and paired helical filament-tau pathology in Alzheimer disease. Ann Neurol, 67(4), 462-469.

Barnes IHA, Ibarra-Soria X, Fitzgerald S, Gonzalez JM, Davidson C, Hardy MP, Manthravadi D, Van Gerven L, Jorissen M, Zeng Z, Khan M, Mombaerts P, Harrow J, Logan DW, Frankish A. (2020) Expert curation of the human and mouse olfactory receptor gene repertoires identifies conserved coding regions split across two exons. BMC Genomics, 21(1), 196.

Barrios AW, Núñez G, Sánchez Quinteiro P, Salazar I. (2014) Anatomy, histochemistry, and immunohistochemistry of the olfactory subsystems in mice. Front Neuroanat, 8, 63.

Belluscio L, Koentges G, Axel R, Dulac C. (1999) A map of pheromone receptor activation in the mammalian brain. Cell, 97(2), 209-220.

Bitter T, Gudziol H, Burmeister HP, Mentzel HJ, Guntinas-Lichius O, Gaser C. (2010) Anosmia leads to a loss of gray matter in cortical brain areas. Chem Senses, 35(5), 407-415.

Boillat M, Challet L, Rossier D, Kan C, Carleton A, Rodriguez I. (2015) The vomeronasal system mediates sick conspecific avoidance. Curr Biol, 25, 251–255.

Bonfils, P., Faulcon, P., Tavernier, L., Bonfils, N.A., Malinvaud, D. (2008). [Home accidents associated with anosmia]. Presse Med, 37, 742-745.

Boyce JM, Shone GR. (2006) Effects of ageing on smell and taste. Postgrad Med J, 82(966), 239-241.

Braidy N, Muñoz P, Palacios AG, Castellano-Gonzalez G, Inestrosa NC, Chung RS, Sachdev P, Guillemin GJ. (2012) Recent rodent models for Alzheimer's disease: clinical implications and basic research. J Neural Transm (Vienna), 119(2), 173-195.

Brann JH, Firestein SJ. (2010) Regeneration of new neurons is preserved in aged vomeronasal epithelia. J Neurosci, 30, 15686–15694.

Brechbühl J, Klaey M, Broillet MC. (2008) Grueneberg ganglion cells mediate alarm pheromone detection in mice. Science, 321(5892), 1092-1095.

Breer, H. (2003) Olfactory receptors: molecular basis for recognition and discrimination of odors. Anal Bioanal Chem, 377, 427-433.

Breer H, Boekhoff I. (1992) Second messenger signalling in olfaction. Curr Opin Neurobiol, 2(4), 439-443.
Brennan PA, Zufall F. (2006) Pheromonal communication in vertebrates. Nature, 444(7117), 308-315.

Breton-Provencher V, Lemasson M, Peralta MR 3rd, Saghatelyan A. (2009) Interneurons produced in adulthood are required for the normal functioning of the olfactory bulb network and for the execution of selected olfactory behaviors. J Neurosci, 29, 15245–15257.

Bronson FH. (1971) Rodent pheromones. Biol Reprod, 4(3), 344-357.

Bruce HM. (1959) An exteroceptive block to pregnancy in the mouse. Nature, 184, 105.

Buck LB. (2000) The molecular architecture of odor and pheromone sensing in mammals. Cell, 100(6), 611-618.

Buck L, Axel R. (1991) A novel multigene family may encode odorant receptors: a molecular basis for odor recognition. Cell, 65(1), 175-187.

Bufe B, Schumann T, Zufall F. (2012) Formyl peptide receptors from immune and vomeronasal system exhibit distinct agonist properties. J Biol Chem, 287(40), 33644-33655.

Bufe B, Teuchert Y, Schmid A, Pyrski M, Perez-Gomez A, Eisenbeis J, et al. (2019) Bacterial MgrB peptide activates chemoreceptor Fpr3 in the mouse

accessory olfactory system and drives avoidance behaviour. Nat Commun, 10, 4889.

Buschhüter D, Smitka M, Puschmann S, Gerber JC, Witt M, Abolmaali ND, Hummel T. (2008) Correlation between olfactory bulb volume and olfactory function. Neuroimage, 42(2), 498-502.

Buzek A, Serwańska-Leja K, Zaworska-Zakrzewska A, Kasprowicz-Potocka M. (2022) The Shape of the Nasal Cavity and Adaptations to Sniffing in the Dog (Canis familiaris) Compared to Other Domesticated Mammals: A Review Article. Animals (Basel), 12(4), 517.

Chamero P, Marton TF, Logan DW, Flanagan K, Cruz JR, Saghatelian A, et al. (2007) Identification of protein pheromones that promote aggressive behaviour. Nature, 450, 899–902.

Chamero, P., Katsoulidou, V., Hendrix, P., Bufe, B., Roberts, R., Matsunami, H., et al. (2011) G protein G o is essential for vomeronasal function and aggressive behavior in mice. Proc. Natl. Acad. Sci. U.S.A., 108, 12898–12903.

Chamero P, Weiss J, Alonso MT, Rodríguez-Prados M, Hisatsune C, Mikoshiba K, Leinders-Zufall T, Zufall F. (2017) Type 3 inositol 1,4,5-trisphosphate receptor is dispensable for sensory activation of the mammalian vomeronasal organ. Sci Rep, 7, 10260.

Chandrashekar J, Mueller KL, Hoon MA, Adler E, Feng L, Guo W, Zuker CS, Ryba NJ. (2000) T2Rs function as bitter taste receptors. Cell, 100(6), 703-711.

Chaudhury D, Manella L, Arellanos A, Escanilla O, Cleland TA, Linster C. (2010) Olfactory bulb habituation to odor stimuli. Behav Neurosci, 124(4), 490-499.

Cheetham SA, Thom MD, Jury F, Ollier WER, Beynon RJ, Hurst JL. (2007) The genetic basis of individual-recognition signals in the mouse. Curr Biol, 17, 177–277.

Cheng N, Cai H, Belluscio L. (2011) In vivo olfactory model of APP-induced neurodegeneration reveals a reversible cell-autonomous function. J Neurosci, 31(39), 13699-13704.

Choudhury ES, Moberg P, Doty RL. (2003) Influences of age and sex on a microencapsulated odor memory test. Chem Senses, 28(9), 799-805.

Cichy A, Ackels T, Tsitoura C, Kahan A, Gronloh N, Söchtig M, Engelhardt CH, Ben-Shaul Y, Müller F, Spehr J, Spehr M. (2015) Extracellular pH regulates excitability of vomeronasal sensory neurons. J Neurosci, 35(9), 4025-4039.

Dan X, Wechter N, Gray S, Mohanty JG, Croteau DL, Bohr VA. (2021) Olfactory dysfunction in aging and neurodegenerative diseases. Ageing Res Rev, 70, 101416.

Daramola OO, Becker SS. (2015) An algorithmic approach to the evaluation and treatment of olfactory disorders. Curr Opin Otolaryngol Head Neck Surg, 23(1), 8-14.

Deacon RMJ, Koros E, Bornemann KD, Rawlins JNP. (2009) Aged Tg2576 mice are impaired on social memory and open field habituation tests. Behav Brain Res, 197, 466–468.

Devanand, D. P., Michaels-Marston, K. S., Liu, X., Pelton, G. H., Padilla, M., Marder, K., et al. (2000). Olfactory deficits in patients with mild cognitive impairment predict Alzheimer's disease at follow-up. Am. J. Psychiatry, 157, 1399–1405.

Doty, R. L., Shaman, P., Applebaum, S. L., Giberson, R., Siksorski, L., and Rosenberg, L. (1984a). Smell identification ability: changes with age. Science, 226, 1441–1443.

Doty, R. L., Petersen, I., Mensah, N., and Christensen, K. (2011). Genetic and environmental influences on odor identification ability in the very old. Psychol. Aging, 26, 864–871.

Doty RL. (2012) Olfactory dysfunction in Parkinson disease. Nat Rev Neurol, 8(6), 329-339.

Doty RL. (2014) Human Pheromones: Do They Exist? In: Mucignat-Caretta C, editor. Neurobiology of Chemical Communication. CRC Press/Taylor & Francis; Chapter 19.

Doty RL, Kamath V. (2014) The influences of age on olfaction: a review. Front Psychol, 5, 20.

Doty, RL, Perl, DP, Steele, JC, Chen, KM, Pierce, JD Jr, Reyes, P, et al. (1991). Odor identification deficit of the parkinsonism-dementia complex of Guam: equivalence to that of Alzheimer's and idiopathic Parkinson's disease. Neurology, 41, 77–80.

Duchamp-Viret P, Chaput MA, Duchamp A. (1999) Odor response properties of rat olfactory receptor neurons. Science, 284(5423), 2171-2174.

Dulac C. (2000) Sensory coding of pheromone signals in mammals. Curr Opin Neurobiol, 10(4), 511-518.

Dulac C, Axel R. (1995) A novel family of genes encoding putative pheromone receptors in mammals. Cell, 83(2), 195-206.

Dulac C, Torello AT. (2003) Molecular detection of pheromone signals in mammals: from genes to behavior. Nat Rev Neurosci, 4(7), 551-562.

Enwere E, Shingo T, Gregg C, Fujikawa H, Ohta S, Weiss S. (2004) Aging results in reduced epidermal growth factor receptor signaling, diminished olfactory neurogenesis, and deficits in fine olfactory discrimination. J Neurosci, 24, 8354–8365.

Ferencz B, Gerritsen L. (2015) Genetics and underlying pathology of dementia. Neuropsychol Rev, 25(1), 113-124.

Ferrero DM, Moeller LM, Osakada T, Horio N, Li Q, Roy DS, Cichy A, Spehr M et al. (2013) A juvenile mouse pheromone inhibits sexual behavior through the vomeronasal system. Nature, 502, 368–371.

Firestein, S. (2001) How the olfactory system makes sense of scents. Nature, 413, 211-218.

Fornazieri MA, dos Santos CA, Bezerra TF, Pinna Fde R, Voegels RL, Doty RL. (2015) Development of normative data for the Brazilian adaptation of the University of Pennsylvania Smell Identification Test. Chem Senses, 40(2), 141-149.

Fortes-Marco L, Lanuza E, Martinez-Garcia F, Agustín-Pavón C. (2015) Avoidance and contextual learning induced by a kairomone, a pheromone, and a common odorant in female CD1 mice. Front Neurosci, 9, 336.

Friard O, Gamba M. (2016) BORIS: a free, versatile open-source event-logging software for video/audio coding and live observations. Methods Ecol Evol, 7, 1325–1330.

Fu X, Yan Y, Xu PS, Geerlof-Vidavsky I, Chong W, Gross ML, Holy TE. (2015) A Molecular Code for Identity in the Vomeronasal System. Cell, 163(2), 313-323.

Gallarda BW, Lledo PM. (2012) Adult neurogenesis in the olfactory system and neurodegenerative disease. Curr Mol Med, 12(10), 1253-1260.

Gangrade BK, Dominic CJ. (1984) Studies of the male-originating pheromones involved in the Whitten effect and Bruce effect in mice. Biol Reprod, 31(1), 89-96.

Garratt M, Stockley P, Armstrong SD, Beynon RJ, Hurst JL. (2011) The scent of senescence: sexual signaling and female preference in house mice. J Evol Biol, 11, 2398–2409.

Gheusi G, Cremer H, McLean H, Chazal G, Vincent JD, Lledo PM. (2000) Importance of newly generated neurons in the adult OB for odor discrimination. Proc Natl Acad Sci U S A, 97, 1823–1828.

Giacobini P, Benedetto A, Tirindelli R, Fasolo A. (2000) Proliferation and migration of receptor neurons in the vomeronasal organ of the adult mouse. Brain Res Dev Brain Res, 123, 33–40.

Godfrey PA, Malnic B, Buck LB. (2004) The mouse olfactory receptor gene family. Proc Natl Acad Sci U S A, 101(7), 2156-2161.

Guo Z, Packard A, Krolewski RC, Harris MT, Manglapus GL, Schwob JE. (2010) Expression of pax6 and sox2 in adult olfactory epithelium. J Comp Neurol, 18, 4395–4418.

Haga S, Hattori T, Sato T, Sato K, Matsuda S, Kobayakawa R, Sakano H, Yoshihara Y, Kikusui T, Touhara K. (2010) The male mouse pheromone ESP1 enhances female sexual receptive behavior through a specific vomeronasal receptor. Nature, 466(7302), 118-122.

Halpern M. (1987) The organization and function of the vomeronasal system. Annu Rev Neurosci, 10, 325-362.

Halpern M, Martínez-Marcos A. (2003) Structure and function of the vomeronasal system: an update. Prog Neurobiol, 70, 245–318.

Harb MR, Sousa N, Zihl J, Almeida OFX (2014) Reward compo- nents of feeding behavior are preserved during mouse aging. Front Aging Neurosci 6:242

Hasegawa-Ishii S, Shimada A, Imamura F. (2019) Neuroplastic changes in the olfactory bulb associated with nasal inflammation in mice. J Allergy Clin Immunol, 143(3), 978-989.e3.

Hasen NS, Gammie SC. (2009) Trpc2 gene impacts on maternal aggression, accessory olfactory bulb anatomy and brain activity. Genes Brain Behav, 8(7), 639-649.

Haughey NJ, Nath A, Chan SL, Borchard AC, Rao MS, Mattson MP. (2002) Disruption of neurogenesis by amyloid beta-peptide, and perturbed neural progenitor cell homeostasis, in models of Alzheimer's disease. J Neurochem, 83(6), 1509-1524.

Hawkes C. (2006) Olfaction in neurodegenerative disorder. Adv Otorhinolaryngol, 63, 133-151.

He J, Ma L, Kim S, Nakai J, Yu CR. (2008) Encoding gender and individual information in the mouse vomeronasal organ. Science, 320(5875), 535-538.

Henkin RI, Schmidt L, Velicu I. (2013) Interleukin 6 in hyposmia. JAMA Otolaryngol Head Neck Surg, 139(7), 728-734.

Herbert J. (1997) Stress, the brain, and mental illness. BMJ, 315(7107), 530-535.

Herrada G, Dulac C. (1997) A novel family of putative pheromone receptors in mammals with a topographically organized and sexually dimorphic distribution. Cell, 90(4), 763-773.

Huang Y, Mucke L. (2012) Alzheimer mechanisms and therapeutic strategies. Cell, 148(6), 1204-1222.

Huang H, Nie S, Cao M, Marshall C, Gao J, Xiao N, Hu G, Xiao M. (2016) Characterization of AD-like phenotype in aged APPSwe/PS1dE9 mice. Age (Dordr), 38(4), 303-322.

Hummel T, Kobal G, Gudziol H, Mackay-Sim A. (2007) Normative data for the "Sniffin' Sticks" including tests of odor identification, odor discrimination, and olfactory thresholds: an upgrade based on a group of more than 3,000 subjects. Eur Arch Otorhinolaryngol, 264(3), 237-243.

Hummel T, Nordin, S. (2005) Olfactory disorders and their consequences for quality of life. Acta Otolaryngol, 125, 116-121.

Hummel, T, Welge-Luessen, A. (2006) Assessment of olfactory function. Adv Otorhinolaryngol, 63, 84-98.

Iurilli G, Datta SR. (2017) Population coding in an innately relevant olfactory area. Neuron, 93, 1180–1197.

Isogai Y, Si S, Pont-Lezica L, Tan T, Kapoor V, Murthy VN, Dulac C. (2011) Molecular organization of vomeronasal chemoreception. Nature, 478(7368), 241-245.

Jacobson L. (1813) Anatomisk beskrivelse over et nyt organ I huusdyrenes naese. Veter Salesk Skr, 2, 209–246.

Jagetia S, Milton AJ, Stetzik LA, Liu S, Pai K, Arakawa K, Mandairon N, Wesson DW. (2018) Inter- and intra-mouse variability in odor preferences revealed in an olfactory multiple-choice test. Behav Neurosci, 132, 88–98.

Jakupovic J, Kang N, Baum MJ. (2008) Effect of bilateral accessory olfactory bulb lesions on volatile urinary odor discrimination and investigation as well as mating behavior in male mice. Physiol Behav, 93(3), 467-473.

Jankowsky JL, Fadale DJ, Anderson J, Xu GM, Gonzales V, Jenkins NA, Copeland NG, Lee MK et al. (2004) Mutant presenilins specifically elevate the levels of the 42 residue beta-amyloid peptide in vivo: evidence for augmentation of a 42-specific gamma-secretase. Hum Mol Genet, 13, 159–170.

Jankowsky JL, Slunt HH, Ratovitski T, Jenkins NA, Copeland NG, Borchelt DR. (2001) Co-expression of multiple transgenes in mouse CNS: a comparison of strategies. Biomol Eng, 17, 157–165.

Janus C, Flores AY, Xu G, Borchelt DR. (2015) Behavioral abnormalities in APPSwe/PS1dE9 mouse model of AD-like pathology: comparative analysis across multiple behavioral domains. Neurobiol Aging, 36(9), 2519-2532.

Jessen F, Amariglio RE, Buckley RF, van der Flier WM, Han Y, Molinuevo JL, Rabin L, Rentz DM et al. (2020) The characterisation of subjective cognitive decline. Lancet Neurol, 19, 271–278.

Johns MA, Feder HH, Komisaruk BR, Mayer AD. (1978) Urine-induced reflex ovulation in anovulatory rats may be a vomeronasal effect. Nature, 272(5652), 446-448.

Johns MA. (1986) The role of the vomeronasal organ in behavioral control of reproduction. Ann. N. Y. Acad. Sci., 474, 148–157.

Kaneda H, Maeshima K, Goto N, Kobayakawa T, Ayabe-Kanamura S, Saito S. (2000) Decline in taste and odor discrimination abilities with age, and relationship between gustation and olfaction. Chem Senses, 25(3), 331-337.

Kaneko N, Debski EA, Wilson MC, Whitten WK. (1980) Puberty acceleration in mice. II. Evidence that the vomeronasal organ is a receptor for the primer pheromone in male mouse urine. Biol Reprod, 22(4), 873-878.

Karlson, P, Lüscher, M. (1959) 'Pheromones': a New Term for a Class of Biologically Active Substances. Nature, 183, 55–56.

Katada, S, Hirokawa, T, Oka, Y, Suwa, M, Touhara, K. (2005) Structural basis for a broad but selective ligand spectrum of a mouse olfactory receptor: mapping the odorant-binding site. J Neurosci, 25, 1806-1815.

Katreddi RR, Forni PE. (2012) Mechanisms underlying pre- and postnatal development of the vomeronasal organ. Cell Mol Life Sci, 78, 5069–5082.

Kass MD, Czarnecki LA, McGann JP. (2018) Stable olfactory sensory neuron in vivo physiology during normal aging. Neurobiol Aging, 69, 33–37.

Kelliher KR, Spehr M, Li XH, Zufall F, Leinders-Zufall T. (2006) Pheromonal recognition memory induced by TRPC2-independent vomeronasal sensing. Eur J Neurosci, 23(12), 3385-3390.

Kelliher KR. (2007) The combined role of the main olfactory and vomeronasal systems in social communication in mammals. Horm Behav, 52(5), 561-570.

Khan M, Vaes E, Mombaerts P. (2013) Temporal patterns of odorant receptor gene expression in adult and aged mice. Mol Cell Neurosci, 57, 120–129.

Kim B, Haney S, Milan AP, Joshi S, Aldworth Z, Rulkov N, Kim AT, Bazhenov M, Stopfer A. (2023) Olfactory receptor neurons generate multiple response motifs, increasing coding space dimensionality. Elife, 12, e79152.

Kimchi T, Xu J, Dulac C. (2007) A functional circuit underlying male sexual behaviour in the female mouse brain. Nature, 448(7157), 1009-1014.

Kobayakawa K, Kobayakawa R, Matsumoto H, Oka Y, Imai T, Ikawa M, Okabe M, Ikeda T, et al. (2007) Innate versus learned odour processing in the mouse olfactory bulb. Nature, 450, 503–508.

Kondo K, Kikuta S, Ueha R, Suzukawa K, Yamasoba T. (2020) Age-Related Olfactory Dysfunction: Epidemiology, Pathophysiology, and Clinical Management. Front Aging Neurosci, 12, 208.

Konstantinidis I, Hummel T, Larsson M. (2006) Identification of unpleasant odors is independent of age. Arch Clin Neuropsychol, 21(7), 615-621.

Kurien BT, Everds NE, Scofield RH. (2004) Experimental animal urine collection.

La Joie R, Perrotin A, Egret S, Pasquier F, Tomadesso C, Mézenge F, Desgranges B, de La Sayette V, et al. (2016) Qualitative and quantitative assessment of self-reported cognitive difficulties in nondemented elders: association with medical help seeking, cognitive deficits, and β-amyloid imaging. Alzheimers Dement, 5, 23–34.

Landis BN, Konnerth CG, Hummel T. (2004) A study on the frequency of olfactory dysfunction. Laryngoscope, 114(10), 1764-1769.

Lee S, Boot LM. (1955) Spontaneous pseudopregnancy in mice. Acta Physiol. Pharmacol. Neurol., 4, 422–443.

Lee AC, Tian H, Grosmaitre X, Ma M. (2009) Expression patterns of odorant receptors and response properties of olfactory sensory neurons in aged mice. Chem Senses, 34, 695–703.

Leinders-Zufall T, Lane AP, Puche AC, Ma W, Novotny MV, Shipley MT, Zufall F. (2000) Ultrasensitive pheromone detection by mammalian vomeronasal neurons. Nature, 405, 792-796.

Leypold BG, Yu CR, Leinders-Zufall T, Kim MM, Zufall F, Axel R. (2002) Altered sexual and social behaviors in trp2 mutant mice. Proc Natl Acad Sci U S A, 99(9), 6376-6381.

Liberles SD. (2015) Trace amine-associated receptors: ligands, neural circuits, and behaviors. Curr Opin Neurobiol, 34, 1-7.

Liberles SD, Horowitz LF, Kuang D, Contos JJ, Wilson KL, Siltberg-Liberles J, Liberles DA, Buck LB. (2009) Formyl peptide receptors are candidate chemosensory receptors in the vomeronasal organ. Proc Natl Acad Sci U S A, 106(24), 9842-9847.

Li Q, Liberles SD. (2015) Aversion and attraction through olfaction. Curr Biol, 25, R120–R129.

Livingston G, Huntley J, Sommerlad A, Ames D, Ballard C, Banerjee S, Brayne C, Burns A, Cohen-Mansfield J, Cooper C, Costafreda SG, Dias A, Fox N, Gitlin LN, Howard R, Kales HC, Kivimäki M, Larson EB, Ogunniyi A, Orgeta V, Ritchie K, Rockwood K, Sampson EL, Samus Q, Schneider LS, Selbæk G, Teri L, Mukadam N. (2020) Dementia prevention, intervention, and care: 2020 report of the Lancet Commission. Lancet, 396(10248), 413-446.

Locci A, Orellana H, Rodríguez G, Gottliebson M, McClarty B, Domínguez S, Keszycki R, Dong H. (2021) Comparison of memory, affective behavior, and neuropathology in APPNLGF knock-in mice to 5xFAD and APP/PS1 mice. Behav Brain Res, 404, 113192.

Lomas DE, Keverne EB. (1982) Role of the vomeronasal organ and prolactin in the acceleration of puberty in female mice. J Reprod Fertil, 66(1), 101-107.

Mandairon N, Sacquet J, Garcia S, Ravel N, Jourdan F, Didier A. (2006) Neurogenic correlates of an olfactory discrimination task in the adult olfactory bulb. Eur J Neurosci, 24, 3578-3588.

Mandiyan VS, Coats JK, Shah NM. (2005) Deficits in sexual and aggressive behaviors in Cnga2 mutant mice. Nat Neurosci, 8(12), 1660-1662.

Marchlewska-Koj A. (1977) Pregnancy block elicited by urinary proteins of male mice. Biol Reprod, 17(5), 729-732.

Matsunami H, Buck LB. (1997) A multigene family encoding a diverse array of putative pheromone receptors in mammals. Cell, 90(4), 775-784.

McCotter, Rollo E. (1912). "The connection of the vomeronasal nerves with the accessory olfactory bulb in the opossum and other mammals." The Anatomical Record, 6(8), 299-318.

Mechin V, Pageat P, Teruel E, Asproni P. (2021) Histological and immunohistochemical characterization of vomeronasal organ aging in mice. Animals, 11, 1211.

Meredith M. (2001) Human vomeronasal organ function: a critical review of best and worst cases. Chem Senses, 26(4), 433-445.

Miyamichi K, Amat F, Moussavi F, Wang C, Wickersham I, Wall NR, Taniguchi H, Tasic B, Huang ZJ, He Z, Callaway EM, Horowitz MA, Luo L. (2011) Cortical representations of olfactory input by trans-synaptic tracing. Nature, 472(7342), 191-196.

Mobley AS, Rodríguez-Gil DJ, Imamura F, Greer CA. (2014) Aging in the olfactory system. Trends Neurosci, 37, 77–84.

Moine F, Brechbühl J, Nenniger Tosato M, Beaumann M, Broillet MC. (2018) Alarm pheromone and kairomone detection via bitter taste receptors in the mouse Grueneberg ganglion. BMC Biol, 16(1), 12.

Mombaerts P. (2006) Axonal wiring in the mouse olfactory system. Annu Rev Cell Dev Biol, 22, 713-737.

Mombaerts P, Wang F, Dulac C, Chao SK, Nemes A, Mendelsohn M, Edmondson J, Axel R. (1996) Visualizing an olfactory sensory map. Cell, 87, 675-686.

Moreno M, Richard M, Landrein B, Sacquet J, Didier A, Mandairon N. (2014) Alteration of olfactory perceptual learning and its cellular basis in aged mice. Neurobiol Aging, 35, 680-691.

Mori K, Yoshihara Y. (1995) Molecular recognition and olfactory processing in the mammalian olfactory system. Prog Neurobiol, 45(6), 585-619.

Munger SD, Leinders-Zufall T, Zufall F. (2009) Subsystem organization of the mammalian sense of smell. Annu Rev Physiol, 71, 115-140.

Murphy C, Cain WS, Gilmore MM, Skinner RB. (1991). Sensory and semantic factors in recognition memory for odors and graphic stimuli: elderly versus young persons. Am J Psychol, 104, 161-192.

Murphy C, Nordin S, Acosta L. (1997). Odor learning, recall, and recognition memory in young and elderly adults. Neuropsychology, 11, 126-137.

Murphy C, Schubert CR, Cruickshanks KJ, Klein BEK, Klein R, Nondahl DM. (2002). Prevalence of olfactory impairment in older adults. JAMA, 288, 2307-2312.

Nadler JJ, Moy SS, Dold G, Trang D, Simmons N, Pérez A, Young NB, Barbaro RP et al. (2004). Automated apparatus for quantitation of social approach behaviors in mice. Genes Brain Behav, 3, 303-314.

Nagayama S, Homma R, Imamura F. (2014). Neuronal organization of olfactory bulb circuits. Front Neural Circuits, 8, 98.

Novotny MV. (2003). Pheromones, binding proteins and receptor responses in rodents. Biochem Soc Trans, 31(Pt 1), 117-122.

Ogg MC, Bendahamane M, Fletcher ML. (2015). Habituation of glomerular responses in the olfactory bulb following prolonged odor stimulation reflects reduced peripheral input. Front Mol Neurosci, 8, 53.

Panaliappan TK, Wittmann W, Jidigam VK, Mercurio S, Bertolini JA, Sghari S, Bose R, Patthey C et al. (2018). Sox2 is required for olfactory pit formation and olfactory neurogenesis through BMP restriction and Hes5 upregulation. Development, 145, dev153791.

Pankevich DE, Baum MJ, Cherry JA. (2004). Olfactory sex discrimination persists, whereas the preference for urinary odorants from estrous females disappears in male mice after vomeronasal organ removal. J Neurosci, 24(42), 9451-9457.

Pardo-Bellver C, Martínez-Bellver S, Martínez-García F, Lanuza E, and Teruel-Martí V. (2017). Synchronized Activity in The Main and Accessory Olfactory Bulbs and Vomeronasal Amygdala Elicited by Chemical Signals in Freely Behaving Mice. Sci. Rep., 7, 9924.

Parrish-Aungst S, Shipley MT, Erdelyi F, Szabo G, Puche AC. (2007). Quantitative analysis of neuronal diversity in the mouse olfactory bulb. J Comp Neurol, 501, 825-836.

Pérez-Gómez A, Stein B, Leinders-Zufall T, Chamero P. (2014). Signaling mechanisms and behavioral function of the mouse basal vomeronasal neuroepithelium. Front Neuroanat, 8, 135.

Pérez-Gómez A, Bleymehl K, Stein B, Pyrski M, Birnbaumer L, Munger SD, et al. (2015). Innate predator odor aversion driven by parallel olfactory subsystems that converge in the ventromedial hypothalamus. Curr Biol, 25, 1340-1346.

Powers JB, Winans SS. (1975). Vomeronasal organ: critical role in mediating sexual behavior of the male hamster. Science, 187(4180), 961-963.

Raisman G. (1972). An experimental study of the projection of the amygdala to the accessory olfactory bulb and its relationship to the concept of a dual olfactory system. Exp Brain Res, 14(4), 395-408.

Rawson NE, Gomez G, Cowart BJ, Kriete A, Pribitkin E, Restrepo D. (2012). Age-associated loss of selectivity in human olfactory sensory neurons. Neurobiol Aging, 33, 1913-1919.

Reiserer RS, Harrison FE, Syverud DC, McDonald MP. (2007). Impaired spatial learning in the APPSwe + PSEN1DeltaE9 bigenic mouse model of Alzheimer's disease. Genes Brain Behav, 6, 54-65.

Richard MB, Taylor SR, Greer CA. (2010). Age-induced disruption of selective olfactory bulb synaptic circuits. Proc Natl Acad Sci U S A, 107, 15613-15618.

Roberts RO, Christianson TJ, Kremers WK, Mielke MM, Machulda MM, Vassilaki M, Alhurani RE, Geda YE et al. (2016). Association between olfactory dysfunction and amnestic mild cognitive impairment and Alzheimer disease dementia. JAMA Neurol, 73, 93-101.

Rivière S, Challet L, Fluegge D, Spehr M, Rodriguez I. (2009). Formyl peptide receptor-like proteins are a novel family of vomeronasal chemosensors. Nature, 459, 574–577.

Rodriguez I, Feinstein P, Mombaerts P. (1999). Variable patterns of axonal projections of sensory neurons in the mouse vomeronasal system. Cell, 97(2), 199-208.

Rodriguez I. (2016). Vomeronasal Receptors: V1Rs, V2Rs, and FPRs. In: Zufall F., Munger S.D., editors. Chemosensory Transduction: The Detection of Odors, Tastes, and Other Chemostimuli, 1st ed. Volume 10. Academic Press; Cambridge, MA, USA.

Ruysh F. (1703). Thesaurus Anatomicus III. Amsterdam: Wolters. p. 49. Table IV, Figure V.

Ryba NJ, Tirindelli R. (1997). A new multigene family of putative pheromone receptors. Neuron, 19(2), 371-379.

Saiz-Sanchez D, De La Rosa-Prieto C, Ubeda-Bañon I, Martinez-Marcos A. (2013). Interneurons and beta-amyloid in the olfactory bulb, anterior olfactory nucleus and olfactory tubercle in APPxPS1 transgenic mice model of Alzheimer's disease. Anat Rec (Hoboken), 296(9), 1413-1423.

Sam M, Vora S, Malnic B, Ma W, Novotny MV, Buck LB. (2001). Odorants may arouse instinctive behaviors. Nature, 412(6843), 142.

Sanderson DJ, Bannerman DM. (2011). Competitive short-term and long-term memory processes in spatial habituation. J Exp Psychol Anim Behav Process, 37, 189-199.

Saraiva LR, Kondoh K, Ye X, Yoon KH, Hernandez M, Buck LB. (2016). Combinatorial effects of odorants on mouse behavior. Proc Natl Acad Sci U S A, 113, E3300–E3306.

Sathyanesan A, Feijoo AA, Mehta ST, Nimarko AF, Lin W. (2013). Expression profile of G-protein βγ subunit gene transcripts in the mouse olfactory sensory epithelia. Front Cell Neurosci, 7, 84.

Scalia F, Winans SS. (1975). The differential projections of the olfactory bulb and accessory olfactory bulb in mammals. J Comp Neurol, 161(1), 31-55.

Scangas GA, Bleier BS. (2017). Anosmia: Differential diagnosis, evaluation, and management. Am J Rhinol Allergy, 31(1), 3-7.

Schneider J, Dickinson MH, Levine JD. (2012). Social structures depend on innate determinants and chemosensory processing in Drosophila. Proc Natl Acad Sci U S A, 109 Suppl 2(Suppl 2), 17174-9.

Schubert CR, Cruickshanks KJ, Fischer ME, Huang GH, Klein BE, Klein, R, et al. (2012). Olfactory impairment in an adult population: the Beaver Dam Offspring Study. Chem. Senses, 37, 325–334.

Scopa C, Marrocco F, Latina V, Ruggeri F, Corvaglia V, La Regina F, Ammassari-Teule M, Middei S et al. (2020). Impaired adult neurogenesis is an early event in Alzheimer's disease neurodegeneration, mediated by intracellular Aβ oligomers. Cell Death Differ, 27, 934–948.

Segura B, Baggio HC, Solana E, Palacios EM, Vendrell P, Bargalló N, Junqué C. (2013). Neuroanatomical correlates of olfactory loss in normal aged subjects. Behav Brain Res, 246, 148-53.

Semmering ST. (1809). Abbildungen der menschlichen Organe des Geruches. Frankfurt: Varrentrap und Wenner.

Seo JH, Pyo S, Shin YK, Nam BG, Kang JW, Kim KP, Lee HY, Cho SR. (2018). The Effect of Environmental Enrichment on Glutathione-Mediated Xenobiotic Metabolism and Antioxidation in Normal Adult Mice. Front Neurol, 9, 425.

Smith TD, Laitman JT, Bhatnagar KP. (2014). The shrinking anthropoid nose, the human vomeronasal organ, and the language of anatomical reduction. Anat Rec (Hoboken), 297(11), 2196-204.

Sosulski DL, Bloom ML, Cutforth T, Axel R, Datta SR. (2011). Distinct representations of olfactory information in different cortical centres. Nature, 472(7342), 213-6.

Spehr M, Wetzel CH, Hatt H, Ache BW. (2002). 3-phosphoinositides modulate cyclic nucleotide signaling in olfactory receptor neurons. Neuron, 33(5), 731-9.

Stevens JC, Plantinga A, Cain WS. (1982). Reduction of odor and nasal pungency associated with aging. Neurobiol Aging, 3(2), 125-32.

Stevens JC, Cain WS. (1987). Old-age deficits in the sense of smell as gauged by thresholds, magnitude matching, and odor identification. Psychol Aging, 2(1), 36-42.

Stowers L, Holy TE, Meister M, Dulac C, Koentges G. (2002). Loss of sex discrimination and male-male aggression in mice deficient for TRP2. Science, 295, 1493–1500.

Sullivan SL, Ressler KJ, Buck LB. (1995). Spatial patterning and information coding in the olfactory system. Curr Opin Genet Dev, 5(4), 516-23.

Sultan-Styne K, Toledo R, Walker C, Kallkopf A, Ribak CE, Guthrie KM. (2009). Long-term survival of olfactory sensory neurons after target depletion. J Comp Neurol, 515(6), 696-710.

Takigami S, Mori Y, Ichikawa M. (2000). Projection pattern of vomeronasal neurons to the accessory olfactory bulb in goats. Chem. Senses, 25, 387–393.

Takigami S, Mori Y, Tanioka Y, Ichikawa M. (2004). Morphological evidence for two types of mammalian vomeronasal system. Chem Senses, 29, 301–310.

Taroc EZM, Katreddi RR, Forni PE. (2020). Identifying Isl1 genetic lineage in the developing olfactory system and in GnRH-1 neurons. Front Physiol, 11, 601923.

Tikhonova MA, Romaschenko AV, Akulov AE, Ho YJ, Kolosova NG, Moshkin MP, Amstislavskaya TG. (2015). Comparative study of perception and processing of socially or sexually significant odor information in male rats with normal or accelerated senescence using fMRI. Behav Brain Res, 294, 89–94.

Trotier D, Eloit C, Wassef M, Talmain G, Bensimon JL, Døving KB, Ferrand J. (2000). The vomeronasal cavity in adult humans. Chem Senses. 369-80.

Tucker ES, Lehtinen MK, Maynard T, Zirlinger M, Dulac C, Rawson N, Pevny L, La-Mantia AS. (2010). Proliferative and transcriptional identity of distinct classes of neural precursors in the mammalian olfactory epithelium. Development, 137, 2471–2481.

Ueha R, Shichino S, Ueha S, Kondo K, Kikuta S, Nishijima H, Matsushima K, Yamasoba T. (2018). Reduction of proliferating olfactory cells and low expression of extracellular matrix genes are hallmarks of the aged olfactory mucosa. Front Aging Neurosci, 10, 86.

Valech N, Tort-Merino A, Coll-Padrós N, Olives J, León M, Rami L, Molinuevo JL. (2018). Executive and language subjective cognitive decline complaints discriminate preclinical Alzheimer's disease from normal aging. J Alzheimers Dis, 61, 689–703.

Vandenbergh JG. (1969). Male odor accelerates female sexual maturation in mice. Endocrinology, 84, 658–660.

Verret L, Jankowsky JL, Xu GM, Borchelt DR, Rampon C. (2007). Alzheimer's-type amyloidosis in transgenic mice impairs survival of newborn neurons derived from adult hippocampal neurogenesis. J Neurosci, 27, 6771–6780.

Webster SJ, Bachstetter AD, Nelson PT, Schmitt FA, Van Eldik LJ. (2014). Using mice to model Alzheimer's dementia: an overview of the clinical disease and the preclinical behavioral changes in 10 mouse models. Front Genet, 5, 88.

Weiß E, Kretschmer D. (2018). Formyl-Peptide Receptors in Infection, Inflammation, and Cancer. Trends Immunol, 39(10), 815-829.

Wesson DW, Levy E, Nixon RA, Wilson DA. (2010). Olfactory dysfunction correlates with amyloid-beta burden in an Alzheimer's disease mouse model. J Neurosci, 30, 505-514.

Whitten WK. (1956). Modification of the oestrous cycle of the mouse by external stimuli associated with the male. J Endocrinol, 13(4), 399-404.

Wilson RS, Arnold SE, Tang Y, Bennett DA. (2006). Odor identification and decline in different cognitive domains in old age. Neuroepidemiology, 26(2), 61-7.

Wilson RS, Yu L, Bennett DA. (2011). Odor identification and mortality in old age. Chem Senses, 36(1), 63-7.

Winans SS, Scalia F. (1970). Amygdaloid nucleus: new afferent input from the vomeronasal organ. Science, 170(3955), 330-2.

Witt M, Thiemer R, Meyer A, Schmitt O, Wree A. (2018). Main Olfactory and Vomeronasal Epithelium Are Differently Affected in Niemann-Pick Disease Type C1. Int J Mol Sci, 19(11), 3563.

Wong FK, Bercsenyi K, Sreenivasan V, Portalés A, Fernández-Otero M, Marín O. (2018). Pyramidal cell regulation of interneuron survival sculpts cortical networks. Nature, 557, 668–673.

Wyatt TD. (2017). Pheromones. Curr Biol, 27(15), R739-R743.

Wysocki CJ. (1979). Neurobehavioral evidence for the involvement of the vomeronasal system in mammalian reproduction. Neurosci Biobehav Rev, 3(4), 301-41.

Wysocki CJ, Gilbert AN. (1989). National Geographic Smell Survey. Effects of age are heterogenous. Ann N Y Acad Sci, 561, 12-28.

Wysocki CJ, Nyby J, Whitney G, Beauchamp GK, Katz Y. (1982). The vomeronasal organ: primary role in mouse chemosensory gender recognition. Physiol Behav, 29(2), 315-27.

Xu F, Schaefer M, Kida I, Schafer J, Liu N, Rothman DL, Hyder F, Restrepo D, Shepherd GM. (2005). Simultaneous activation of mouse main and accessory olfactory bulbs by odors or pheromones. J Comp Neurol, 489(4), 491-500.

Yang M, Crawley JN. (2009). Simple behavioral assessment of mouse olfaction. Curr Protoc Neurosci, 8, Unit 8.24.

Zeng Q, Zheng M, Zhang T, He G. (2016). Hippocampal neurogenesis in the APP/PS1/nestin-GFP triple transgenic mouse model of Alzheimer's disease. Neuroscience, 314, 64–74.

Zhang C, McNeil E, Dressler L, Siman R. (2007). Long-lasting impairment in hippocampal neurogenesis associated with amyloid deposition in a knock-in mouse model of familial Alzheimer's disease. Exp Neurol, 204, 77–87.

Zufall F, Leinders-Zufall T. (2000). The cellular and molecular basis of odor adaptation. Chem Senses, 25(4), 473-81.

ANNEX I - Author scientific publications

Molecular Neurobiology (2023) 60:4641–4658
https://doi.org/10.1007/s12035-023-03362-3

Natural and Pathological Aging Distinctively Impacts the Pheromone Detection System and Social Behavior

Adrián Portalés[1] · **Pablo Chamero**[2] · **Sandra Jurado**[1]

Received: 29 November 2022 / Accepted: 19 April 2023 / Published online: 2 May 2023

Abstract

Normal aging and many age-related disorders such as Alzheimer's disease cause deficits in olfaction; however, it is currently unknown how natural and pathological aging impacts the detection of social odors which might contribute to the impoverishment of social behavior at old age further worsening overall health. Analysis of the vomeronasal organ, the main gateway to pheromone-encoded information, indicated that natural and pathological aging distinctively affects the neurogenic ability of the vomeronasal sensory epithelium. Whereas cell proliferation remained majorly preserved in 1-year-old APP/PS1 mice, naturally aged animals exhibited significant deficiencies in the number of mature, proliferative, and progenitor cells. These alterations may support age-related deficits in the recognition of social cues and the display of social behavior. Our findings indicate that aging disrupts the processing of social olfactory cues decreasing social odor exploration, discrimination, and habituation in both wild-type senescent (2-year-old) mice and in 1-year-old double mutant model of Alzheimer's disease (APP/PS1). Furthermore, social novelty was diminished in 1-year-old APP/PS1 mice, indicating that alterations in the processing of social cues are accelerated during pathological aging. This study reveals fundamental differences in the cellular processes by which natural and pathological aging disrupts the exploration of social information and social behavior.

Keywords Aging · Pheromone · Vomeronasal system · Social behavior · Odor discrimination · Neurodegeneration

Abbreviations

AD	Alzheimer's disease
AOB	Anterior olfactory bulb
APP	Amyloid precursor protein
C	VNO central zone
CTF	Corrected total fluorescence
FFT	Food finding test
I	VNO intermediate zone
IA	Isoamyl acetate
M	VNO marginal zone
MOB	Main olfactory bulb
MOE	Main olfactory epithelium
NSE	Non-sensory epithelium
OCT	Optimal cutting temperature
OMP	Olfactory marker protein
PCNA	Proliferative cell nuclear antigen
PS1	Presenilin 1
SCL	Supporting cell layer
Sox2	SRY-box transcription factor 2
VL	Vomeronasal lumen
VNO	Vomeronasal organ
VSE	Vomeronasal sensory epithelium

Introduction

Social recognition is essential for survival allowing to appropriately adapt behavior across a variety of contexts [1, 2]. As aging progresses, social odors have been shown to elicit attenuated responses [3], a phenomenon interpreted as a natural consequence of age-related decline in sensory perception. In humans, social impoverishment has been identified as a major aggravating factor for decreased life expectancy [4, 5] and an indicator of the appearance of dementia and neurodegenerative disorders such as Alzheimer's disease (AD) [6, 7]. Despite the central role of social interaction in maintaining overall well-being, the mechanisms by which

✉ Sandra Jurado
sjurado@umh.es

[1] Instituto de Neurociencias de Alicante, Consejo Superior de Investigaciones Científicas - Universidad Miguel Hernández (CSIC-UMH), 03550 Sant Joan d´Alacant, Spain

[2] Laboratoire de Physiologie de La Reproduction Et Des Comportements, CNRS, IFCE, INRAE, University of Tours, 37380 Nouzilly, France

aging, natural or pathological, alters social information processing remain unclear.

Mouse social communication strongly depends on chemosignals comprised by volatile and non-volatile molecules (pheromones) [8, 9]. Volatile odors are primarily detected at the main olfactory epithelium (MOE) which projects to the main olfactory bulb (MOB), whereas pheromones are mainly detected by the vomeronasal sensory epithelium (VSE) [10–12] which connects to the accessory olfactory bulb (AOB) [13]. Despite the segregated connectivity, both systems have overlapping functions [14, 15].

A remarkable property of the VSE is that it contains proliferative niches capable of generating functional neurons during adulthood [16–19]. The neurogenic properties of olfactory structures are known to decline with age, which it is likely to underlie the olfactory deficits associated to both natural aging and neurodegenerative disorders [20–22]. However, how natural and pathological aging affects the regenerative capacity of the VSE has been scarcely studied despite being central to socio-sexual cue detection. An elegant study by Brann and Firestein [18] showed that the proliferative capacity of the marginal region of the VSE of 2-year-old animals was attenuated in comparison to young animals. More recently, Mechin et al. (2021) [23] reported a significant reduction in mature olfactory marker protein (OMP)-expressing cells (OMP^+), indicating structural modifications of the aged VNO. However, it is currently unclear whether these cell alterations have any impact in social odor detection, particularly in animal models of neurodegeneration.

To gain insight into these questions, we investigated the impact of natural and pathological aging in social odor-evoked sniffing behavior, social-odor habituation/dishabituation, and sociability during the aging process of wild-type C57/BL6 mice and amyloid precursor protein (APP) and presenilin 1 (PS1) double transgenic mice ($APP/PS1^{Het}$ mice, therein), a widely used animal model of AD [24–26]. Analysis of the number of progenitors, proliferative and mature neurons revealed that naturally aged animals show reduced neuronal proliferation and decreased levels of sensory mature OMP^+ neurons. In contrast, the VSE of 1-year-old $APP/PS1^{Het}$ mice exhibited normal levels of mature neurons and cell regeneration, suggesting that natural and pathological aging distinctively impacts the neurogenic capacity of the VSE.

We explored the functional consequences of these cell alterations observing reduced exploration time of social odors and decreased performance in a social odor habituation-dishabituation test in both senescent and middle-aged $APP/PS1^{Het}$ mice, suggesting that despite the overall normal VSE structure and cell composition, $APP/PS1^{Het}$ animals exhibit an accelerated decay of social cue exploration. Moreover, 1-year-old $APP/PS1^{Het}$ mice exhibited a significant reduction of social novelty which was not apparent in naturally aged animals, exposing fundamental differences in how natural and pathological aging impacts not only the pheromone detection system but also the display of social behavior.

Materials and Methods

Animals Experiments were performed in either control C57/BL6 mice (young adult: 2–4 months old; middle age: 6–8 months old; old: 12–14 months old; senescent: 20–24 months old) or APP/PS1 mice on a C57/BL6 genetic background (young adult: 2–4 months old; old: 12–14 months old) (Jackson Labs, Stock No. 004462, MMRRC Stock No. 34829). Distinct animals were utilized in each of the test conducted. $APP/PS1^{Het}$ mice express a chimeric mouse/human amyloid precursor protein (Mo/HuAPP-695swe) and a mutant human presenilin 1 (PS1-dE9). These animals develop beta-amyloid deposits at ~ 6 months of age and exhibit early-onset cognitive impairments [24–26] and reduced life expectancy (~ 14–16 months old) in comparison to $APP/PS1^{WT}$ controls, a scenario that prevented the study's extension to a comparable age range to naturally aged animals (20–24 months old). Mice were kept group-housed and experimentally naïve during all their lifetime under pathogen-free conditions. Animals were housed in ventilated cages with free access to food and water on a 12 h light/dark cycle. Although the study was not originally designed to address sexual differences, many experiments included animals of both sexes. However, a meaningful statistical comparison of the results desegregated by sex could be only performed for the social exploration test.

All experiments were performed according to Spanish and European Union regulations regarding animal research (2010/63/EU), and the experimental procedures were approved by the Bioethical Committee at the Instituto de Neurociencias and the Consejo Superior de Investigaciones Científicas (CSIC).

VNO Dissection Mice were perfused transcardially with PBS, pH 7.4, followed by 4% paraformaldehyde in 0.1 M phosphate buffer (PB), pH 7.4. A fixed mouse head was placed under a scope, and the lower jaw was removed to get a palate view. To facilitate VNO extraction, the palate and the nasal septum were removed and the bilateral VNOs were split in two parts with a gentle twisting motion. Finally, the bony capsule that covers each portion was carefully removed to extract the VNOs. Tissue was incubated in a 30% sucrose solution for cryoprotection and kept at − 4 °C until sectioning. Samples were embedded in OCT and frozen at − 80 °C for cryosectioning.

Immunohistochemistry VNOs embedded in OCT medium were sliced in 16 µm thick sections in a cryostat apparatus (Leica CM 3050S). Slices were incubated in blocking solution containing 0.5% Triton X-100 and 5% normal horse serum in 0.1 M TBS for 2 h at room temperature (RT). Primary antibody incubation was performed overnight (o/n) at 4 °C with anti-OMP (Wako goat polyclonal; 1:2000), anti-PCNA (Sigma, rabbit monoclonal; 1:2000), and anti-Sox2 (R&D Systems, goat polyclonal; 1:300). For PCNA immunostaining, slices were incubated in 10 mM citrate buffer (100 °C; pH, 6.0) for 5 min prior staining. Sections were incubated with Alexa Fluor 488- or 594-conjugated secondary antibodies (Jackson Laboratories, 1:500) for 2 h at RT. Hoechst (Sigma, 1:10,000) was added during 5 min after the secondary antibody incubation for nuclei visualization. Imaging was performed using a vertical confocal microscope Leica SPEII. Final images were assembled in Adobe Illustrator.

Sox2 Fluorescence Intensity at the VNO Supporting Cell Layer (SCL) For determining the expression of Sox2 in the VNO SCL where single-cell quantification was limited by the densely packed disposition of the cells, we calculated the corrected total fluorescence (CTF) of the area of interest employing the Freehand ROI tool of Image J. CTF was calculated by subtracting the background fluorescence from a minimum of 3 sections, 16 µm thick, from at least 4 animals per condition.

Stereology, Cell Quantification, and AOB Volume Estimation

The total number of olfactory mature neurons (OMP^+ neurons) in the entire VSE was estimated using stereology (optical fractionator method [27]) employing Stereo Investigator (MBF Bioscience). Two different tools are combined in this unbiased quantification method: a 3D optical dissector for cell counting and a fractionator, based on a systematic, uniform, and random sampling over a known area [28, 29]. The number of neurons was estimated as

$$N = \left(1/h \times 1/ssf \times 1/asf \times \sum Q - t\right)$$

in which $\sum \mathbf{Q}$ is the total cell number in the region of interest acquired using the optical dissector method; **t** stands for the mean mounted section thickness; **h** is the optical dissector height; **asf** is the area sampling fraction and **ssf** is the frequency of sampling (section sampling fraction). For the VSE stereological analysis, sampling was performed with a 20 × objective (Leica, NA 0.6), the counting frame area was 2500 µm^2, and the sampling grid area was 22,500 µm^2. *H* for VSE stereology was 8 µm with 1 µm as upper and lower guard zones and *t* was set at 10 µm. Quantifications were performed for marginal regions of the VSE dividing the area in segments of equal length as previously described [18, 30]. For cell quantification in the anterior–posterior regions, the VSE was distributed in 10 sections per animal. Results were divided by the area to obtain the number of cells/mm^2 in each subdivision. Quantification of the cell number in the marginal area was performed in three slices of each animal delineated with a 50 × 50 dissector employing Stereo Investigator (MBF Bioscience).

VSE volume was calculated by multiplying the sampled area by the slice thickness (16 µm) and the number of series (10 slices per animal). Ten sections per series were analyzed to obtain an estimation of the VSE area and volume in young adults (4 months old), senescent (24 months old), and old (12 months old) APP/PS1^{WT} and old APP/PS1^{Het} mice.

The volume of the AOB was estimated by measuring the AOB area and multiplying the sampled area by the section thickness (50 µm) and the number of analyzed Sects. (5 series per animal).

Odorants

Social and non-social scents were employed to discern the impact of aging in social odor perception. As non-social scents, we used (i) the banana-like odor isoamyl acetate (IA) (Sigma) shown to be primarily detected at the MOE level (Xu et al., 2005) with neutral valence within a broad dilution range [31–33] and (ii) food pellets to perform a food finding test (FFT, see experimental details below). As a social scent, we used urine from conspecifics which has been shown to elicit robust VNO activity [34]. Urine samples were collected according to standard procedures [35]. For habituation-dishabituation tests, frozen urine samples from young cage mates were used to test fine odor discrimination. For sensitivity tests, urine samples were combined in a stock sample used for each round of odor presentations until experiment completion. For female urine, samples obtained at different points of the estrous cycle were pooled to generate a uniform stock.

Behavioral Assessment

All the behavioral experiments using social and non-social stimuli were performed in a dedicated room with continuous air reposition under dim indirect light (20 lx). Odor dilutions were prepared in a room outside the animal house. Odor presentation was performed in a homemade methacrylate box with removable walls for cleaning. The chamber dimensions were 15 cm width, 15 cm length, and 30 cm high. A small hole (1 cm diameter) was performed in the middle of one of the sides located 5 cm above from the box ground to fit standard cotton sticks impregnated with 1 µL of the odorant allowing direct contact with the stick. Habituation to the

testing conditions was performed before odorant presentations consisting of handling (5 min), free exploratory activity in the box and habituation to the cotton stick movement (5 min). Urine was presented embedded in a cotton stick in order to preserve non-volatile pheromones and mimic the natural detection method of physical contact between conspecifics. To avoid variability due to the intensity of the volatile components of the urine, only direct nose contact with the tip of the cotton stick was considered as explorative behavior (sniffing/exploration time). Experiments were monitored by a video recording camera fixed 15 cm above the box. Videos were collected and analyzed offline using SMART video-tracking software (PanLab S.L.).

(a) Odor exploration test: After a period of habituation (10 min), mice were exposed to two control trials (mineral oil for IA assays or water for urine tests) during 1 min separated by intervals of 1 min to avoid odor habituation [36, 37]. Subsequent presentations consisted on serial dilutions of either urine samples (diluted in water: 1:1.000, 1:500, 1:250, 1:100, 1:50, 1:10, and non-diluted (nd)) or IA were tested in ascending order (diluted in mineral oil: $1:5\times10^5$, 1:100.000, 1:10.000, 1:1.000, 1:100). Animals were considered to detect the olfactory stimulus when spent more time investigating the odors than the vehicles (water or mineral oil).

(b) Food finding test (FFT): FFT was performed following standard procedures [38]. The mice were food deprived for 24 h before testing. Five food pellets (~ 35 g) were placed in a corner and covered by 5 cm of litter bedding. Animals were considered to detect the food pellet when spent digging, touching, and holding the food pellet for more than 5 s.

(c) Social odor habituation-dishabituation test: The effect of aging in social odor discrimination and habituation was explored using an adapted habituation-dishabituation test [39]. After a period of cage habituation (10 min), two control trials were performed employing cotton sticks soaked with 1 µL of water (vehicle). Three successive presentations of urine from an animal of the opposite sex (S1a-c) were followed by three presentations of urine from a different subject of the opposite sex (S2a-c) to evaluate fine chemo-olfactory discrimination and habituation. Urine samples came from young animals of the opposite sex to maximize approaching behavior [3]. Each sample presentation lasted 1 min separated by 1 min intervals. Habituation was estimated as a decrease in the exploration time (sniffing) over the cotton stick tip after the first exposure of urine from the same animal (S1a). Dishabituation (discrimination) occurs in response to a new odor presentation (S2a) as a measurable increase in the exploration time. The test allows to explore two consecutive phases of discrimination (H_2O^B-S1a and S1c-S2a) and habituation (S1a-S1b and S2a-S2b). Trend lines between H_2O^B-S1a, S1c-S2a, S1a-S1b, and S2a-S2b were fitted to obtain the slope values indicating the amplitude of the discrimination and habituation effect for each tested condition. Higher positive values indicated more pronounced social discrimination, and higher negative values corresponded to more robust habituation.

(d) Long-term social habituation-dishabituation test: The aforementioned social odor habituation task was adapted to assay social cue memory by presenting the urine sample employed in S1a, 24 h after the first test was performed. Intact social odor memory was manifested as a reduction of the sniffing time during the second presentation of S1a, an effect which was clearly apparent in young animals.

(e) Three-chamber test: Social testing was performed in a cage ($60\times40\times22$ cm) following standard procedures [40]. Dividing walls were made from clear Plexiglas, with openings allowing access into each chamber. The test mouse was first placed in the middle chamber and allowed to explore for 10 min. After the habituation period, an unfamiliar subject of the same sex (mouse 1, $M1^A$) was placed in one of the side chambers. The unfamiliar mouse was enclosed in a small, round wire cage, which allowed nose contact between the bars. In this first session (sociability), the test mouse had a choice of spending time in either the empty chamber (E) or the chamber occupied by $M1^A$. At the end of the sociability session, each mouse was tested in a second 10-min session to evaluate social preference for a new subject. A second, unfamiliar mouse (mouse 2, M2) of the same sex was placed in the chamber that had been empty during the first session. This second unfamiliar mouse was enclosed in an identical wire cage than $M1^A$. The test mouse had a choice between the first, already-investigated mouse ($M1^B$) and the novel unfamiliar mouse (M2) which indicates their social preference or social novelty [40]. Continuous video recordings were collected and analyzed offline using BORIS and SMART video-tracking software (PanLab S.L.). Measures of time spent sniffing E, $M1^{A-B}$, and M2 were quantified for each session.

Data Analysis All data were tested for statistical significance using GraphPad Prism 8. The Shapiro–Wilk test was used to determine data normality. One-way ANOVA with Tukey's test for multiple comparisons with a single variable was implemented for cell quantifications and anatomical data. For the behavioral analysis, a two-way ANOVA

with Tukey's test was used to test multiple comparisons with more than one variable. *P* values are indicated in all figures above the corresponding comparisons. $P \leq 0.05$ was considered statistically significant. *P* values are indicated in all figures above the corresponding comparisons. In addition, a two-way ANOVA with the interaction of age vs. genotype has been applied to all data sets including these variables. Results of these statistical analyses can be found in Supplementary Results. A summary of all data presented in the study with their correspondent *P* values can be found in Supplementary Results. In addition, Supplementary Figures 3, 4, 6, and 7 summarize the *P* and *N* values corresponding to all the statistical comparisons between different ages, genotypes, and dilutions of the social odor sensitivity tests.

Results

Structural Modifications of the Mouse VSE During Natural and Pathological Aging

We sought to investigate the structure of the VSE during natural and pathological aging, as the main gateway of pheromone (non-volatile)-encoded social information [41, 42]. Stereological analysis revealed significantly smaller VSE volumes in 2-year-old (senescent) mice (Fig. 1a; Supplementary Results—Table 1). This observation was supported by the reduced number of olfactory marker protein (OMP)-positive cells (OMP^+ cells) along the rostrocaudal axis of the marginal VSE (Fig. 1c, e; Supplementary Results—Table 2; Supplementary Figure 1).

We hypothesized that the drop in the number of OMP^+ cells in senescent mice could translate into a reduced axonal projection to the AOB, the main VNO target area, resulting in smaller AOB volumes (Supplementary Figure 2). As expected, we observed a reduction in AOB size with no apparent histopathological alterations in 2-year-old mice (Fig. 1b; Supplementary Results—Table 3), indicating that natural aging alters basic structural features of the VNO-AOB axis.

We expanded our analysis to the SRY-box transcription factor 2 (Sox2)-expressing cells ($Sox2^+$ cells) in the supporting cell layer (SCL), a neuronal stem cell marker which also stains mature differentiated sustentacular cells [43–45]. The estimation of the labeling intensity of Sox2 in the SCL showed a drastic reduction in senescent but not in APP/$PS1^{Het}$ mice (Fig. 1d, f; Supplementary Results—Table 4). These results show that natural aging disrupts VSE structure by reducing the number of sensory (OMP^+) and SCL sustentacular ($Sox2^+$) cells, although this may not imply a total elimination of the proliferative capacities [18].

Natural and Pathological Aging Differentially Impacts VSE Cell Proliferation

Because of the lack of data on the characteristics of the VSE neurogenic niche in animal models of neurodegeneration, we conducted an analysis to examine the expression of proliferative cell nuclear antigen (PCNA)-positive cells ($PCNA^+$ cells) in the anterior, medial, and posterior VNO of senescent and APP/$PS1^{Het}$ mice. Consistent with previous reports, cell proliferation in young animals was abundant in the marginal zone of the anterior and medial VSE [18, 30] (Fig. 2a, b). Senescent mice exhibited a significant reduction in $PCNA^+$ cells in the marginal VSE (Fig. 2a, b; Supplementary Results—Table 5), indicating reduced cell proliferation. Surprisingly, the number of $PCNA^+$ cells in APP/$PS1^{Het}$ mice was significantly higher in the anterior VSE whereas it showed a downward trend in the posterior VNE (Fig. 2a, b), suggesting a region-specific increase in cell proliferation in these animals. Importantly, no significant overlap between OMP and PCNA staining was observed which demonstrates that these two markers recognize cell populations at different maturation stages (OMP-PCNA double immunostaining, right panel in Fig. 2a).

We then sought to explore whether the reduced number of proliferative $PCNA^+$ cells in senescent mice could be due to a decrease of stem cell generation by analyzing the number of $Sox2^+$ neural precursor cells in the VSE [46, 47]. We observed a significant reduction in the number of $Sox2^+$ cells in 2-year-old mice but not in APP/$PS1^{Het}$ animals, indicating reduced neurogenic capacity in the naturally aged VSE (Fig. 2c; Supplementary Results—Table 6). Altogether, these findings revealed a fundamental difference in how natural and diseased aging impacts the VSE structure and proliferative capacity.

Late Onset of Social Exploration Deficits During Natural Aging

Our data indicated that natural aging induces significant alterations in the structure, VSE proliferative capacity, and cellular composition; thus, we investigated whether these adaptations might translate into impairments in the processing of socio-sexual information. Cumulative evidence points to olfactory decline as a common symptom of natural and pathological aging [4, 5, 48, 49]. However, most of these studies and diagnostic tests employed synthetic odors with reduced social valence; therefore, the temporal course and severity of the age-related involution of the recognition of social cues, largely processed by the VNO-AOB system, remain unclear.

To explore the impact of natural aging on social odor detection, we conducted an odor-evoked sniffing test in which serial dilutions of urine from young conspecifics of the opposite sex were presented to either male or female subjects over a range

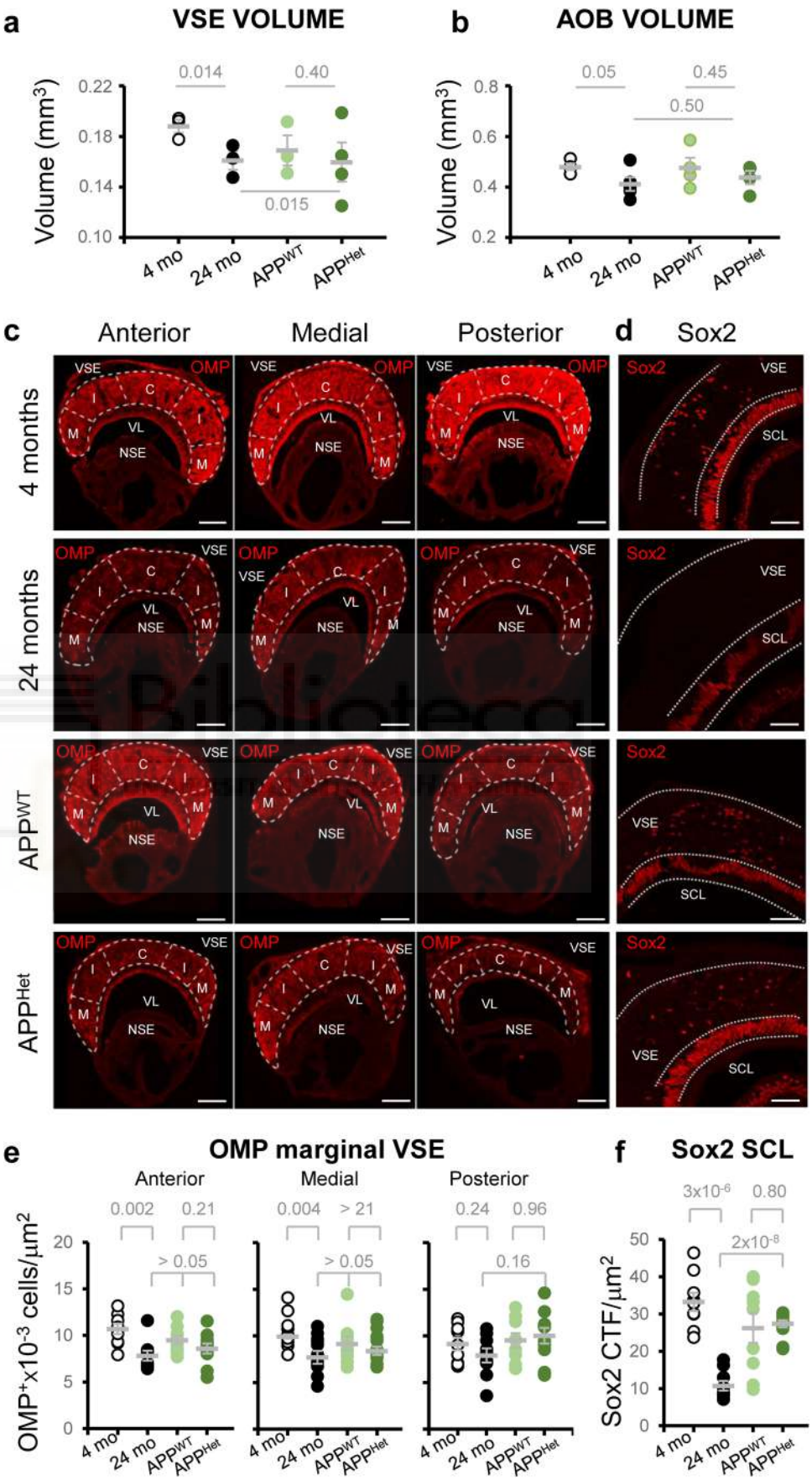

Fig. 1 Structural modifications of the mouse VSE during natural and pathological aging. **a** Dispersion plot of the VSE volume indicates a significant reduction during natural but not pathological aging. **b** Dispersion plot of AOB volume. Thick lines indicate the mean ± SEM. Data were obtained from 4 animals per condition. **c** Representative images of OMP staining in the VSE during natural and pathological aging. Scale bar indicates 100 µm. **d** Representative images of Sox2 staining in the VSE and the supporting cell layer. Scale bar indicates 100 µm. VL: vomeronasal lumen; SCL: supporting cell layer; NSE: non-sensory epithelium; M: marginal zone; I: intermediate zone; C: central zone. **e**, **f** Dispersion plots represent the number of OMP^+ cells in the marginal VSE (number of cells $\times 10^3/\mu m^3$) and the intensity of Sox2 fluorescence in the SCL (Sox2 CTF/μm^2). Thick lines indicate the mean ± SEM. Data were obtained from slices from at least three animals per condition. Statistical comparisons were calculated by two-way ANOVA with Tukey's test. $P \leq 0.05$ was considered statistically significant. P values are indicated above the corresponding comparisons

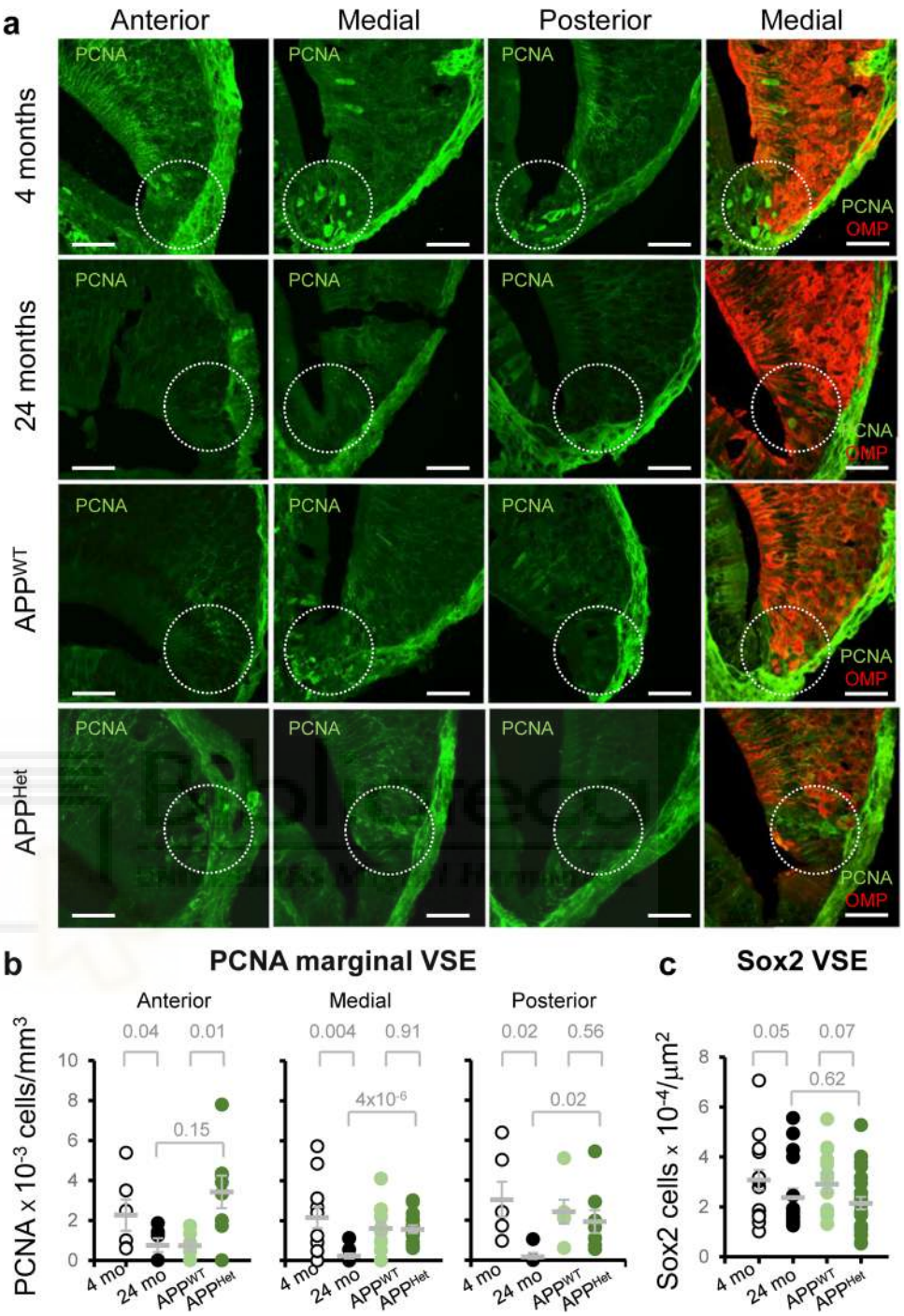

Fig. 2 Natural and pathological aging differentially impacts cell proliferation in the marginal VSE. **a** Representative confocal images of PCNA staining in the VSE proliferative niche during natural and pathological aging. Panels on the right show confocal images of OMP and PCNA double staining in the VSE. To note, there is no overlapping signal between the two markers indicating the identification of cells at different maturation stages. Circles indicate active proliferative marginal region of the VSE. Scale bar represents 20 µm. **b**, **c** Dispersion plots represent the number of $PCNA^+$ cells (number of cells $\times 10^{-3}/mm^3$) and the number of $Sox2^+$ cells (number of cell $\times 10^{-4}/\mu m^2$) in the marginal VSE. Thick lines indicate the mean ± SEM. Data were obtained from slices from at least three animals per condition. Statistical analysis was calculated by two-way ANOVA with Tukey's test for multiple comparisons. $P \leq 0.05$ was considered statistically significant. *P* values are indicated above the corresponding comparisons

of different ages: young adult (2–4 mo.), middle age (6–8 mo.), old (12–14 mo.), and senescent mice (20–24 mo.) (Fig. 3a, see "Materials and Methods" for details on urine sample preparation). Our results indicated a significant reduction in the exploration time throughout various urine dilutions in comparison to adult wild-type mice (Fig. 3b, c; Supplementary Results—Table 7). Raw sniffing time data showed a similar decrease in the exploration of social odors in senescent animals across different dilutions (see details in Supplementary Figures 3 and 4).

Furthermore, senescent mice progressively increased the exploration time in parallel with odor concentration, whereas young adult, middle-aged, and old animals showed a habituation phase at intermediate dilutions (1:500, 1:250, 1:100, and 1:50), indicating effective odor detection and recognition capabilities [50]. Lastly, data analysis disaggregated by sex showed no sex differences in the reduction of urine exploration time (Supplementary Figure 5; but see [51] for an alternative view).

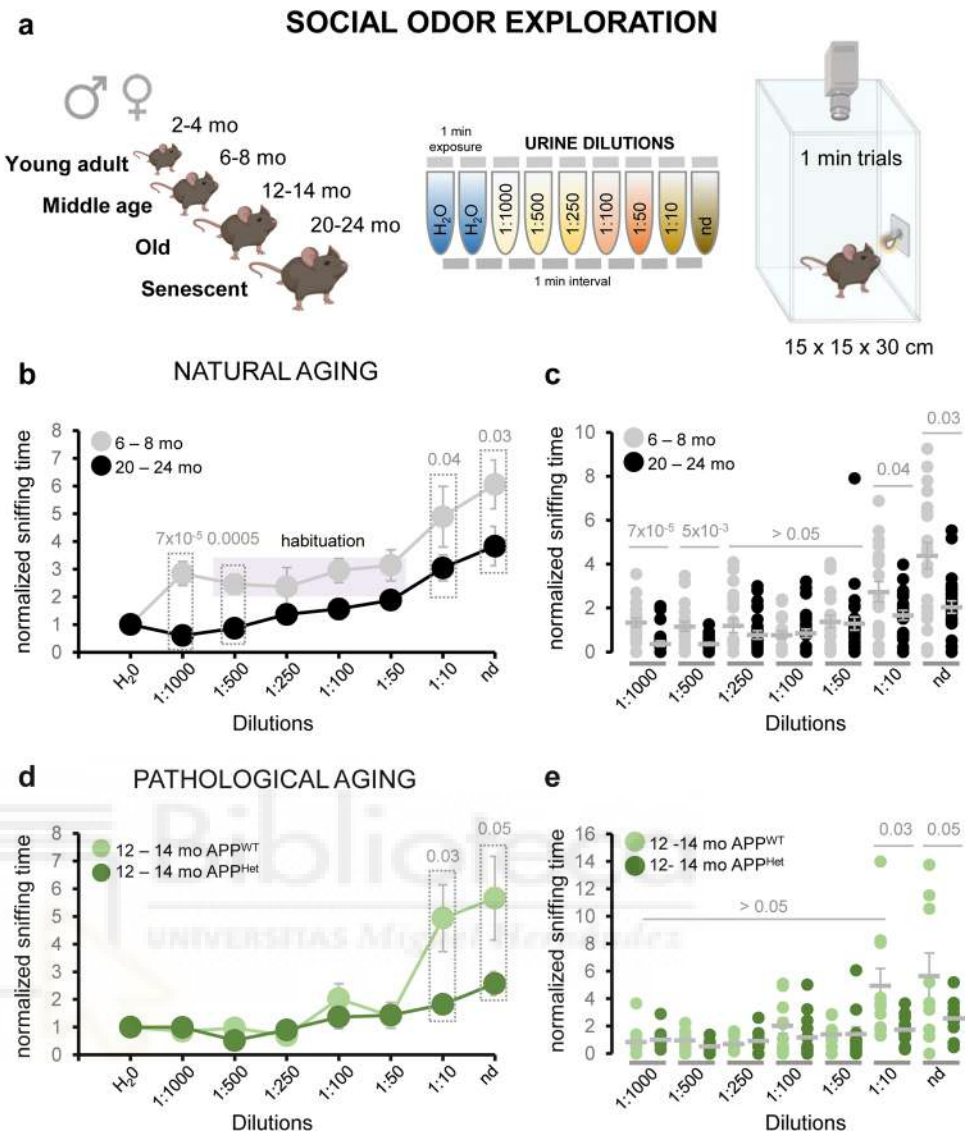

Fig. 3 Natural and pathological aging reduces exploration to social odors. **a** Schematics of the olfactory test used in this study in which urine dilutions are presented as a social signal. **b** Average of the sniffing time of urine serial dilutions normalized to the exploration time of the vehicle (water) of adult and aged wild-type mice. A typical habituation indicated by a purple box was observed in adult mice at intermediate dilutions (1:500, 1:250, 1:100; 1:50). **c** Dispersion plot of the normalized sniffing time of each urine dilution (nd (non-diluted); 1:10; 1:50; 1:100; 1:250; 1:500; 1:1000) for adult and aged wild-type mice. **d** Average of the sniffing time of urine dilutions normalized to the exploration time of the vehicle (water) of middle-aged APP^{WT} controls and middle-aged $APP/PS1^{Het}$ mice. **e** Dispersion plots of normalized sniffing time of middle-aged APP^{WT} controls and $APP/PS1^{Het}$ mice. Grey lines in the dispersion plots indicate mean ± SEM. Data were analyzed by a one-way ANOVA with Tukey's test to test multiple comparisons with more than one variable. $P \leq 0.05$ was considered statistically significant. *P* values are indicated above the corresponding comparisons

Reduction in the Exploration of Social Information Is Accelerated in an Animal Model of Neurodegeneration

Next, we investigated whether pathological aging would alter the exploration of social olfactory cues despite no obvious effects on VSE structure or proliferative capacity. Social odor sensitivity tests in 1-year-old $APP/PS1^{Het}$ mice revealed reduced sniffing times of low urine dilutions when compared to age-matched $APP/PS1^{WT}$ control mice, suggesting that pathological aging accelerates the decline of exploration time of social odors (Fig. 3d, e; Supplementary Results—Table 8). Similar to senescent mice, these results were reproduced when raw sniffing time data were compared (Supplemental Figures 6 and 7).

Natural Aging Mildly Reduces Neutral Odor Exploration

Next, we asked whether non-social odor modalities were also affected in senescent and $APP/PS1^{Het}$ animals. We investigated this question by analyzing the exploration time to both food and synthetic neutral odors. First, we exposed naturally aged and $APP/PS1^{Het}$ mice to serial dilutions of IA, a synthetic banana-like odor of neutral valence when used at high dilutions [32, 33]. Consistent with previous studies, mice across all conditions showed significantly reduced responses to the neutral odorant than to urine (Fig. 4a–d) according to the higher social valence of urine over a synthetic odor [33, 52, 53]. Our results showed no significant differences on

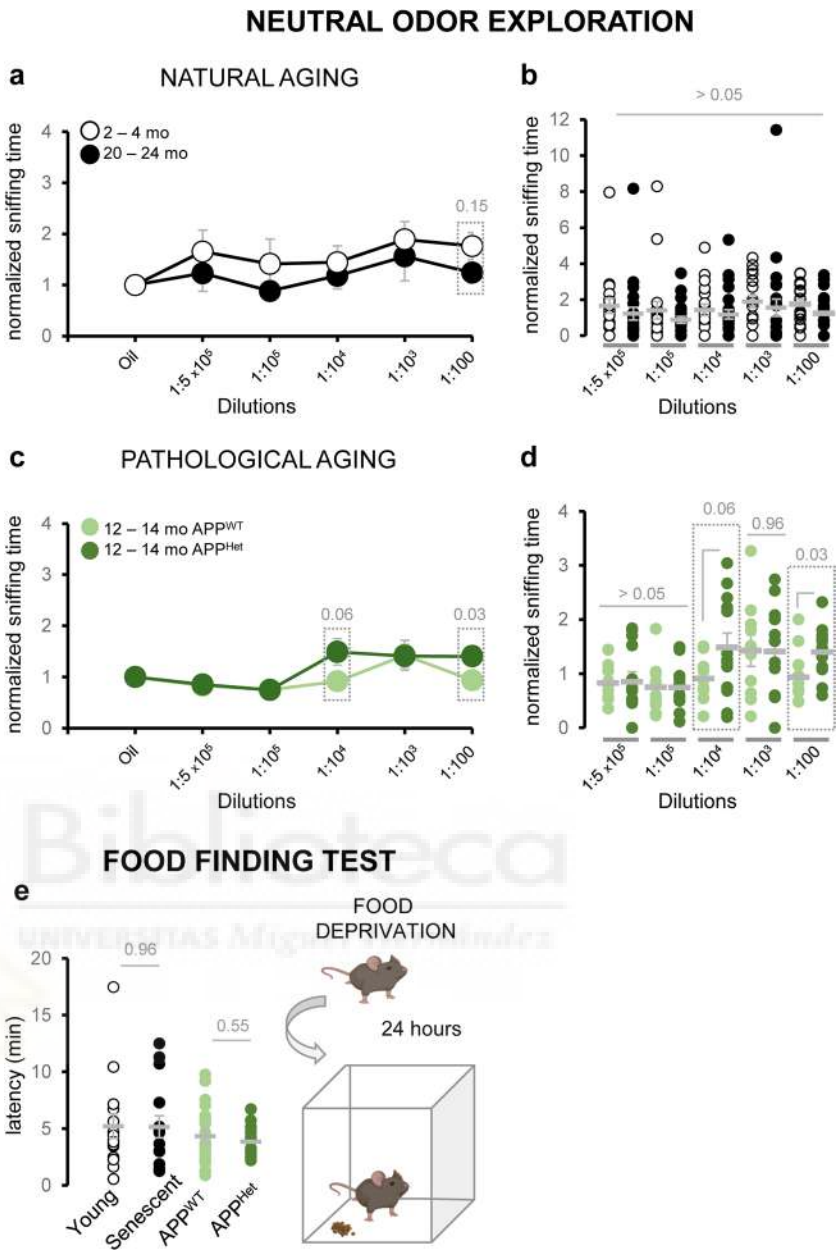

Fig. 4 Aging and neurodegeneration impact social odor recognition more severely than other odor modalities. **a** Average of the sniffing time of young and aged mice in response to a neutral synthetic odor (IA) normalized to the vehicle (mineral oil). **b** Dispersion plots of the normalized sniffing time of young and aged mice in response to various IA dilutions. **c** Average of the sniffing time of middle-aged APP^{WT} and APP/PS1^{Het} mice in response to IA samples normalized to the vehicle (mineral oil). **d** Dispersion plots of normalized sniffing time of APP/PS1^{WT} and APP/PS1^{Het} mice in response to various IA dilutions. Note that APP/PS1^{Het} mice showed higher exploration times for the 1:10^4 and 1:100 IA dilutions. **e** Food-deprived animals performed a food finding test (schematics on the right) which revealed equivalent latencies to find hidden food pellets as shown in the dispersion data plot (left panel). Thick grey lines in the dispersion plot indicate mean ± SEM. Data were analyzed by a one-way ANOVA with Tukey's test to test multiple comparisons with more than one variable. $P \leq 0.05$ was considered statistically significant. *P* values are indicated above the corresponding comparisons

the exploration times of IA in senescent mice and a modest but significant increase, in the sniffing time of the 1:10^4 and 1:100 IA dilutions in APP/PS1^{Het} animals (Fig. 4a–d; Supplementary Results—Tables 9 and 10; Supplementary Figure 8). Similarly, a FFT showed no significant differences in the latency to find food pellets after 24 h of food deprivation in either naturally aged or middle-aged APP/PS1^{Het} mice (Fig. 4e; Supplementary Results—Table 11). These results suggest that deficits in social exploration time at advanced stages of natural aging and in an animal model of AD are more pronounced than other odor modalities.

Social Odor Discrimination and Habituation Are Reduced in Naturally Aged and APP/PS1Het Mice

To further investigate the impact of aging and neurodegeneration in the detection of social information, we performed a habituation–dishabituation test, which relies on the animal's ability to discriminate novel smells [50]. For these experiments, young (2–4 mo.) and aged (20–24 mo.) wild-type animals were presented three consecutive replicates of urine samples from two different animals (S1a-c and S2a-c) (Fig. 5a). Aged animals were able to discriminate between urine sources, but showed reduced sniffing times during the first and second

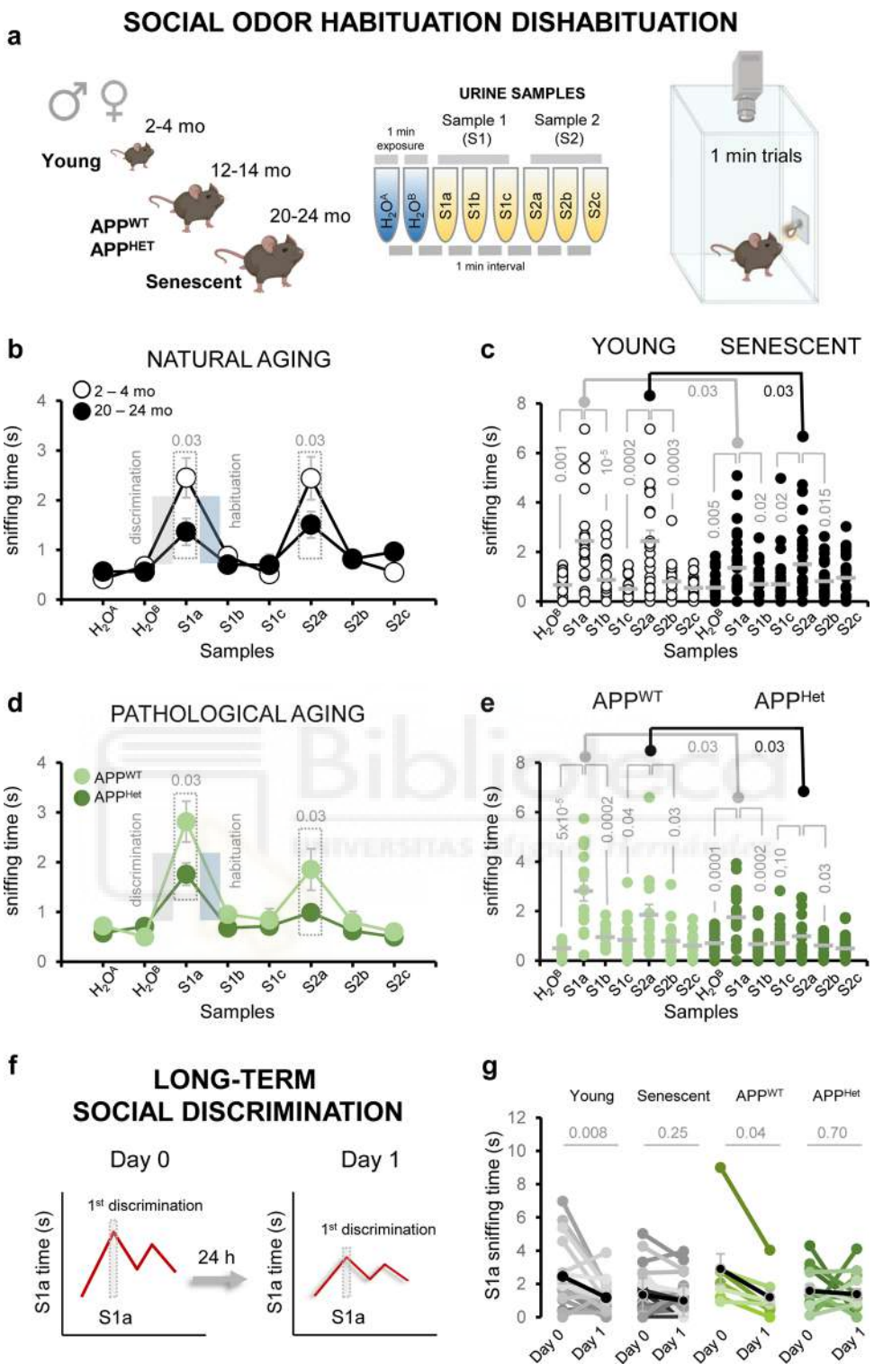

discrimination and habituation phases (Fig. 5b, c). Similarly, middle-aged APP/PS1^{Het} mice also exhibited reduced sniffing times in comparison to aged-matched APP/PS1^{WT} controls (Fig. 5d, e; Supplementary Results—Tables 12 and 13). Analysis of the slope values of the first and second discrimination and habituation phases revealed that senescent mice exhibited significant deficits during both rounds of social habituation–dishabituation, whereas APP/PS1^{Het} mouse impairments were apparent during the second phase of discrimination (Fig. 6; Supplementary Results—Tables 14 and 15).

Then, we adapted the habituation-dishabituation test to assay potential changes in long-term social odor memory

◂**Fig. 5** Social odor discrimination and habituation are reduced in naturally aged and APP/PS1^{Het} mice. **a** Schematics of the social habituation-dishabituation test used in this study: after habituation to the experimental cage, the animal was exposed to the same urine sample three times (S1a-c) which induces a typical increase in exploration time (1st discrimination) to be followed by a reduction in the sniffing time (1st habituation). Dishabituation induced by a urine sample from a new subject (S2a) elicits a second round of habituation–habituation (see "Materials and Methods" for details). **b** Average sniffing time of the social habituation-dishabituation test performed by young and aged wild-type mice. **c** Dispersion plot of the sniffing time of young and aged animals during the social habituation-dishabituation test. **d** Average sniffing time of the social habituation-dishabituation test performed by middle-aged APP/PS1^{WT} controls and age-matched APP/PS1^{Het} mice. **e** Dispersion plot of the sniffing time of middle-aged APP/PS1^{WT} controls and APP/PS1^{Het} mice during the social habituation-dishabituation test. **f** The habituation-dishabituation test was modified to assess potential deficits in long-term discrimination due to natural or pathological aging by presenting the same S1a sample 24 h after. **g** Paired data corresponding to the sniffing time during the first and second S1a presentation (24 h later) is plotted for each condition. Thick lines in dispersion plots and black dots in **g** indicate mean ± SEM. Data were analyzed by a one-way ANOVA with Tukey's test to test multiple comparisons with more than one variable. $P \leq 0.05$ was considered statistically significant. P values are indicated above the corresponding comparisons

(Fig. 5f). To this aim, animals were exposed to the same S1a urine sample 24 h after the first presentation. A reduction of the sniffing time during the first discrimination phase was interpreted as an indicator of memory. This reduction was clearly observed in young adults, but absent in naturally aged and 1-year-old APP/PS1^{Het} mice (Fig. 5g; Supplementary Results—Table 16), suggesting long-term social odor memory impairments during both natural and pathological aging.

Age-Related Deficits in Social Discrimination and Habituation Are Not Influenced by Previous Experience

Next, we compared animals exposed to either familiar (littermate urine, L) or novel social odors (novel urine, N) in the habituation-dishabituation test (Fig. 7a). Aged animals performed poorly in the L-N dishabituation task (no significant increase in sniffing time), suggesting that the reduction in social odor discrimination and habituation is independent of previous experience.

Since impairments in social odor discrimination were more severe in naturally aged mice, we asked whether these deficits also extended to the recognition of animal's own odors, as the loss of self-awareness is a disrupting symptom of common occurrence in senescent subjects [54, 55]. To this aim, animals were presented samples of their own urine (O) during the second discrimination phase of the habituation-dishabituation test (Fig. 7c, d). Our data indicated that animal's own urine was effective to elicit a typical discrimination (dishabituation) response (Fig. 7; Supplementary Results—Tables 17 and 18), suggesting that self-recognition is preserved in senescent mice.

Social Novelty Is Disrupted During Pathological Aging

Last, we explored whether the observed impairments in social odor exploration and discrimination may negatively impact social interaction in naturally aged and APP/PS1^{Het} mice. To this aim, we performed a three-chamber test [40, 56] (Fig. 8a) to assess general sociability and social novelty in senescent and APP/PS1^{Het} animals. Our data indicated a reduction in social novelty in middle-aged APP1/PS1^{Het} mice, which was not detected in 2-year-old animals (Fig. 8b–e; Supplementary Results—Tables 19 and 20). Although senescent mice did not show significant impairments in either sociability or social novelty, they exhibited a mild increase in the latency to approach M1 during the sociability phase (Supplementary Figure 9), consistent with the overall decrease in the exploration time of social odors (Supplementary Figures 3 and 4). These findings exposed exacerbated deficits in an animal model of AD, suggesting a distinct impact of natural and pathological aging on the display of social behavior.

Discussion

The quality of social life has been proposed as a predictive factor for developing dementia or mental illness [6, 57]. However, the impairment of social functions with age is poorly understood with some authors suggesting that social deficits might be the consequence of generalized brain impairments [58] or a symptom which might be developed independently [59, 60]. Our results revealed that both natural and pathological aging affects several key aspects of social information processing including the exploration of social odors and social odor discrimination and habituation, with no obvious disruption of other odor modalities, suggesting specific alterations that affect how the aged brain integrates social information. To gain insight into the mechanisms underlying these deficits, we explored the age-related adaptions of the VSE, a central gateway for pheromone-encoded information in mammals [10–12] and part of the accessory olfactory system whose aging process has been largely overlooked in contrast to other aspects of olfaction [61].

Our data showed VSE alterations during natural aging but not in APP/PS1^{Het} mice, a standardized animal model of AD. Whereas the VSE of APP/PS1^{Het} mice maintained stable neurogenic capabilities, senescent wild-type animals showed a reduction in proliferative and stem cells (PCNA^{+} and Sox2^{+} cells) in the marginal VSE in comparison to

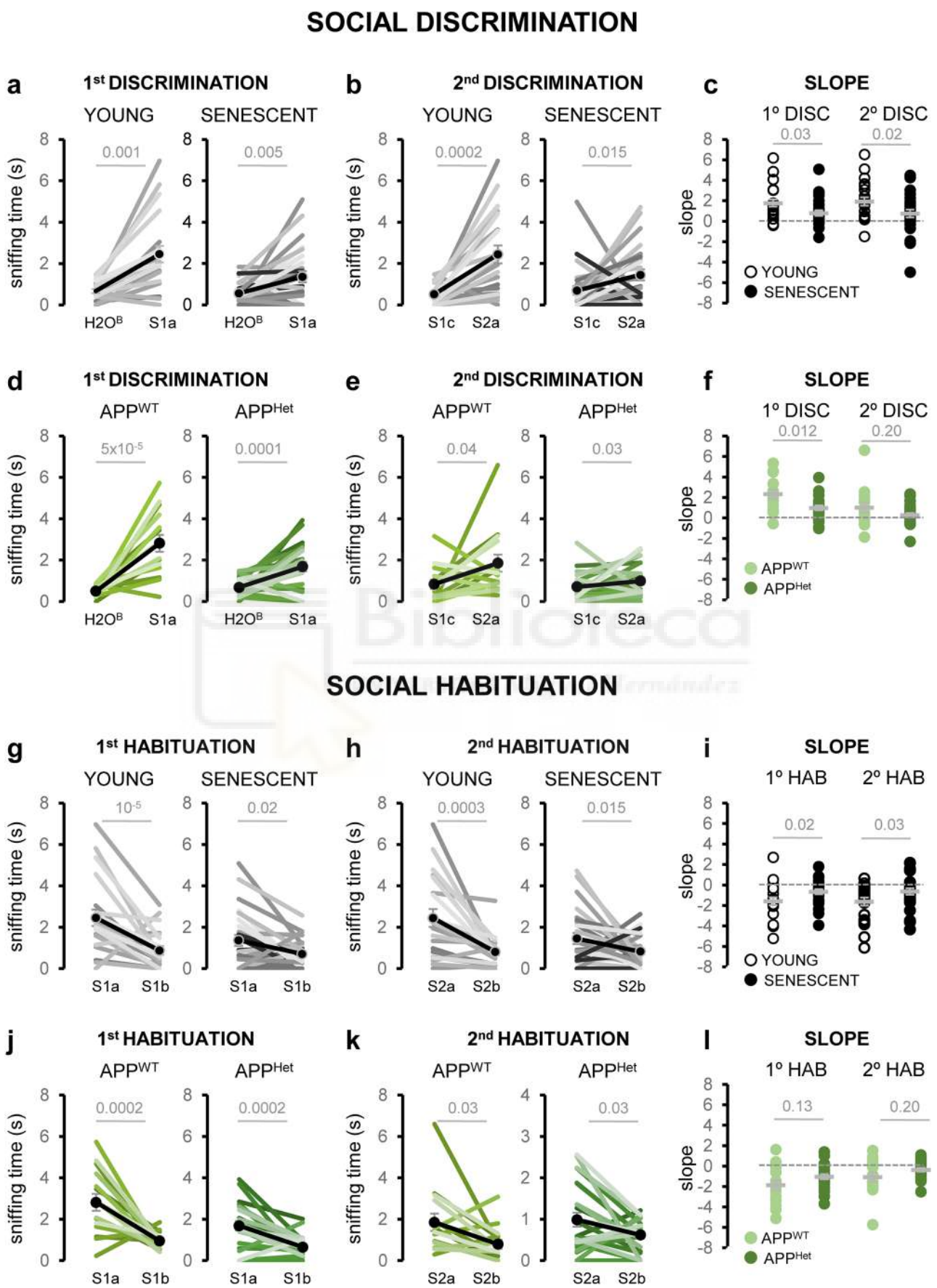
SOCIAL DISCRIMINATION
a
1st DISCRIMINATION
YOUNG
SENESCENT
sniffing time (s)
0.001
0.005
H2OB
S1a
b
2nd DISCRIMINATION
0.0002
0.015
S1c
S2a
c
SLOPE
1º DISC
2º DISC
0.03
0.02
slope
YOUNG
SENESCENT
d
1st DISCRIMINATION
APPWT
APPHet
5x10-5
0.0001
e
2nd DISCRIMINATION
0.04
0.03
f
SLOPE
0.012
0.20
SOCIAL HABITUATION
g
1st HABITUATION
10-5
0.02
S1a
S1b
h
2nd HABITUATION
0.0003
0.015
S2a
S2b
i
SLOPE
1º HAB
2º HAB
0.02
0.03
j
1st HABITUATION
0.0002
0.0002
k
2nd HABITUATION
0.03
0.03
l
SLOPE
1º HAB
2º HAB
0.13
0.20

◂**Fig. 6** Analysis of the social discrimination and habituation decay during natural and pathological aging. **a** Paired data of the sniffing time of young and aged wild-type animals corresponding to the first discrimination phase (H_2O-S1a). **b** Paired data of the sniffing time of young and aged wild-type animals corresponding to the second discrimination phase (S1c-S2a). **c** Dispersion plots of the slope values corresponding to the first and second discrimination phases of young and aged mice. **d** Paired data of the sniffing time of APP^{WT} and APP^{Het} mice corresponding to the first discrimination phase (H_2O-S1a). **e** Paired data of the sniffing time of APP^{WT} and APP^{Het} mice corresponding to the second discrimination phase (S1c-S2a). **f** Dispersion plots of APP^{WT} and APP^{Het} mice corresponding to the slope values of the first and second discrimination phases. **g** Paired data of the sniffing time of young and aged wild-type animals corresponding to the first habituation phase (S1a-S1b). **h** Paired data of the sniffing time of the young and aged wild-type animals corresponding to the second habituation phase (S2a-S2b). **i** Dispersion plots of the slope values of young and aged mice corresponding to the first and second habituation phases. **j** Paired data of the sniffing time of APP^{WT} and APP^{Het} mice corresponding to the first habituation phase (S1a-S1b). **k** Paired data of the sniffing time of APP^{WT} and APP^{Het} mice corresponding to the second habituation phase (S2a-S2b). **l** Dispersion plots of the slope values of APP^{WT} and APP^{Het} mice corresponding to the first and second habituation phases. Black dots in **a**, **b**, **d**, **e**, **g**, **h**, **j**, **k** and thick lines in **c**, **f**, **i**, **l** indicate mean ± SEM. Data were analyzed by one-way ANOVA with Tukey's test. $P \leq 0.05$ was considered statistically significant. *P* values are indicated above the corresponding comparisons

young animals (Fig. 2), which in turn could explain the reduction of mature OMP^+ neurons, SCL sustentacular $Sox2^+$ cells, and organ volume (Fig. 1), although this may not imply a total elimination of proliferative capacities in old mice [18]. Our findings are consistent with two previous studies [18, 23], which reported an overall thinning of the vomeronasal sensory epithelium [23] and reduced VSE neurogenesis in the marginal zone of 2-year-old animals [18]. Here, we provide novel information from a commonly used AD animal model ($APP/PS1^{Het}$), revealing an unexpected preservation of the VSE proliferative capabilities in middle-aged $APP/PS1^{Het}$ mice. These results contrast with the reduction of SVZ neurogenesis reported in similar animal models [62–65], suggesting that VSE neurogenesis might be less susceptible to lesions (see [18]) and pathological conditions than other proliferative areas.

A relevant aspect of our work is that most previous studies addressing olfactory decline employed synthetic or neutral odors, thus remaining uncertain the specific effect of healthy and diseased aging in the recognition of social cues. To gain insight into this question, we investigated the exploration time and the habituation-dishabituation response to social odors (urine) (Figs. 3, 5, and 6). Our findings revealed that despite the distinctive effects of natural and pathological aging on VSE structure and cell composition, both processes impaired the exploration of socio-sexual cues, social discrimination-habituation, and social behavior, suggesting fundamental differences in the mechanisms by which healthy and diseased aging impact social information processing.

Further experiments are needed to establish causality, but our results suggest that the observed VSE alterations in senescent mice underlie deficits in urine exploration time (Fig. 3, Supplementary Figs. 3 and 4) which could impair the processing of social information. VSE volume data from middle-aged $APP/PS1^{WT}$ control animals suggest that VSE structural changes might appear around 1-year-old (Fig. 1a), although their functional consequences might not become apparent until advanced stages of aging (2-year-old). This scenario suggests a parsimonious VNO decay that matches the aging of other olfactory areas like the OB. As such, several studies have shown that several symptoms of OB aging like reduced regeneration rate of olfactory sensory neurons (OSNs), decreased number of synaptic contacts [66], expression loss of odorant receptor genes [67, 68], or changes in the OSN dynamic range [69] are only clearly detectable in 2-year-old mice. This evidence suggests that although age-related changes may start earlier in the olfactory system [21], functional and behavioral deficits may exhibit a late onset, suggesting compensatory mechanisms to preserve the processing of olfactory cues relevant for the survival of aged animals [70, 71]. In contrast to the natural steady decline, pathological conditions may accelerate functional deficits even in the absence of peripheral organs modifications, suggesting alterations in the central processing of social information. As such, defects in the exploration of social odors were found exacerbated in middle-aged $APP/PS1^{Het}$ mice (Fig. 3d, e), a condition likely to aggravate frailty and reduce life expectancy in these animals (as observed for $APP/PSEN1^{Het}$ in our experimental conditions, see "Materials and Methods" for details).

Furthermore, results from the long-term social habituation-dishabituation test (S1a urine sample presentation after 24 h; Fig. 5f, g) revealed significant impairments in both 2-year-old wild-type animals and middle-aged $APP/PS1^{Het}$ mice, suggesting that in parallel to sensory decline, the downstream pathways involved in social cue recognition may be affected during both natural and pathological aging. To control for a potential contribution of novelty in the social habituation-dishabituation test, we presented urine samples from littermate and novel animals finding similar deficits in discrimination (Fig. 7). Interestingly, although senescent animals showed severe discrimination deficits, they preserved the ability to differentiate between urine from a novel subject and their own, preventing to further explore the underlying mechanisms of subjective perception loss, a disrupting symptom of senescence and dementia which currently lacks appropriate animal models for preclinical studies [72].

Age-related decline of olfactory detection is likely to occur due to alterations of both the main olfactory epithelium and the VNO [67, 73], thus potentially affecting other odor modalities. Here, we sought to explore this question

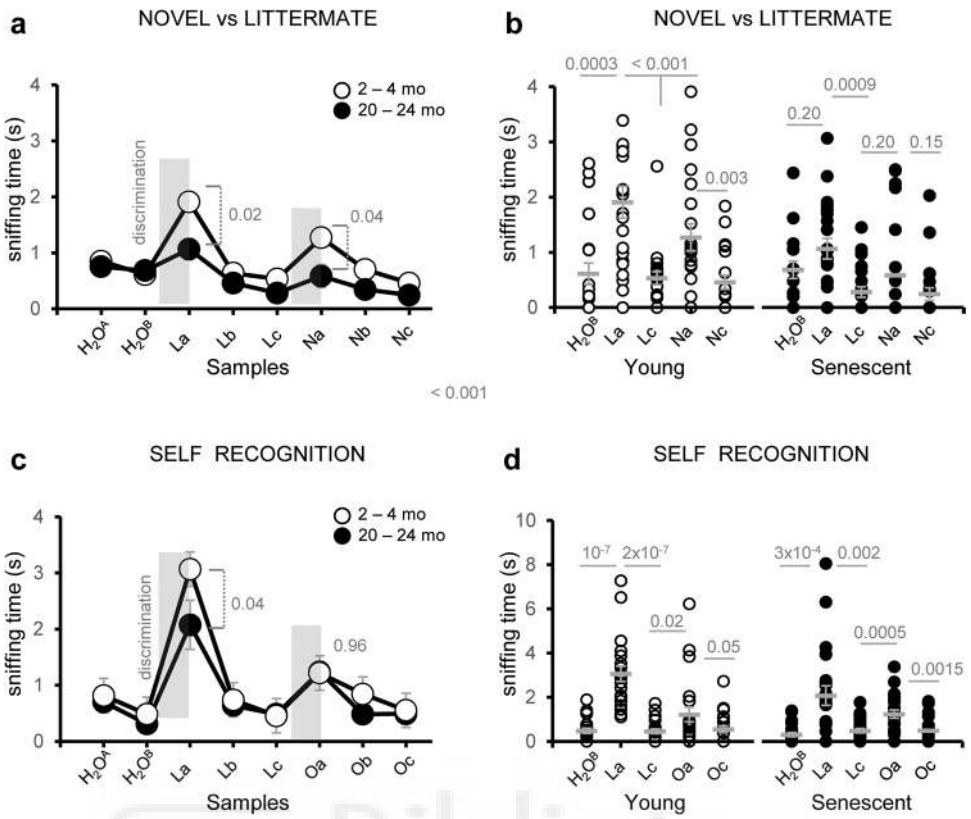

Fig. 7 Age-related deficits in social discrimination and habituation are not influenced by previous experience. **a** Average sniffing time of social habituation-dishabituation test in response to odors from novel (N) or littermate (L) subjects of young and naturally aged mice. **b** Dispersion plot of the exploration time of young and senescent animals in response to novel or littermate urine samples. **c** Average sniffing time of social habituation-dishabituation test in response to littermate and animal's own urine (O). **d** Dispersion plot of exploration time of young and naturally aged animals in response to their own or littermate urine samples. Thick grey lines in dispersion plots indicate mean ± SEM. Data were analyzed by a one-way ANOVA with Tukey's test to test multiple comparisons with more than one variable. $P \leq 0.05$ was considered statistically significant. P values are indicated above the corresponding comparisons

by performing odor-evoked sniffing tests employing social and neutral synthetic odors (Fig. 4). Quantification of the exploration time across various IA dilutions exposed no significant differences between senescent and young mice and even enhanced responses in APP/PS1^{Het} mice. This mild effect in the exploration of IA is probably partly due to the animals' lower interest in exploring neutral odors as compared to conspecifics urine, as previously shown [33, 52, 53]. Nonetheless, results from a FFT revealed no changes in the latency time to find the hidden food pellets (Fig. 4e) indicating that defects in social odor detection related to natural and pathological aging might be more severe than other odor modalities like food odors, which drive vital behaviors such as foraging and feeding, reported to be mainly preserved at old age [74]. In rodents, the differentiation between learned and innate responses is believed to be maintained in advanced processing stages [52, 75]. However, this categorization may be an oversimplification since MOB mitral-tufted cells have been found to project to both the piriform cortex (associated with learned responses) and the posterolateral cortical amygdala (associated with innate responses). Additionally, recent research indicates that the patterns of activity in the piriform cortex and posterolateral cortical amygdala are essentially identical in response to odors of different types (e.g., conspecifics and predators) and valences (e.g., aversive, neutral, and appetitive) [76]. Therefore, the impairments in social odor exploration and discrimination may rise from maladaptations of the VNO-AOB axis, consistent with the observed decrease in AOB volume (Fig. 1b). Future studies should deepen into the anatomical and functional properties of the VNO-AOB circuit in order to obtain a complete picture on how healthy and pathological aging affects social information processing.

Finally, we sought to determine how the age-related defects in social odor sensitivity, discrimination, and memory shaped social behavior. Results from a three-chamber test (Fig. 8) indicated that sociability was overall preserved in senescent and APP/PS1^{Het} animals. In contrast, social novelty was found impaired in APP/PS1^{Het} mice consistently with previous studies [77–79]. However, it is important

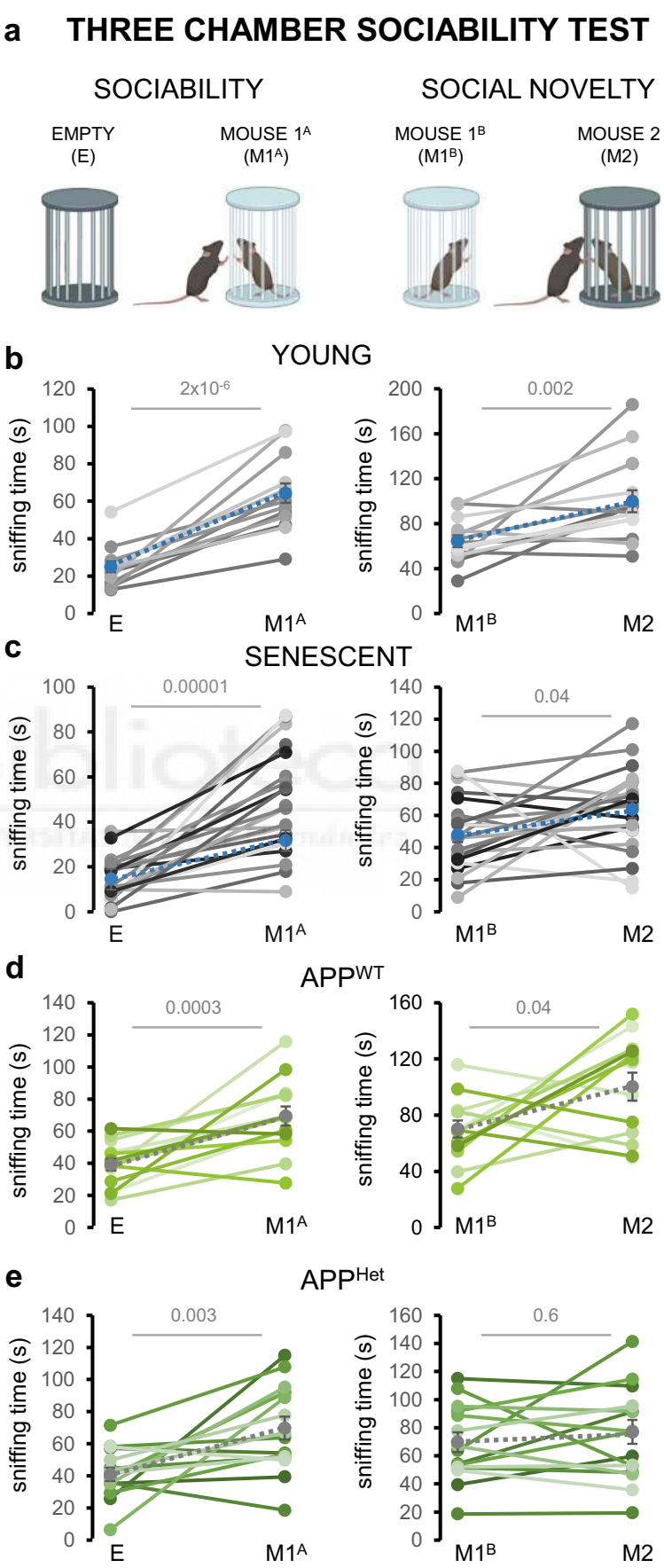

Fig. 8 Social novelty is disrupted during pathological aging. **a** Schematics of the three-chamber test used in this study to test sociability and social novelty. In the sociability phase, the sniffing time of E and $M1^A$ is compared. Social novelty is estimated by quantifying the sniffing time of exploring $M1^B$ versus M2 (see "Materials and Methods"). **b** Paired data of the sniffing times of young wild-type mice during the sociability (E-$M1^A$) and social novelty ($M1^B$-M2) phases. **c** Paired data of the sniffing times of aged wild-type mice during sociability and social novelty. **d** Paired data of the sniffing times of middle-aged APP^{WT} mice during sociability and social novelty. **e** Paired data of the sniffing times of middle-aged APP^{Het} mice during sociability and social novelty. Colored dots in the paired plots indicate mean ± SEM. Data were analyzed by a one-way ANOVA with Tukey's test to test multiple comparisons with more than one variable. $P \leq 0.05$ was considered statistically significant. *P* values are indicated above the corresponding comparisons

to note that our testing conditions in which the empty pencil cup is presented during the habituation may have exacerbated the curiosity towards $M1^A$, potentially obscuring latent deficits in the social phase of the test.

Social novelty impairments in APP/$PS1^{Het}$ mice could be linked to the decline in social discrimination observed in the habituation-dishabituation test (Figs. 5d, e and 6d, f) which may impair the recognition of M2 as a novel subject [80, 81]. Consistent with the overall decrease in the exploration time of social odors (Fig. 3, Supplementary Figs. 3 and 4), aged animals exhibited an increase in the latency to approach novel or familiar mice ($M1^A$, $M1^B$, M^2) and a reduced number of approaches (Supplementary Fig. 9), which could be related to potential locomotion deficits that did not prevent and adequate performance of the three chamber test. These findings indicate that despite the reduction in social odor exploration and discrimination, overall sociability and novelty are majorly preserved in naturally aged mice. In contrast, the APP/PS1 neurodegenerative model shows a measurable impairment in social novelty, which might result from an overall problem in learning and memory as it is one of the main trademarks of AD and a common feature in transgenic mouse models for Aβ amyloidosis [25, 26, 78, 79]. This evidence supports the possibility that neuronal circuits underlying specific social functions (sociability vs. social memory) may be particularly susceptible to pathological aging.

Conclusion

Olfactory deficits are a common symptom of natural and pathological aging. While multiple age-related changes of the olfactory sensory epithelium have been described, the aging of the pheromone detection system, a major gateway for social information, has been largely overlooked. This study reveals that whereas natural aging reduces VSE cell proliferation, mature sensory neurons and organ volume, a common animal model of AD exhibits normal proliferation capacities and no obvious morphological alterations. Despite exhibiting distinctive effects at the cellular level, both natural and pathological aging disrupt the detection of social odors in a more severe way than other odor modalities (i.e., neutral or food odors). Furthermore, social detection and social behavior impairments were exacerbated in APP/$PS1^{Het}$ mice, indicating pathological aging impacts the downstream processing of social information even in the absence of VSE alterations.

Supplementary Information The online version contains supplementary material available at https://doi.org/10.1007/s12035-023-03362-3.

Acknowledgements We are grateful to the teams of the Imaging and Animal Facilities at the Instituto de Neurociencias (CSIC-UMH) and all members of the Jurado and Chamero laboratories for their support during the realization of this work.

Author Contribution The project was led by S.J. Brain sample preparation, data acquisition, and analysis were done by A.P. Result interpretation, manuscript preparation, and editing were done by S.J., P.C., and A.P. with help of members from the Jurado Lab at the Instituto de Neurociencias (CSIC-UMH). All authors read and approved the final manuscript.

Funding Open Access funding provided thanks to the CRUE-CSIC agreement with Springer Nature. This work was supported by grants of the Spanish Ministry of Science and Innovation SAF2017-82524-R and PID2020-113878RB-I00 (to S.J.), the "Severo Ochoa" Program for Centres of Excellence in R&D (SEV-2013–0317 and SEV-2017–0723), the Generalitat Valenciana Prometeo/2019/014 (to S.J.), and a FPI contract (BES-2017–081243) to A.P.; Agence National de la Recherche (ANR): ANR-20-CE92-0003 (to P.C.) and Region Centre Val de Loire: 201900134883 (to P.C.).

Data Availability The datasets supporting the conclusions of this article are included within the article and its additional files.

Declarations

Ethics Approval All experiments were performed according to Spanish and European Union regulations regarding animal research (2010/63/EU), and the experimental procedures were approved by the Bioethical Committee at the Instituto de Neurociencias and the Consejo Superior de Investigaciones Científicas (CSIC).

Consent to Participate Not applicable.

Consent for Publication Not applicable.

Competing Interests The authors declare no competing interests.

References

1. Adolphs R (2001) The neurobiology of social cognition. Curr Opin Neurobiol 11:231–239
2. Brennan PA, Kendrick KM (2006) Mammalian social odours: attraction and individual recognition. Philos Trans R Soc Lond B Biol Sci 361:2061–2078
3. Garratt M, Stockley P, Armstrong SD, Beynon RJ, Hurst JL (2011) The scent of senescence: sexual signaling and female preference in house mice. J Evol Biol 11:2398–2409
4. Murphy C, Schubert CR, Cruickshanks KJ, Klein BEK, Klein R, Nondahl DM (2002) Prevalence of olfactory impairment in older adults. JAMA 288:2307–2312

5. Doty RL, Kamath V (2014) The influences of age on olfaction: a review. Front Psychol 5:20. https://doi.org/10.3389/fpsyg.2014.00020
6. Wilson RS, Krueger KR, Arnold SE, Schneider JA, Kelly JF, Barnes LL, Tang Y, Bennett DA (2007) Loneliness and risk of Alzheimer disease. Arch Gen Psychiatry 64:234–240
7. Donovan NJ, Okereke OI, Vannini P, Amariglio RE, Rentz DM, Marshall GA, Johnson KA, Sperling RA (2016) Association of higher cortical amyloid burden with loneliness in cognitively normal older adults. JAMA Psychiat 73:1230–1237
8. Chamero P, Leinders-Zufall T, Zufall F (2012) From genes to social communication: molecular sensing by the vomeronasal organ. Trends Neurosci 35:597–606
9. Li Y, Dulac C (2018) Neural coding of sex-specific social information in the mouse brain. Curr Opin Neurobiol 53:120–130
10. Jacobson L (1813) Anatomisk beskrivelse over et nyt organ I huusdyrenes naese. Veter Salesk Skr 2:209–246
11. Halpern M, Martínez-Marcos A (2003) Structure and function of the vomeronasal system: an update. Prog Neurobiol 70:245–318
12. Munger SD, Leinders-Zufall T, Zufall F (2009) Subsystem organization of the mammalian sense of smell. Annu Rev Physiol 71:115–140
13. Ennis M, Puche AC, Holy T, Shipley MT (2015) The olfactory system. In The Rat Nervous System, 4th edn. Elsevier Inc., pp 761–803. https://doi.org/10.1016/B978-0-12-374245-2.00027-9
14. Zufall F, Leinders-Zufall T (2007) Mammalian pheromone sensing. Curr Opin Neurobiol 17:483–489
15. Baum MJ, Kelliher KR (2009) Complementary roles of the main and accessory olfactory systems in mammalian mate recognition. Annu Rev Physiol 71:141–160
16. Wilson KC, Raisman G (1980) Age-related changes in the neurosensory epithelium of the mouse vomeronasal organ: extended period of postnatal growth in size and evidence for rapid cell turnover in the adult. Brain Res 185:103–113
17. Weiler E, McCulloch MA, Farbman AI (1999) Proliferation in the vomeronasal organ of the rat during postnatal development. Eur J Neurosci 11:700–711
18. Brann JH, Firestein SJ (2010) Regeneration of new neurons is preserved in aged vomeronasal epithelia. J Neurosci 30:15686–15694
19. Oboti L, Ibarra-Soria X, Pérez-Gómez A, Schimd A, Pyrski M, Paschek N, Kircher S, Logan DW et al (2015) Pregnancy and estrogen enhance neural progenitor-cell proliferation in the vomeronasal sensory epithelium. BMC Biol 13:104. https://doi.org/10.1186/s12915-015-0211-8
20. Ahlenius H, Visan V, Kokaia M, Lindvall O, Koaia Z (2009) Neuronal stem and progenitor cells retain their potential for proliferation and differentiation into functional neurons despite lower number in aged brain. J Neurosci 29:4408–4419
21. Mobley AS, Rodríguez-Gil DJ, Imamura F, Greer CA (2014) Aging in the olfactory system. Trends Neurosci 37:77–84
22. Devanand DP (2016) Olfactory identification deficits, cognitive decline and dementia in older adults. Am J Geriatr Psychiatry 24:1151–1157
23. Mechin V, Pageat P, Teruel E, Asproni P (2021) Histological and immunohistochemical characterization of vomeronasal organ aging in mice. Animals 11:1211
24. Jankowsky JL, Fadale DJ, Anderson J, Xu GM, Gonzales V, Jenkins NA, Copeland NG, Lee MK et al (2004) Mutant presenilins specifically elevate the levels of the 42 residue beta-amyloid peptide in vivo: evidence for augmentation of a 42-specific gamma secretase. Hum Mol Genet 13:159–170
25. Jankowsky JL, Slunt HH, Ratovitski T, Jenkins NA, Copeland NG, Borchelt DR (2001) Co-expression of multiple transgenes in mouse CNS: a comparison of strategies. Biomol Eng 17:157–165
26. Reiserer RS, Harrison FE, Syverud DC, McDonald MP (2007) Impaired spatial learning in the APPSwe + PSEN1DeltaE9 bigenic mouse model of Alzheimer's disease. Genes Brain Behav 6:54–65
27. Wong FK, Bercsenyi K, Sreenivasan V, Portalés A, Fernández-Otero M, Marín O (2018) Pyramidal cell regulation of interneuron survival sculpts cortical networks. Nature 557:668–673
28. West MJ, Gundersen HJ (1990) Unbiased stereological estimation of the number of neurons in the human hippocampus. J Comp Neurol 296:1–22
29. Parrish-Aungst S, Shipley MT, Erdelyi F, Szabo G, Puche AC (2007) Quantitative analysis of neuronal diversity in the mouse olfactory bulb. J Comp Neurol 501:825–836
30. Giacobini P, Benedetto A, Tirindelli R, Fasolo A (2000) Proliferation and migration of receptor neurons in the vomeronasal organ of the adult mouse. Brain Res Dev Brain Res 123:33–40
31. Root CM, Denny CA, Hen R, Axel R (2014) The participation of cortical amygdala in innate, odour-driven behaviour. Nature 515:269–273
32. Fortes-Marco L, Lanuza E, Martinez-Garcia F, Agustín-Pavón C (2015) Avoidance and contextual learning induced by a kairomone, a pheromone and a common odorant in female CD1 mice. Front Neurosci 9:336
33. Saraiva LR, Kondoh K, Ye X, Yoon KH, Hernandez M, Buck LB (2016) Combinatorial effects of odorants on mouse behavior. Proc Natl Acad Sci U S A 113:E3300–E3306
34. Chamero P, Weiss J, Alonso MT, Rodríguez-Prados M, Hisatsune C, Mikoshiba K, Leinders-Zufall T, Zufall F (2017) Type 3 inositol 1,4,5-trisphosphate receptor is dispensable for sensory activation of the mammalian vomeronasal organ. Sci Rep 7:10260
35. Kurien BT, Everds NE, Scofield RH (2004) Experimental animal urine collection: a review. Lab Anim 38:333–361
36. Breton-Provencher V, Lemasson M, Peralta MR 3rd, Saghatelyan A (2009) Interneurons produced in adulthood are required for the normal functioning of the olfactory bulb network and for the execution of selected olfactory behaviors. J Neurosci 29:15245–15257
37. Sanderson DJ, Bannerman DM (2011) Competitive short-term and long-term memory processes in spatial habituation. J Exp Psychol Anim Behav Process 37:189–199
38. Deacon RMJ, Koros E, Bornemann KD, Rawlins JNP (2009) Aged Tg2576 mice are impaired on social memory and open field habituation tests. Behav Brain Res 197:466–468
39. Gheusi G, Cremer H, McLean H, Chazal G, Vincent JD, Lledo PM (2000) Importance of newly generated neurons in the adult OB for odor discrimination. Proc Natl Acad Sci U S A 97:1823–1828
40. Nadler JJ, Moy SS, Dold G, Trang D, Simmons N, Pérez A, Young NB, Barbaro RP et al (2004) Automated apparatus for quantitation of social approach behaviors in mice. Genes Brain Behav 3:303–314
41. Cheetham SA, Thom MD, Jury F, Ollier WER, Beynon RJ, Hurst JL (2007) The genetic basis of individual-recognition signals in the mouse. Curr Biol 17:177–277
42. Ferrero DM, Moeller LM, Osakada T, Horio N, Li Q, Roy DS, Cichy A, Spehr M et al (2013) A juvenile mouse pheromone inhibits sexual behaviour through the vomeronasal system. Nature 502:368–371
43. Guo Z, Packard A, Krolewski RC, Harris MT, Manglapus GL, Schwob JE (2010) Expression of pax6 and sox2 in adult olfactory epithelium. J Comp Neurol 18:4395–4418
44. Taroc EZM, Katreddi RR, Forni PE (2020) Identifying Isl1 genetic lineage in the developing olfactory system and in GnRH-1 neurons. Front Physiol 11:601923
45. Katreddi RR, Forni PE (2012) Mechanisms underlying pre- and postnatal development of the vomeronasal organ. Cell Mol Life Sci 78:5069–5082

46. Tucker ES, Lehtinen MK, Maynard T, Zirlinger M, Dulac C, Rawson N, Pevny L, La-Mantia AS (2010) Proliferative and transcriptional identity of distinct classes of neural precursors in the mammalian olfactory epithelium. Development 137:2471–2481
47 Panaliappan TK, Wittmann W, Jidigam VK, Mercurio S, Bertolini JA, Sghari S, Bose R, Patthey C et al (2018) Sox2 is required for olfactory pit formation and olfactory neurogenesis through BMP restriction and Hes5 upregulation. Development 145:dev153791
48. Rawson NE, Gomez G, Cowart BJ, Kriete A, Pribitkin E, Restrepo D (2012) Age-associated loss of selectivity in human olfactory sensory neurons. Neurobiol Aging 33:1913–1919
49. Roberts RO, Christianson TJ, Kremers WK, Mielke MM, Machulda MM, Vassilaki M, Alhurani RE, Geda YE et al (2016) Association between olfactory dysfunction and amnestic mild cognitive impairment and Alzheimer disease dementia. JAMA Neurol 73:93–101
50. Yang M, Crawley JN (2009) Simple behavioral assessment of mouse olfaction. Curr Protoc Neurosci 8. Unit 8.24 https://doi.org/10.1002/0471142301.ns0824s48
51. Martínez B, Karunanayaka P, Wang J, Tobia MJ, Vasavada M, Eslinger PJ, Yang QX (2017) Different patterns of age-related central olfactory decline in men and women as quantified by olfactory fMRI. Oncotarget 8:79212–79222
52. Kobayakawa K, Kobayakawa R, Matsumoto H, Oka Y, Imai T, Ikawa M, Okabe M, Ikeda T et al (2007) Innate versus learned odour processing in the mouse olfactory bulb. Nature 450:503–508
53. Jagetia S, Milton AJ, Stetzik LA, Liu S, Pai K, Arakawa K, Mandairon N, Wesson DW (2018) Inter- and intra-mouse variability in odor preferences revealed in an olfactory multiple-choice test. Behav Neurosci 132:88–98
54. La Joie R, Perrotin A, Egret S, Pasquier F, Tomadesso C, Mézenge F, Desgranges B, de La Sayette V et al (2016) Qualitative and quantitative assessment of self-reported cognitive difficulties in nondemented elders: association with medical help seeking, cognitive deficits, and β-amyloid imaging. Alzheimers Dement 5:23–34
55. Valech N, Tort-Merino A, Coll-Padrós N, Olives J, León M, Rami L, Molinuevo JL (2018) Executive and language subjective cognitive decline complaints discriminate preclinical Alzheimer's disease from normal aging. J Alzheimers Dis 61:689–703
56. Yang M, Silverman JL, Crawley JN (2011) Automated three-chambered social approach task for mice. Curr Protoc Neurosci 8(8):26. https://doi.org/10.1002/0471142301.ns0826s56
57. Cohen S, Wills TA (1985) Stress, social support, and the buffering hypothesis. Psychol Bull 98:310–357
58. Moran JM, Jolly E, Mitchell JP (2012) Social-cognitive deficits in normal aging. J Neurosci 32:5553–5561
59. Spalletta G, Baldinetti BI, Fadda L, Perri R, Scalmana S, Serra L, Caltagirone C (2004) Cognition and behaviour are independente and hetreogenous dimensions in Alzheimer's disease. J Neurol 251:68–95
60. Mohs RC, Schmeidler J, Aryan M (2000) Longitudinal studies of cognitive, functional and behavioural changes in patients with Alzheimer's disease. Sta Med 19:1401–1409
61. Murphy C (2019) Olfactory and other sensory impairments in Alzheimer disease. Nat Rev Neurol 15:11–24
62. Verret L, Jankowsky JL, Xu GM, Borchelt DR, Rampon C (2007) Alzheimer's-type amyloidosis in transgenic mice impairs survival of newborn neurons derived from adult hippocampal neurogenesis. J Neurosci 27:6771–6780
63. Zhang C, McNeil E, Dressler L, Siman R (2007) Long-lasting impairment in hippocampal neurogenesis associated with amyloid deposition in a knock-in mouse model of familial Alzheimer's disease. Exp Neurol 204:77–87
64. Zeng Q, Zheng M, Zhang T, He G (2016) Hippocampal neurogenesis in the APP/PS1/nestin-GFP triple transgenic mouse model of Alzheimer's disease. Neuroscience 314:64–74
65. Scopa C, Marrocco F, Latina V, Ruggeri F, Corvaglia V, La Regina F, Ammassari-Teule M, Middei S et al (2020) Impaired adult neurogenesis is an early event in Alzheimer's disease neurodegeneration, mediated by intracellular Aβ oligomers. Cell Death Difer 27:934–948
66. Richard MB, Taylor SR, Greer CA (2010) Age-induced disruption of selective olfactory bulb synaptic circuits. Proc Natl Acad Sci U S A 107:15613–15618
67. Lee AC, Tian H, Grosmaitre X, Ma M (2009) Expression patterns of odorant receptors and response properties of olfactory sensory neurons in aged mice. Chem Senses 34:695–703
68. Khan M, Vaes E, Mombaerts P (2013) Temporal patterns of odorant receptor gene expression in adult and aged mice. Mol Cell Neurosci 57:120–129
69. Kass MD, Czarnecki LA, McGann JP (2018) Stable olfactory sensory neuron in vivo physiology during normal aging. Neurobiol Aging 69:33–37
70. Tobiansky DJ, Hattori T, Scott JM, Nutsch VL, Roma PG, Dominguez JM (2012) Mating-relevant olfactory stimuli activate the rat brain in an age-dependent manner. NeuroReport 23:1077–1083
71. Tikhonova MA, Romaschenko AV, Akulov AE, Ho YJ, Kolosova NG, Moshkin MP, Amstislavskaya TG (2015) Comparative study of perception and processing of socially or sexually significant odor information in male rats with normal or accelerated senescence using fMRI. Behav Brain Res 294:89–94
72. Jessen F, Amariglio RE, Buckley RF, van der Flier WM, Han Y, Molinuevo JL, Rabin L, Rentz DM et al (2020) The characterisation of subjective cognitive decline. Lancet Neurol 19:271–278
73. Ueha R, Shichino S, Ueha S, Kondo K, Kikuta S, Nishijima H, Matsushima K, Yamasoba T (2018) Reduction of proliferating olfactory cells and low expression of extracellular matrix genes are hallmarks of the aged olfactory mucosa. Front Aging Neurosci 10:86
74. Harb MR, Sousa N, Zihl J, Almeida OFX (2014) Reward components of feeding behavior are preserved during mouse aging. Front Aging Neurosci 6:242
75. Li Q, Liberles SD (2015) Aversion and attraction through olfaction. Curr Biol 25:R120–R129
76. Iurilli G, Datta SR (2017) Population coding in an innately relevant olfactory area. Neuron 93:1180–1197
77. Cheng D, Spiro AS, Jenner AM, Garner B, Karl T (2014) Long-term cannabidiol treatment prevents the development of social recognition memory deficits in Alzheimer's disease transgenic mice. J Alzheimers Dis 42:1383–1396
78. Olesen LØ, Bouzinova EV, Severino M, Sivasaravanaparan M, Hasselstrøm JB, Finsen B, Wiborg O (2016) Behavioural phenotyping of APPswe/PS1δE9 mice: age related changes and effect of long-term paroxetine treatment. PLoS One 11:e0165144. https://doi.org/10.1371/journal.pone.0165144
79. Locci A, Orellana H, Rodríguez G, Gottliebson M, McClarty B, Domínguez S, Keszycki R, Dong H (2021) Comparison of memory, affective behavior, and neuropathology in APPNLGF knock-in mice to 5xFAD and APP/PS1 mice. Behav Brain Res 404:113192
80. Enwere E, Shingo T, Gregg C, Fujikawa H, Ohta S, Weiss S (2004) Aging results in reduced epidermal growth factor receptor signaling, diminished olfactory neurogenesis, and deficits in fine olfactory discrimination. J Neurosci 24:8354–8365
81. Moreno M, Richard M, Landrein B, Sacquet J, Didier A, Mandairon N (2014) Alteration of olfactory perceptual learning and its cellular basis in aged mice. Neurobiol Aging 35:680–691

SUPPLEMENTARY INFORMATION

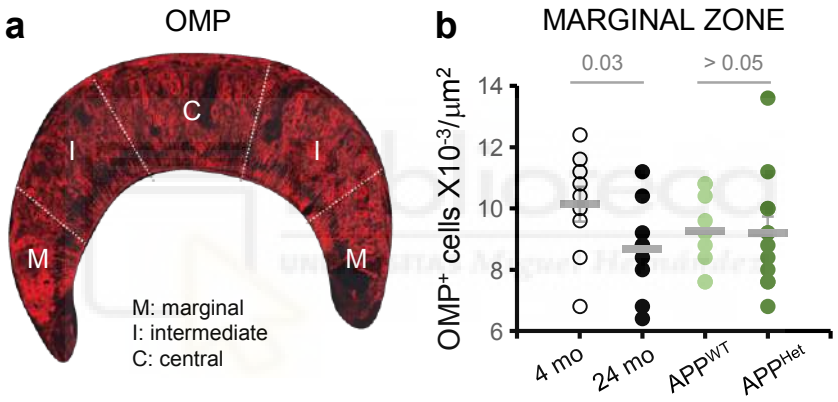

Supplementary Figure 1

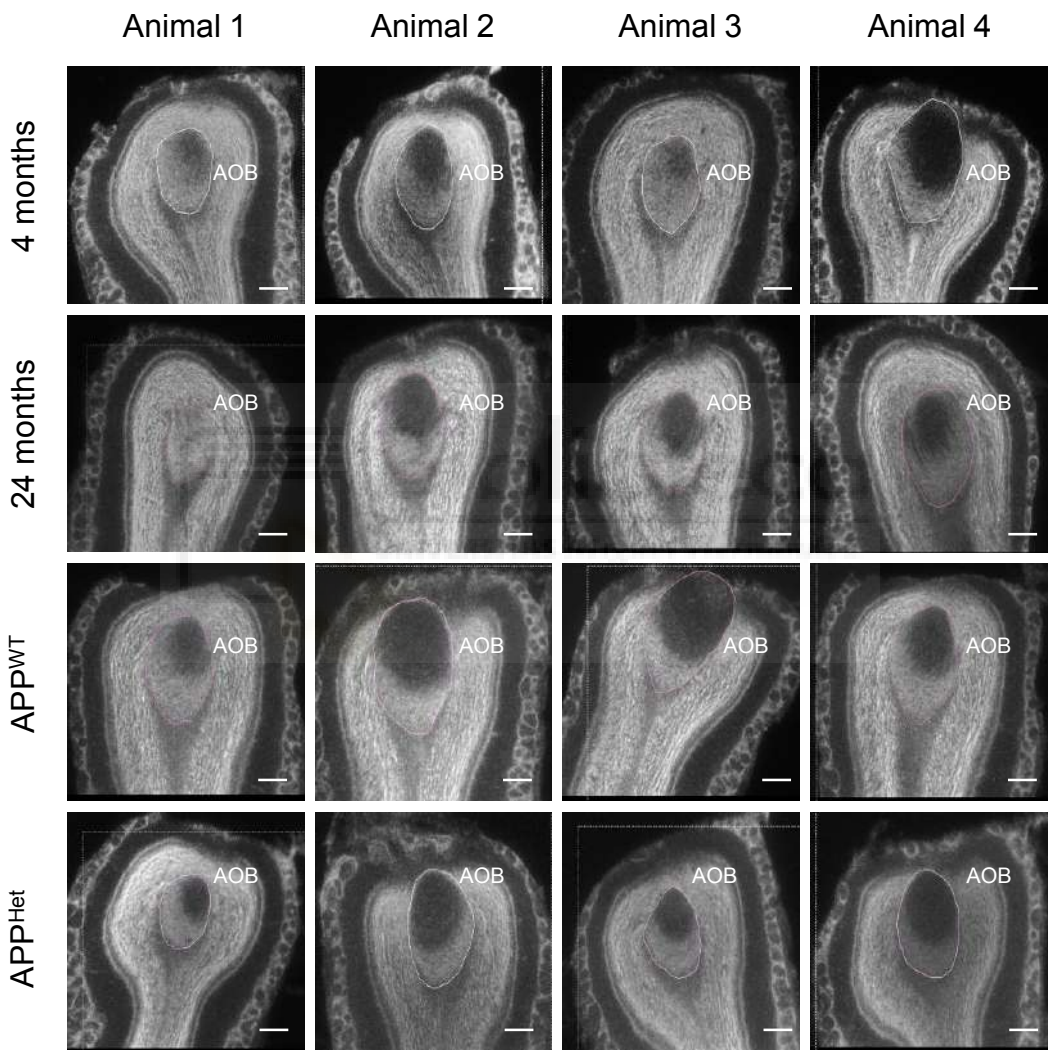

Supplementary Figure 2

SOCIAL ODOR EXPLORATION – NATURAL AGING

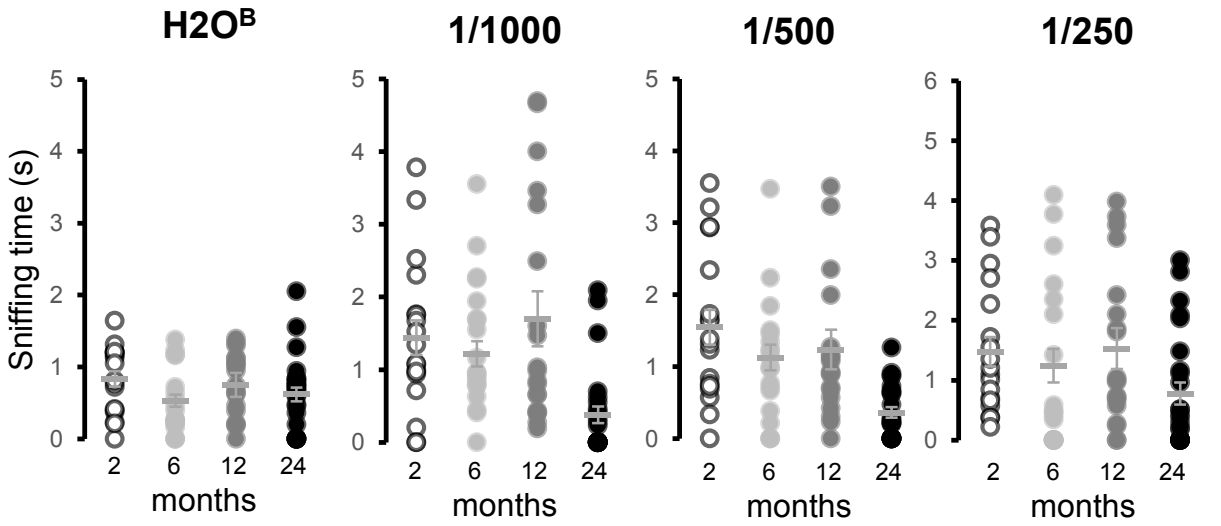

One-way ANOVA

H2O^B	
Comparison	***P***
4 m vs 8 m	**0.02**
4 m vs 12 m	ns
2 m vs 24 m	ns
8 m vs 12 m	ns
8 m vs 24 m	ns
12 m vs 24 m	ns

1:1000 urine dilution	
Comparison	***P***
4 m vs 8 m	ns
4 m vs 12 m	ns
4 m vs 24 m	**0.0007**
8 m vs 12 m	ns
8 m vs 24 m	**0.0004**
12 m vs 24 m	**0.002**

1:500 urine dilution	
Comparison	***P***
4 m vs 8 m	ns
4 m vs 12 m	ns
4 m vs 24 m	**0.0002**
44 m vs 12 m	ns
4 m vs 24 m	**0.0005**
12 m vs 24 m	**0.0008**

1:250 urine dilution	
Comparison	***P***
4 m vs 8 m	ns
4 m vs 12 m	ns
4 m vs 24 m	**0.03**
8 m vs 12 m	ns
8 m vs 24 m	ns
12 m vs 24 m	**0.04**

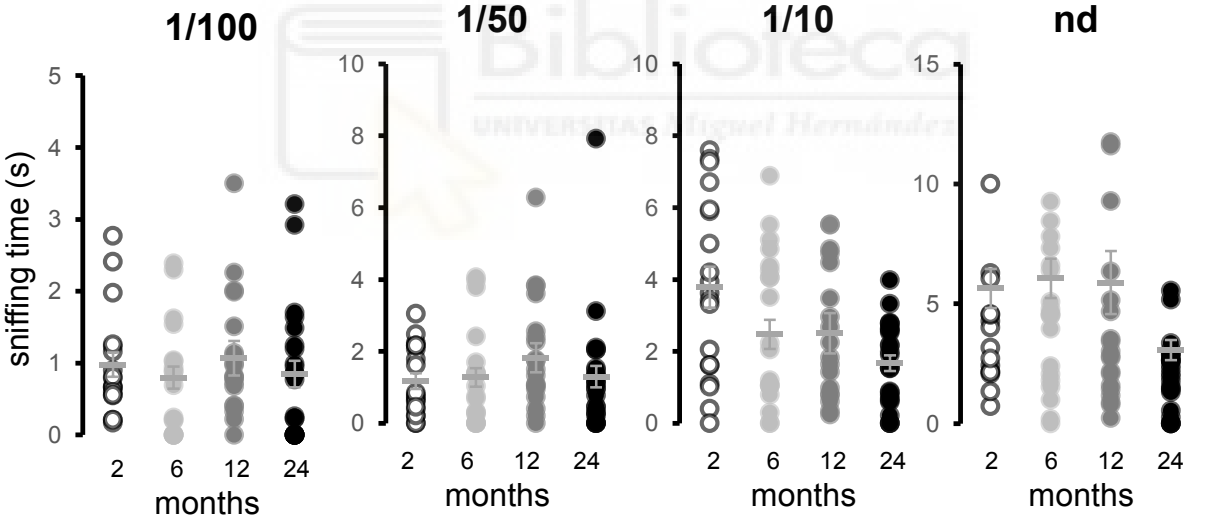

One-way ANOVA

1:100 urine dilution	
Comparison	***P***
4 m vs 8 m	ns
4 m vs 12 m	ns
4 m vs 24 m	ns
8 m vs 12 m	ns
8 m vs 24 m	ns
12 m vs 24 m	ns

1:50 urine dilution	
Comparison	***P***
4 m vs 8 m	ns
4 m vs 12 m	ns
4 m vs 24 m	ns
8 m vs 12 m	ns
8 m vs 24 m	ns
12 m vs 24 m	ns

1:10 urine dilution	
Comparison	***P***
4 m vs 8 m	**0.08**
4 m vs 12 m	**0.04**
4 m vs 24 m	**0.002**
8 m vs 12 m	ns
8 m vs 24 m	ns
12 m vs 24 m	ns

Non diluted	
Comparison	***P***
4 m vs 8 m	ns
4 m vs 12 m	ns
4 m vs 24 m	**0.04**
8 m vs 12 m	ns
8 m vs 24 m	**0.003**
12 m vs 24 m	**0.02**

dilution / age	*H_2O^B*	*1:000*	*1:500*	*1:250*	*1.100*	*1:50*	*1:10*	*nd*
	n	**n**	***n***	***n***	***n***	***n***	***n***	***n***
4 months	18	18	18	18	18	18	18	18
8 months	20	20	20	20	20	20	20	20
12 months	20	20	20	20	20	20	20	20
24 months	25	25	25	25	25	25	25	25

Supplementary Figure 3

SOCIAL ODOR EXPLORATION – NATURAL AGING

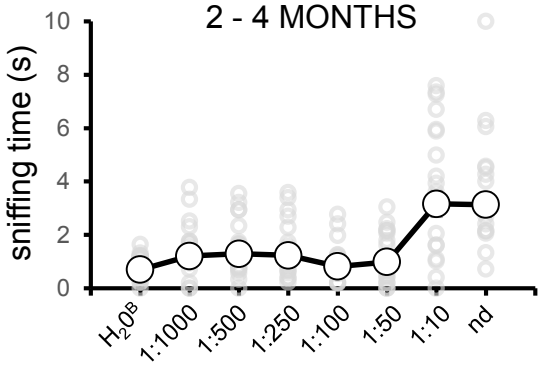

One Way ANOVA – Tukey test

2 months	
Comparison	***P***
H_2O^B vs 1/1000	0.91
H_2O^B vs 1/500	0.81
1/1000 vs 1/500	1.00
H_2O^B vs 1/250	0.88
1/250 vs 1/1000	1.00
1/250 vs 1/500	1.00
H_2O^B vs 1/100	0.99
1/100 vs 1/1000	0.97
1/100 vs 1/500	0.93
1/100 vs 1/250	0.99
H_2O^B vs 1/50	0.99
1/50 vs 1/1000	0.99
1/500 vs 1/50	0.99
1/250 vs 1/50	0.99

2 months	
Comparison	***P***
1/100 vs 1/50	0.99
H_2O^B vs 1/10	1.5×10^{-7}
1/10 vs 1/1000	5.0×10^{-5}
1/10 vs 1/500	1.3×10^{-4}
1/10 vs 1/250	7.0×10^{-5}
1/10 vs 1/100	5.8×10^{-7}
1/10 vs 1/50	3.0×10^{-6}
Nd vs H_2O^B	1.0×10^{-6}
Nd vs 1/1000	2.2×10^{-4}
Nd vs 1/500	5.2×10^{-4}
Nd vs 1/250	3.0×10^{-4}
Nd vs 1/100	4.0×10^{-6}
Nd vs 1/50	1.8×10^{-5}
Nd vs 1/10	1.00

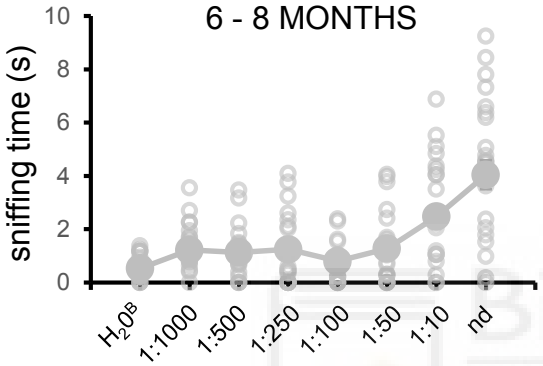

One Way ANOVA – Tukey test

6 months	
Comparison	***P***
H_2O^B vs 1/1000	0.63
H_2O^B vs 1/500	0.85
1/1000 vs 1/500	0.99
H_2O^B vs 1/250	0.82
1/250 vs 1/1000	0.99
1/250 vs 1/500	1.00
H_2O^B vs 1/100	0.99
1/100 vs 1/1000	0.94
1/100 vs 1/500	0.99
1/100 vs 1/250	0.98
H_2O^B vs 1/50	0.53
1/50 vs 1/1000	1.0
1/500 vs 1/50	0.99
1/250 vs 1/50	0.99

6 months	
Comparison	***P***
1/100 vs 1/50	0.90
H_2O^B vs 1/10	6.4×10^{-5}
1/10 vs 1/1000	0.07
1/10 vs 1/500	0.02
1/10 vs 1/250	0.03
1/10 vs 1/100	0.0016
1/10 vs 1/50	0.07
Nd vs H_2O^B	2.2×10^{-8}
Nd vs 1/1000	8.3×10^{-8}
Nd vs 1/500	4.1×10^{-8}
Nd vs 1/250	$4,3 \times 10^{-8}$
Nd vs 1/100	4.5×10^{-8}
Nd vs 1/50	7.0×10^{-8}
Nd vs 1/10	0.01

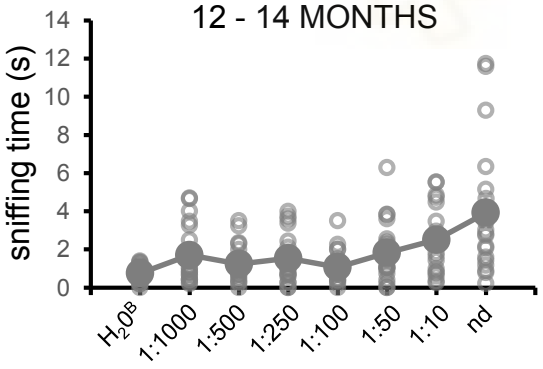

One Way ANOVA – Tukey test

12 months	
Comparison	***P***
H_2O^B vs 1/1000	0.67
H_2O^B vs 1/500	0.98
1/1000 vs 1/500	0.99
H_2O^B vs 1/250	0.85
1/250 vs 1/1000	0.99
1/250 vs 1/500	0.99
H_2O^B vs 1/100	0.99
1/100 vs 1/1000	0.94
1/100 vs 1/500	0.99
1/100 vs 1/250	0.99
H_2O^B vs 1/50	0.50
1/50 vs 1/1000	1.0
1/500 vs 1/50	0.95
1/250 vs 1/50	0.99

12 months	
Comparison	***P***
1/100 vs 1/50	0.85
H_2O^B vs 1/10	0.04
1/10 vs 1/1000	0.84
1/10 vs 1/500	0.31
1/10 vs 1/250	0.67
1/10 vs 1/100	0.17
1/10 vs 1/50	0.92
Nd vs H_2O^B	1.3×10^{-6}
Nd vs 1/1000	0.002
Nd vs 1/500	7.2×10^{-5}
Nd vs 1/250	8.0×10^{-4}
Nd vs 1/100	2.0×10^{-5}
Nd vs 1/50	0.005
Nd vs 1/10	0.20

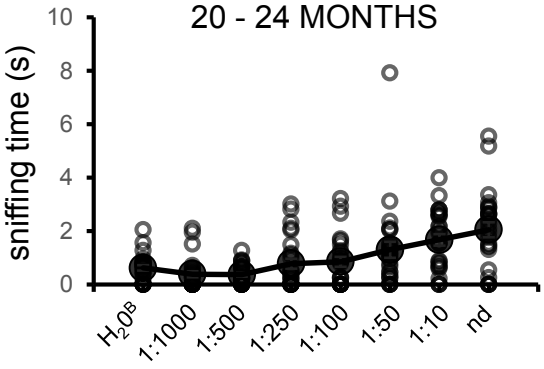

One Way ANOVA – Tukey test

24 months	
Comparison	***P***
H_2O^B vs 1/1000	0.99
H_2O^B vs 1/500	0.98
1/1000 vs 1/500	1.0
H_2O^B vs 1/250	0.99
1/250 vs 1/1000	0.87
1/250 vs 1/500	0.84
H_2O^B vs 1/100	0.99
1/100 vs 1/1000	0.73
1/100 vs 1/500	0.69
1/100 vs 1/250	1.0
H_2O^B vs 1/50	0.25
1/50 vs 1/1000	0.03
1/500 vs 1/50	0.03
1/250 vs 1/50	0.6

24 months	
Comparison	***P***
1/100 vs 1/50	0.76
H_2O^B vs 1/10	0.007
1/10 vs 1/1000	3.4×10^{-4}
1/10 vs 1/500	2.6×10^{-4}
1/10 vs 1/250	0.04
1/10 vs 1/100	0.08
1/10 vs 1/50	0.88
Nd vs H_2O^B	3.4×10^{-5}
Nd vs 1/1000	8.4×10^{-7}
Nd vs 1/500	6.3×10^{-7}
Nd vs 1/250	$4,6 \times 10^{-4}$
Nd vs 1/100	0.001
Nd vs 1/50	0.14
Nd vs 1/10	0.89

Supplementary Figure 4

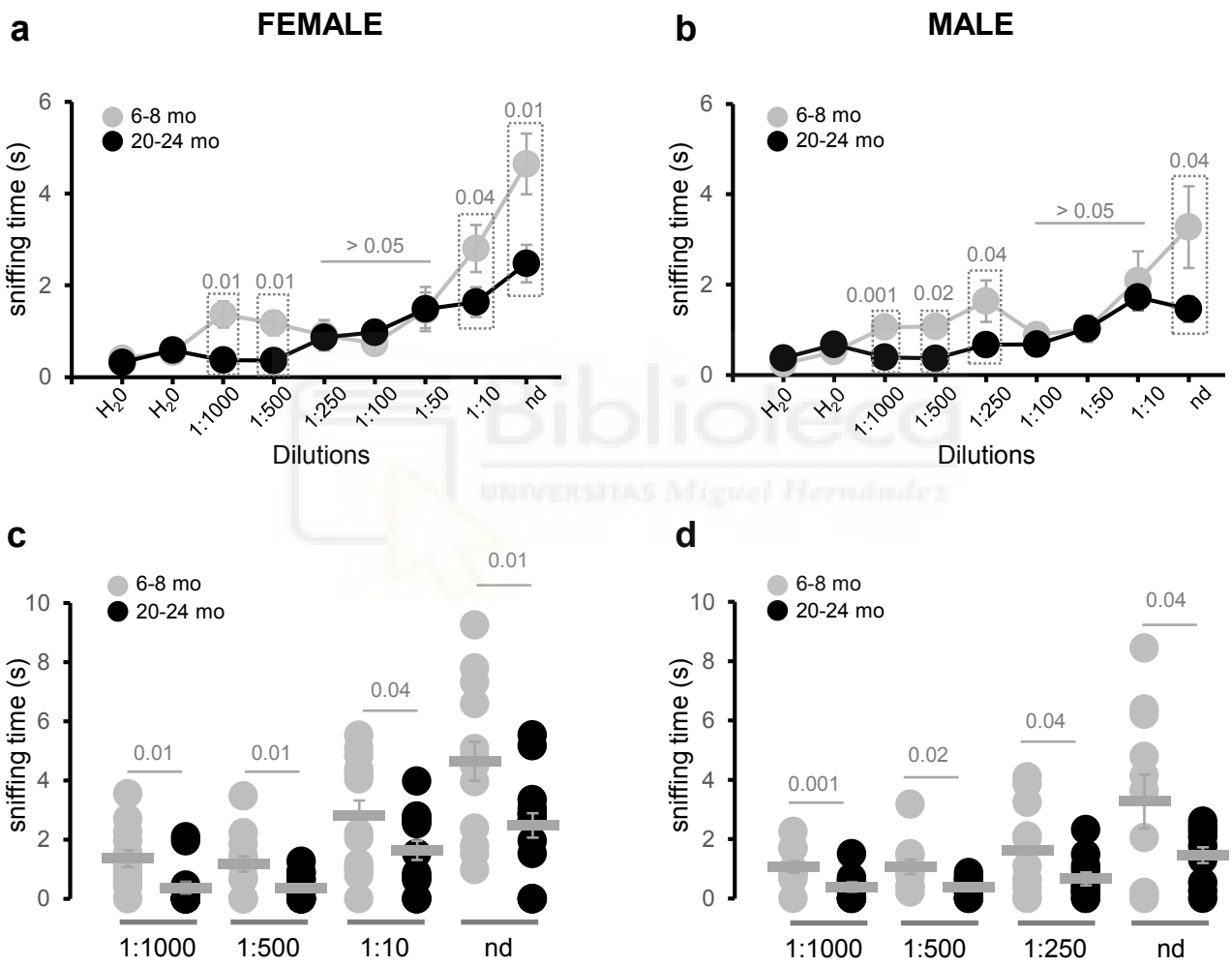

Supplementary Figure 5

SOCIAL ODOR EXPLORATION - PATHOLOGICAL AGING

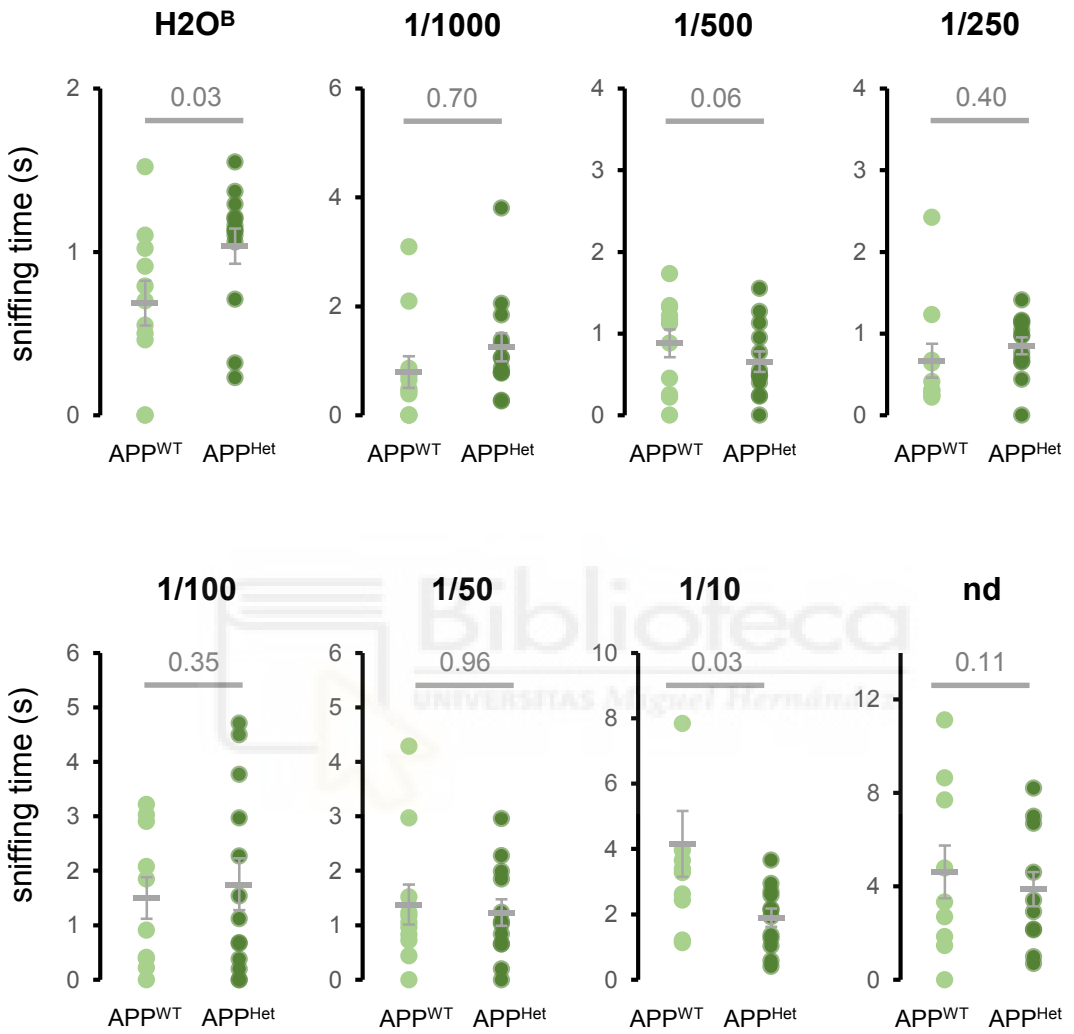

dilution / genotype	H_2O_B	1:1000	1:500	1:250	1.100	1:50	1:10	nd
	n	*n*	*n*	*n*	*n*	*n*	*n*	*n*
APP^{WT}	11	11	11	11	11	11	11	11
APP^{Het}	12	12	12	12	12	12	12	12

Supplementary Figure 6

SOCIAL ODOR EXPLORATION – PATHOLOGICAL AGING

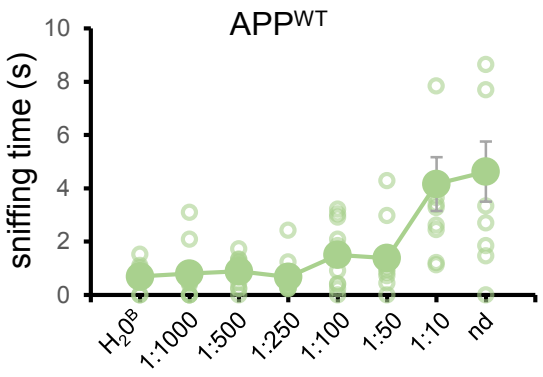

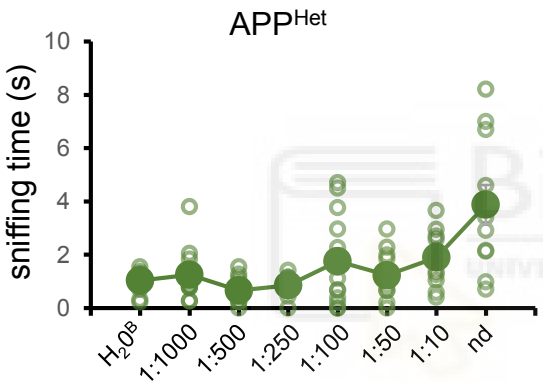

One Way ANOVA – Tukey test

APP^{WT}	
Comparison	***P***
H_2O^B vs 1/1000	1.00
H_2O^B vs 1/500	1.00
1/1000 vs 1/500	1.00
H_2O^B vs 1/250	1.00
1/250 vs 1/1000	1.00
1/250 vs 1/500	0.99
H_2O^B vs 1/100	0.97
1/100 vs 1/1000	0.99
1/100 vs 1/500	0.99
1/100 vs 1/250	0.97
H_2O^B vs 1/50	0.98
1/50 vs 1/1000	0.99
1/500 vs 1/50	0.99
1/250 vs 1/50	0.98

APP^{WT}	
Comparison	***P***
1/100 vs 1/50	1.00
H_2O^B vs 1/10	0.001
1/10 vs 1/1000	0.002
1/10 vs 1/500	0.003
1/10 vs 1/250	0.002
1/10 vs 1/100	0.04
1/10 vs 1/50	0.02
Nd vs H_2O^B	3.1×10^{-4}
Nd vs 1/1000	5.0×10^{-4}
Nd vs 1/500	7.2×10^{-4}
Nd vs 1/250	4.1×10^{-4}
Nd vs 1/100	0.01
Nd vs 1/50	0.005
Nd vs 1/10	0.99

One Way ANOVA – Tukey test

APP^{Het}	
Comparison	***P***
H_2O^B vs 1/1000	0.99
H_2O^B vs 1/500	0.99
1/1000 vs 1/500	0.91
H_2O^B vs 1/250	0.99
1/250 vs 1/1000	0.99
1/250 vs 1/500	0.99
H_2O^B vs 1/100	0.79
1/100 vs 1/1000	0.96
1/100 vs 1/500	0.30
1/100 vs 1/250	0.99
H_2O^B vs 1/50	0.99
1/50 vs 1/1000	1.00
1/500 vs 1/50	0.93
1/250 vs 1/50	0.99

APP^{Het}	
Comparison	***P***
1/100 vs 1/50	0.95
H_2O^B vs 1/10	0.63
1/10 vs 1/1000	0.88
1/10 vs 1/500	0.18
1/10 vs 1/250	0.38
1/10 vs 1/100	0.99
1/10 vs 1/50	0.90
Nd vs H_2O^B	6.6×10^{-6}
Nd vs 1/1000	3.7×10^{-5}
Nd vs 1/500	3.4×10^{-7}
Nd vs 1/250	1.5×10^{-6}
Nd vs 1/100	0.002
Nd vs 1/50	4.7×10^{-5}
Nd vs 1/10	0.005

Supplementary Figure 7

NEUTRAL ODOR EXPLORATION

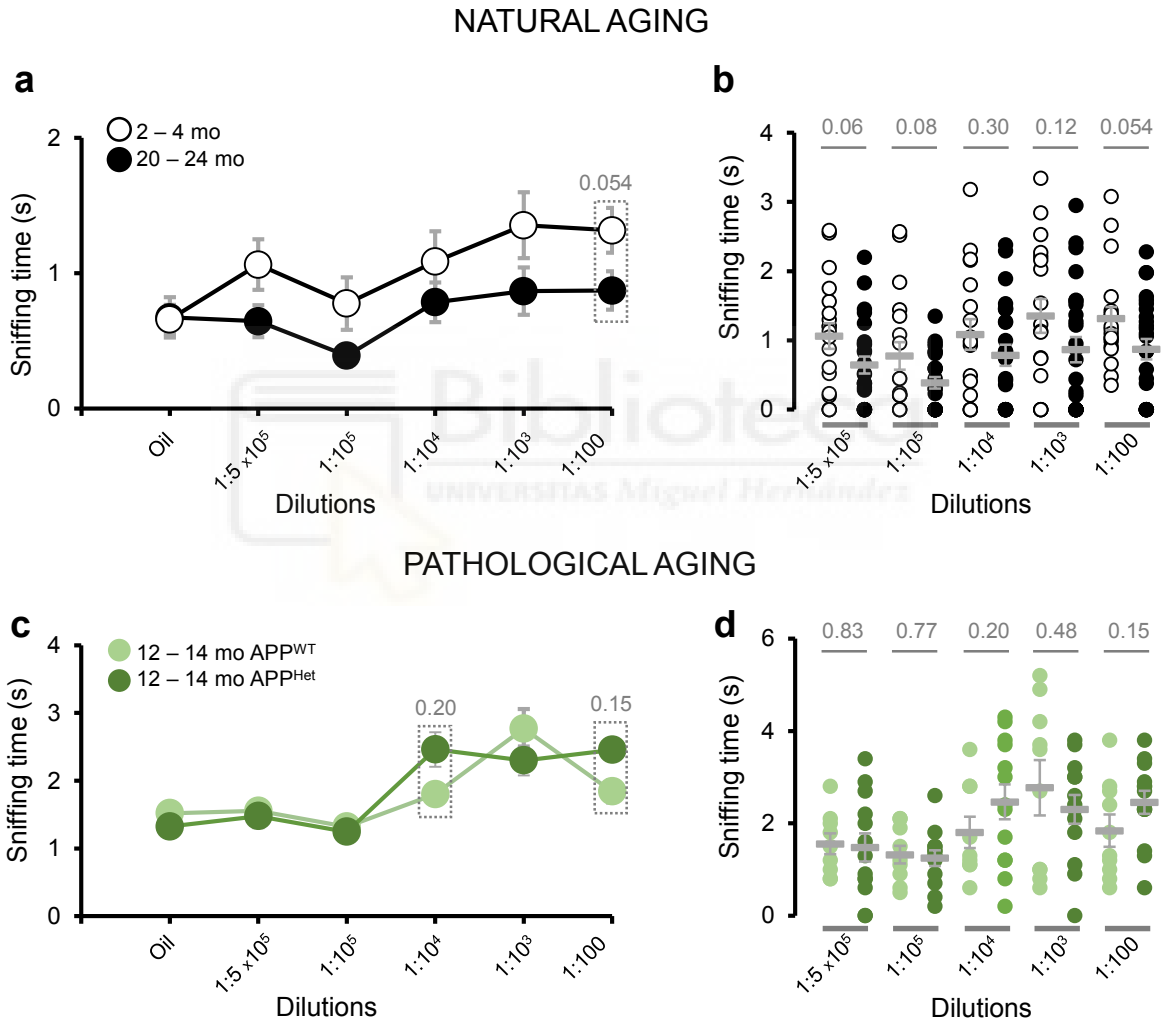

Supplementary Figure 8

THREE CHAMBER SOCIABILITY TEST

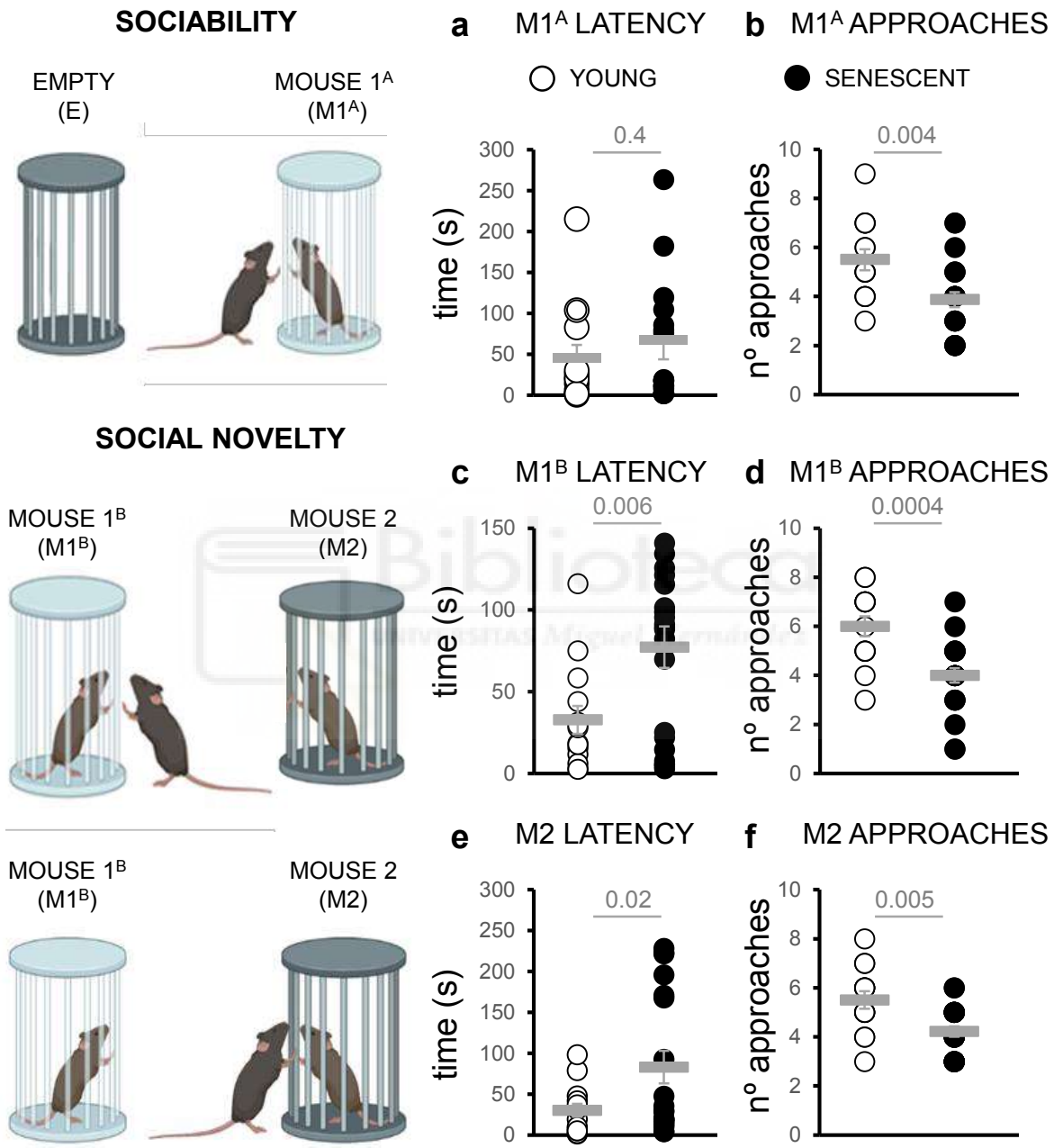

Supplementary Figure 9

Supplementary Results

Table 1. Figure 1a. VSE Volume (mm^3)

Age - Genotype	VSE Volume (mm^3)	N (mice)	One-way ANOVA Comparisons	One way ANOVA P value	Two-way ANOVA Age – Genotype interaction P value
4 months	0.190 ± 0.008	4	4 months vs 24 months	0.014	0.37
24 months	0.160 ± 0.007	4	APP^{WT} vs APP^{HET}	0.40	
1-year-old APP^{WT}	0.170 ± 0.007	4	4 months vs APP^{HET}	0.015	
1-year-old APP^{HET}	0.160 ± 0.008	4	24 months vs APP^{HET}	0.015	

Table 2. Figure 1e. Number of OMP+ cells / area

Age - Genotype	VSE region	OMP+ / um^2 x 10^{-3}	N (mice)	One way ANOVA Comparisons	One way ANOVA P value	Two-way ANOVA Age – Genotype Interaction P value
4 months	Anterior	10.69 ± 0.56	4	**Anterior**		**Anterior** 0.47
24 months	Anterior	7.80 ± 0.53	4	4 months vs 24 months	0.002	**Central** 0.87
1-year-old APP^{WT}	Anterior	9.50 ± 0.45	4	APP^{WT} vs APP^{HET}	0.21	**Posterior** 0.37
1-year-old APP^{HET}	Anterior	8.60 ± 0.53	4			
4 months	Medial	9.92 ± 0.23	4	**Central**		
24 months	Medial	7.70 ± 0.70	4	4 months vs 24 months	0.004	
1-year-old APP^{WT}	Medial	9.15 ± 0.78	4	APP^{WT} vs APP^{HET}	0.21	
1-year-old APP^{HET}	Medial	8.40 ± 0.40	4			
4 months	Posterior	9.15 ± 0.70	4	**Posterior**		
24 months	Posterior	7.90 ± 0.75	4	4 months vs 24 months	0.24	
1-year-old APP^{WT}	Posterior	9.53 ± 0.77	4	APP^{WT} vs APP^{HET}	0.96	
1-year-old APP^{HET}	Posterior	10.00 ± 0.84	4	24 mo vs APP^{HET}	0.16	

Table 3. Figure 1b AOB Volume (mm^3)

Age - Genotype	AOB Volume (mm^3)	N (mice)	One-way ANOVA Comparisons	One-way ANOVA P value	Two-way ANOVA Age – Genotype Interaction P value
4 months	0.48 ± 0.03	4	4 months vs 24 months	0.05	0.82
24 months	0.41 ± 0.03	4	APP^{WT} vs APP^{HET}	0.45	
1-year-old APP^{WT}	0.48 ± 0.04	4	4 months vs APP^{HET}	0.22	
1-year-old APP^{HET}	0.44 ± 0.03	4	24 months vs APP^{HET}	0.50	

Table 4. Figure 1f. Sox2 CTF / area - SCL

Age - Genotype	Sox2 CTF/um^2	N (mice)	One-way ANOVA Comparisons	One-way ANOVA P value	Two-way ANOVA Age – Genotype interaction P value
4 months	33.24 ± 2.43	4	4 months vs 24 months	$3x10^{-6}$	0.63
24 months	10.74 ± 1.32	4	APP^{WT} vs APP^{HET}	0.78	
1-year-old APP^{WT}	26.23 ± 3.95	4	24 months vs APP^{HET}	$2x10^{-8}$	
1-year-old APP^{HET}	27.37 ± 0.96	4			

Table 5. Figure 2b. Number of PCNA+ cells / area

Age - Genotype	VSE region	PCNA+ / um^2 x 10^{-3}	N (mice)	One-way ANOVA Comparisons	One-way ANOVA P value	Two-way ANOVA Age – Genotype Interaction P value
4 months	Anterior	2.26 ± 0.80	4	**Anterior**		**Anterior** 0.74
24 months	Anterior	0.75 ± 0.35	4	4 months vs 24 months	0.04	**Central** 0.014
1-year-old APP^{WT}	Anterior	0.73 ± 0.30	4	APP^{WT} vs APP^{HET}	0.01	**Posterior** 0.006
1-year-old APP^{HET}	Anterior	3.42 ± 0.82	4	24 months vs APP^{HET}	0.015	
4 months	Medial	2.15 ± 0.52	4	**Central**		
24 months	Medial	0.23 ± 0.13	4	4 months vs 24 mo	0.004	
1-year-old APP^{WT}	Medial	1.61 ± 0.32	4	APP^{WT} vs APP^{HET}	0.91	
1-year-old APP^{HET}	Medial	1.57 ± 0.20	4	24 months vs APP^{HET}	$4x10^{-6}$	
4 months	Posterior	3.04 ± 0.90	4	**Posterior**		
24 months	Posterior	0.17 ± 0.08	4	4 months vs 24 months	0.02	
1-year-old APP^{WT}	Posterior	2.42 ± 0.60	4	APP^{WT} vs APP^{HET}	0.56	
1-year-old APP^{HET}	Posterior	1.93 ± 0.57	4	24 months vs APP^{HET}	0.02	

Table 6. Figure 2c. Sox2$^+$ cells / area - VSE

Age - Genotype	Sox2$^+$ cells /um^2	N (mice)	One-way ANOVA Comparisons	One-way ANOVA P value	Two-way ANOVA Age – Genotype Interaction P value
4 months	3.08 ± 0.40	4	4 months vs 24 months	0.05	0.53
24 months	2.37 ± 0.36	4	APP^{WT} vs APP^{HET}	0.07	
1-year old APP^{WT}	2.92 ± 0.38	4	24 months vs APP^{HET}	0.62	
1-year old APP^{HET}	2.15 ± 0.24	4			

Table 7. Figure 3 b-c. Social odor exploration. Natural aging

	Normalized sniffing time (s)		One-way ANOVA P value
Dilution	**Middle age N = 20 mice**	**Senescent N = 25 mice**	Middle age vs Senescent
1:1000	2.80 ± 0.43	0.60 ± 0.20	$7x10^{-5}$
1:500	2.50 ± 0.35	0.86 ± 0.20	0.0005

1:250	2.36 ± 0.70	1.37 ± 0.36	0.20
1:100	2.95 ± 0.43	1.56 ± 0.37	0.05
1:50	3.14 ± 0.55	1.90 ± 0.33	0.10
1:10	4.90 ± 1.10	3.04 ± 0.50	0.04
ND	6.06 ± 0.88	3.83 ± 0.71	0.03

Table 8. Figure 3 d-e. Social odor exploration. Pathological aging

	Normalized sniffing time (s)		**P value**
Dilution	**APP^{WT} N = 11 mice**	**APP^{HET} N = 12 mice**	APP^{WT} vs APP^{HET}
1:1000	0.84 ± 0.31	1.00 ± 0.20	0.70
1:500	0.97 ± 0.20	0.52 ± 0.10	0.06
1:250	0.70 ± 0.14	0.90 ± 0.17	0.40
1:100	2.03 ± 0.55	1.37 ± 0.43	0.35
1:50	1.40 ± 0.26	1.43 ± 0.46	0.96
1:10	4.94 ± 1.21	1.82 ± 0.27	0.03
ND	5.65 ± 1.51	2.58 ± 0.43	0.05

Dilution	**Two-way ANOVA Age – Genotype Interaction P value**
1:1000	0.02
1:500	0.0003
1:250	0.015
1:100	0.88
1:50	0.53
1:10	0.51
ND	0.33

Table 9. Figure 4 a-b. Neutral odor exploration. Natural aging

	Normalized sniffing time (s)		**One-way ANOVA P value**
Dilution	**Young N = 18 mice**	**Senescent N = 20 mice**	Young vs Senescent
$1:5x10^5$	1.65 ± 0.42	1.23 ±0.35	0.50
$1:10^5$	1.41 ± 0.50	0.90 ± 0.20	0.33
$1:10^4$	1.44 ± 0.32	1.20 ±0.26	0.54
$1:10^3$	1.90 ± 0.35	1.56 ± 0.50	0.60
1:100	1.76 ± 0.26	1.24 ± 0.20	0.15

Table 10. Figure 4 c-d. Neutral odor exploration. Pathological aging

	Normalized sniffing time (s)		**One-way ANOVA P value**
Dilution	**APP^{WT} N = 10 mice**	**APP^{HET} N = 13 mice**	APP^{WT} vs APP^{HET}
$1:5x10^5$	0.82 ± 0.11	0.85 ± 0.18	0.90
$1:10^5$	0.75 ± 0.15	0.75 ± 0.11	0.97
$1:10^4$	0.91 ± 0.13	1.50 ± 0.25	0.06
$1:10^3$	1.42 ± 0.30	1.40 ± 0.22	0.96
1:100	0.93 ±0.16	1.40 ± 0.12	0.03

Dilution	Two-way ANOVA Age – Genotype Interaction P value
1:5x10^5	0.50
1:10^5	0.71
1:10^4	0.99
1:10^3	0.80
1:100	0.46

Table 11. Figure 4e. Food finding test latency (min)

Condition	Latency (min)	N (mice)	One-way ANOVA Comparisons	One-way ANOVA P value	Two-way ANOVA Age-Genotype interaction P value
4 months	5.22 ± 1.08	15	4 mo vs 24 mo	0.96	0.13
24 months	5.15 ± 0.95	15	APP^{WT} vs APP^{HET}	0.55	
1-year-old APP^{WT}	3.87 ± 0.32	16			
1-year-old APP^{HET}	4.27 ± 0.58	20			

Table 12. Figure 5 b, c. Figure 6 a, b, g, h. Social habituation – Natural aging

	Sniffing time (s)		One-way ANOVA P value
Test phase	**Young N = 21 mice**	**Senescent N = 26 mice**	Young vs Senescent
Water control	0.67 ± 0.10	0.56 ± 0.11	0.30
S1a	2.45 ± 0.40	1.36 ± 0.27	0.03
S1b	0.87 ± 0.20	0.70 ± 0.14	0.50
S1c	0.51 ± 0.10	0.70 ± 0.21	0.44
S2a	2.44 ± 0.43	1.51 ± 0.27	0.03
S2b	0.81 ± 0.15	0.82 ± 0.14	0.94
S2c	0.55 ± 0.11	0.96 ± 0.18	0.06

Table 13. Figure 5 d, e. Figure 6 d, e, j, k. Social habituation – Pathological aging

	Sniffing time (s)		One way-ANOVA P value
Test phase	**APPWT N = 15 mice**	**APPHET N = 24 mice**	APP^{WT} vs APP^{HET}
Water control	0.50 ± 0.07	0.71 ± 0.09	0.70
S1a	2.81 ± 0.40	1.75 ± 0.22	0.03
S1b	0.95 ± 0.10	0.68 ± 0.10	0.08
S1c	0.84 ± 0.22	0.71 ± 0.13	0.62
S2a	1.85 ± 0.42	1.00 ± 0.17	0.03
S2b	0.80 ± 0.22	0.62 ± 0.08	0.50
S2c	0.60 ± 0.13	0.50 ± 0.09	0.53

Dilution	Two-way ANOVA Age – Genotype Interaction P value
Water control	0.51
S1a	0.70
S1b	0.15
S1c	0.84
S2a	0.33
S2b	0.17

S2c	0.70

Table 14. Figure 6 c, i. Social habituation – discrimination slopes – Natural aging

	Slope		P value
Test phase	**Young N = 21 mice**	**Senescent N = 26 mice**	Middle age vs Senescent
1st discrimination	1.78 ± 0.36	0.80 ± 0.30	0.03
2nd discrimination	1.92 ± 0.40	0.75 ± 0.40	0.02
1st habituation	-1,57 ± 0.40	-0.65 ± 0.24	0.02
2nd habituation	-1.62 ± 0.40	-0.62 ± 0.32	0.03

Table 15. Figure 6 f, l. Social habituation – discrimination slopes – Pathological aging

	Slope		P value
Test phase	**APP^{WT} N = 15 mice**	**APP^{HET} N = 24 mice**	APP^{WT} vs APP^{HET}
1st discrimination	2.32 ± 0.43	0.97 ± 0.24	0.012
2nd discrimination	1.01 ± 0.51	0.27 ± 0.20	0.20
1st habituation	-1.86 ± 0.50	-1.03 ± 0.24	0.13
2nd habituation	-1.06 ± 0.44	-0.37 ± 0.18	0.20

Test phase	**Two-way ANOVA Age – Genotype Interaction P value**
1st discrimination	0.41
2nd discrimination	0.19
1st habituation	0.65
2nd habituation	0.007

Table 16. Figure 5 g. Long-term social discrimination

	Sniffing time (s)		One-way ANOVA P value	Two-way ANOVA Age – Genotype interaction P value
Test phase	**Day 0**	**Day 1**	**Day 0 vs Day 1**	0.98
4 months (n = 19 mice)	2.45 ± 0.07	1.20 ± 0.20	0.008	
24 months (n = 20 mice)	1.36 ± 0.30	1.12 ± 0.30	0.25	
1-year-old APP^{WT} (n = 8 mice)	3.12 ± 0.90	1.65 ± 0.60	0.04	
1-year-old APP^{HET} (n = 13 mice)	1.60 ± 0.40	1.40 ± 0.33	0.70	

Table 17. Figure 7. Social habituation – Novel vs littermate

	Sniffing time (s)		One-way ANOVA P value
Test phase	**Young N = 21 mice**	**Senescent N = 23 mice**	Young vs Senescent
Water control	0.61 ± 0.20	0.68 ± 0.16	0.70
La	1.91 ± 0.30	1.10 ± 0.20	0.02
Lc	0.53 ± 0.11	0.30 ± 0.09	0.3
Na	1.27 ± 0.25	0.60 ± 0.20	0.04
Nc	0.45 ± 0.13	0.24 ± 0.11	0.2

Table 18. Figure 7. Social habituation – Self recognition

	Sniffing time (s)		One-way ANOVA P value
Test phase	**Young N = 21 mice**	**Senescent N = 23 mice**	Young vs Senescent
Water control	0.48 ± 0.11	0.31 ± 0.09	0.70
La	3.06 ± 0.35	2.07 ± 0.43	0.04
Lc	0.45 ± 0.10	0.48 ± 0.10	0.64
Oa	1.22 ± 0.33	1.23 ± 0.18	0.96
Oc	0.84 ± 0.13	0.48 ± 0.13	0.90

Table 19. Figure 8 b, c. Three chamber sociability test – Natural aging

Test phase	**Sniffing time (s)**		**One-way ANOVA P value**
	Young N = 14 mice	**Senescent N = 22 mice**	
Sociability			**Empty vs $M1^A$**
Empty	25.06 ± 2.96	14.50 ± 1.90	Middle age: $2x10^{-6}$
$M1^A$	64.35 ± 5.23	47.24 ± 4.60	Senescent: $1x10^{-5}$
Social novelty			**$M1^B$ vs M2**
$M1^B$	62.37 ± 5.01	49.15 ± 4.20	Middle age: 0.002
M2	99.93 ± 9.83	63.70 ± 5.30	Senescent: 0.04

Table 20. Figure 8 c,d. Three chamber sociability test – Pathological aging

Test phase	**Sniffing time (s)**		**One-way ANOVA P value**
	APP^{WT} N = 14 mice	**APP^{HET} N = 15 mice**	
Sociability			**Empty vs $M1^A$**
Empty	39.15 ± 3.63	41.00 ± 4.07	APP^{WT}: 0.0003
$M1^A$	69.40 ± 6.05	69.73 7.10	APP^{HET}: 0.003
Social novelty			**$M1^B$ vs M2**
$M1^B$	71.30 ± 5.75	65.12 ± 6.70	APP^{WT}: 0.04
M2	93.07 ± 11.70	77.02 ± 8.43	APP^{HET}: 0.60

Test phase	**Two-way ANOVA Age – Genotype interaction P value**
Sociability M1A - Empty	0.96
Social novelty M2 – M1B	0.83